

DR. XUE WU (Orcid ID : 0000-0002-0511-9436)

DR. MELISSA FISHEL (Orcid ID : 0000-0002-9436-6382)

DR. HEIKO KONIG (Orcid ID : 0000-0002-6871-7388)

Article type : Original Article

Pharmacological inhibition of Carbonic Anhydrase IX and XII to enhance targeting of acute myeloid leukemia cells under hypoxic conditions.

Fangli Chen¹, Emilia Licarete^{1,5}, Xue Wu¹, Daniela Petrusca¹, Callista Maguire⁴, Max Jacobsen⁴, Austyn Colter⁴, George E. Sandusky⁴, Magdalena Czader⁴, Maegan L. Capitano¹, James P. Ropa¹, H. Scott Boswell¹, Fabrizio Carta⁶, Claudiu T. Supuran⁶, Brian Parkin⁷, Melissa Fishel^{1,2,3}, Heiko Konig¹

¹Melvin and Bren Simon Comprehensive Cancer Center, Indiana University, Indianapolis, IN, USA

²Department of Pediatrics, Wells Center for Pediatric Research, Indiana University, Indianapolis, IN, USA

³Department of Pharmacology & Toxicology, Indiana University, Indianapolis, IN, USA

⁴Department of Pathology and Laboratory Medicine, Indiana University, Indianapolis, IN, USA

⁵Department of Molecular Biology and Biotechnology, Faculty of Biology and Geology, Babes-Bolyai University, 400006 Cluj-Napoca, Romania

⁶NEUROFARBA Department, Pharmaceutical and Nutraceutical Section, University of Florence, Italy

⁷Division of Hematology and Oncology, Department of Internal Medicine, University of Michigan, Ann Arbor, MI, USA.

Address correspondence to:

This is the author manuscript accepted for publication and has undergone full peer review but has not been through the copyediting, typesetting, pagination and proofreading process, which may lead to differences between this version and the [Version of Record](#). Please cite this article as [doi: 10.1111/JCMM.17027](https://doi.org/10.1111/JCMM.17027)

This article is protected by copyright. All rights reserved

Heiko Konig, MD PhD, Department of Medicine, Division of Hematology/Oncology, Indiana University School of Medicine, Melvin and Bren Simon Comprehensive Cancer Center, 980 W. Walnut St., Walther Hall R3 – C321G, Indianapolis, IN 46202.

Phone: 317/274-3590; Fax: 317/274-0396; Email: hkonig@iupui.edu

Running title: Dual CA IX and XII targeting in AML.

Key words: Acute myeloid leukemia, Carbonic Anhydrases, pH regulation, Drug resistance, Hypoxia.

Abstract

Acute myeloid leukemia (AML) is an aggressive form of blood cancer that carries a dismal prognosis. Several studies suggest that the poor outcome is due to a small fraction of leukemic cells that elude treatment and survive in specialized, oxygen (O₂)-deprived niches of the bone marrow. Although several AML drug targets such as FLT3, IDH1/2 and CD33 have been established in recent years, survival rates remain unsatisfactory which indicates that other, yet unrecognized, mechanisms influence the ability of AML cells to escape cell death and to proliferate in hypoxic environments. Our data illustrates that Carbonic Anhydrases IX and XII (CA IX/ XII) are critical for leukemic cell survival in the O₂-deprived milieu. CA IX and XII function as transmembrane proteins that mediate intracellular pH under low O₂ conditions. Because maintaining a neutral pH represents a key survival mechanism for tumor cells in O₂-deprived settings, we sought to elucidate the role of dual CA IX/ XII inhibition as a novel strategy to eliminate AML cells under hypoxic conditions. Our findings demonstrate that the dual CA IX/ XII inhibitor FC531 may prove to be of value as an adjunct to chemotherapy for the treatment of AML.

Introduction

Acute myeloid leukemia (AML) represents a heterogeneous, malignant disorder of the hematopoietic system that is characterized by rapid cell growth, dysregulated apoptosis and impaired differentiation of leukemic blasts(1). While standard anti-neoplastic therapies, including recently approved targeted agents (e. g. inhibitors of FLT3 and IDH1/2), and allogeneic stem cell transplantation frequently lead to remissions, most patients relapse due to the development of drug resistance and minimal residual disease (MRD)(1, 2). The substrate of

MRD is the survival of a small drug-resistant population of leukemic cells in specific “sanctuaries” such as the bone marrow (BM) niche(3-5). Recent data suggests that distinct regions of the BM niche are severely deprived of oxygen (O₂)(6-9). Although factors such as BM stromal cells and Hypoxia Inducible Factor (HIF) signaling have been implicated in niche-associated leukemic cell survival and MRD development, therapeutic approaches to disrupt leukemic cell-BM stromal interaction and HIF-targeted strategies have yielded limited success to date(10-18). As a result, there remains a significant knowledge gap regarding the most relevant targets in AML.

Carbonic Anhydrases (CA) IX and XII have recently emerged as attractive targets in multiple tumors(19-22). CAs function as transmembrane proteins that mediate intracellular pH under low O₂ conditions via the reversible conversion of CO₂ to bicarbonate and protons(23). Lines of evidence suggest that maintaining a close to neutral, intracellular pH represents a key survival mechanism for tumor cells to escape apoptosis and to proliferate in the hypoxic environment(24). Confined to few normal tissues, CA IX is highly expressed in many solid tumor types and has been associated with poor prognosis, disease progression and aggressiveness(25, 26). A therapeutic effect of CA IX inhibition has been demonstrated in preclinical *in vivo* studies of renal cell and colorectal cancer where specific inhibition of CA IX activity enhanced the effects of tumor irradiation(27, 28). However, the role of CA IX in AML is not well defined. Recent work by Konopleva et al. demonstrated that CA IX expression strongly correlates with the BM blast percentage in AML patients, indicating that CA IX stabilization is closely associated with the extent of leukemic infiltration(29). Compared to CA IX, data on the role of CA XII in human cancers is less abundant. Similar to CA IX, CA XII expression has been shown to be upregulated in several solid malignancies(30-33). In addition, Lounnas et al. as well as others demonstrated that CA XII promotes cancer cell survival, migration, invasion and stemness(34-36). Further work by Kopecka and colleagues strongly suggests that targeting CA XII has the potential to overcome drug resistance as increased expression of CA XII has been found on the surface of chemo-resistant cells(19).

We herein evaluated the expression of CA IX and XII in AML cells under O₂-controlled settings and uncovered a potential role for CA IX and CA XII in AML cells exposed to hypoxic and

chemotherapeutic stress conditions. We therefore visited the approach of dual CA IX and XII inhibition in a diverse panel of AML cells and in patient derived (PDX) AML models. Our data demonstrates that dual CA IX/ XII inhibition exerts anti-leukemic activity *in vitro* and *in vivo*, is well tolerated in single agent mode and when combined with Cytarabine, and improves survival. On the basis of our findings, we propose the further investigation of integrated CA IX/ XII targeting in AML.

Methods

Cell culture and reagents

Molm13 (M13), Molm14 (M14) and the relatively Cytarabine-resistant cell lines OCI-AML3 and THP-1(37) were obtained from the Deutsche Sammlung von Mikroorganismen und Zellkulturen (Braunschweig, Germany). All cells were cultured in RPMI1640 medium with 10% FBS and 100U/mL streptomycin/penicillin in a humidified atmosphere at 37 °C and 5% CO₂. Quizartinib and Cytarabine were purchased from Selleck Chemicals, dissolved in dimethyl sulfoxide (DMSO) at stock concentrations of 10 mM and stored at –80 °C. The dual CA IX/ XII inhibitors FC531 and SLC0111 were synthesized as previously described(22). The dual CA IX/ XII inhibitor CA912 was purchased from Calbiochem (Calbiochem Research Biochemicals, Burlington, MA). All CA IX/ XII inhibitors were dissolved in DMSO at stock concentrations 10 mM and stored at –80 °C. Fluorescein isothiocyanate-AnnexinV antibody and propidium iodide were purchased from BD Pharmingen (556420) and Sigma-Aldrich (P4864). APC-CD11b antibody was purchased from Biolegend (101212).

Patient samples

AML blasts derived from whole blood or the BM from newly diagnosed (ND) and relapsed/refractory (R/R) AML patients (pts) were obtained under guidelines approved by the Institutional Review Board of the Indiana University (Indianapolis, IN, USA). All patients gave informed consent according to the Declaration of Helsinki. Blasts were separated as described elsewhere(38). The clinical characteristics of the patients from whom samples and tissues were derived are listed in **Table 1A** and **B**.

MTT cell viability assay

1×10^4 Molm13, Molm14, THP-1 and OCI-AML3 suspended in RPMI1640 culture medium with 10% FBS were seeded in 96 well plates, after 24h pre-incubation, cells were treated with drug under ambient air (normoxia, 21% O₂) or hypoxic conditions (1% O₂) for 48 hours (h) as outlined for each experiment. For primary cells, 15×10^4 fresh primary cells were suspended in RPMI1640 culture medium with 20% FBS. Cell viability was assessed using MTT (3-(4,5-dimethylthiazol-2-yl)-2,5-diphenyltetrazolium bromide; Roche, Indianapolis, IN, USA) in accordance to the manufacturer's recommended protocols. Unless otherwise specified, all assays were performed in *triplicate* and results were obtained in at least three independent experiments.

Apoptosis assay

5×10^5 leukemia cells were seeded in 6 well plates for 24h pre-incubation, and incubated with Cytarabine, Quizartinib or FC531 under 21% or 1% O₂ conditions for 48h. Leukemia cells were collected from the plates, washed twice with cold PBS and then re-suspended in 100ul binding buffer. 5ul FITC-Annexin V and 10ul propidium iodide stock solution (50 μ g/ml) were added to each sample and incubated at room temperature in the dark for 15 minutes. Cells were analyzed on a FACSCalibur machine (BD Biosciences, San Jose, CA) and the data was analyzed by Flowjo software.

Differentiation assay

5×10^5 leukemia cells were pre-incubated in 6 well plates for 24h and treated with different concentration of FC531 under 1% O₂ conditions for 72h. Leukemia cells were collected from the plates, washed twice with cold PBS and then re-suspended in 100ul PBS. 5ul APC-CD11b antibody were added to each sample and incubated at room temperature in the dark for 30 minutes. CD11b expression was analyzed on a FACSCalibur machine (BD Biosciences, San Jose, CA) and the data was analyzed by FlowJo software.

Intracellular pH assay

Intracellular pH was evaluated using the pHrodo Red AM Intracellular pH Indicator (Thermo Fisher Scientific, Waltham, MA). Molm14 cells treated with FC531 under normoxic and hypoxic

conditions for 48h were analyzed with pHrodo Red AM dye. Results were normalized to cell viability by MTT assay. Intracellular pH calibration buffers were used to create a standard curve of fluorescence intensity for determination of pH values.

RNA isolation and QPCR

Molm13, Molm14, THP-1, OCI-AML3 and primary cells were incubated under normoxic or hypoxic conditions for 48h. Total RNA was extracted by RNeasy Plus Kit (Qiagen) according to the manufacturer's instructions. cDNA was synthesized with reverse transcription kit (Thermo Fisher Scientific) in accordance with the manufacturer's protocols. The PCR primers used in the study were as follows:

- CA IX(F): GTGCCTATGAGCAGTTGCTGTC and CA IX(R): AAGTAGCGGCTGAAGTCAGAGG
- CA XII(F): GACCTTTATCCTGACGCCAGCA and CA XII (R): CATAGGACGGATTGAAGGAGCC
- CA I(F): TAGTGTCTCCTACAACCCAGCC and CA I(R): GCTGTCAGAGAAAGGACCACCT
- CA II(F): GTGACCTGGATTGTGCTCAAGG and CA II(R): GTTGTCCACCATCAGTTCTTCGG
- RN18S1(F): ACCCGTTGAACCCATTCGTGA and RN18S1 (R): GCCTCACTAAACCATCCAATCGG

RN18S1 expression was used as a control for RNA loading. Quantitative PCR reactions were performed using PowerUp SYBR Green PCR Master Mix (Applied Biosystems, USA) on 7900HT Real-Time PCR System.

Droplet Digital (dd) PCR

Genomic DNA from circulating leukocytes was extracted from murine whole blood using QIAamp DNA Micro columns (Qiagen) and amplified with a REPLI-g Single Cell kit (Qiagen). An allele-specific fluorescent locked nucleic acid probe set (IDT, Coralville, IA) for the FLT3-ITD of interest was developed and optimized. ddPCR was then performed using that probe set with the murine leukocyte genomic DNA samples along with wildtype (negative) and mutant (positive) controls on a BioRad RainDrop system as previously described(39).

Animals and establishment of tumor xenografts

All animal studies were performed according to an IACUC-approved protocol and in compliance with the Guide for the Care and Use of Laboratory Animals (National Research Council, 2011). In brief, Molm14 and PDX xenografts were generated by injecting 2×10^5 and 1×10^6 cells into the tail vein of 6-8 weeks old NOD-SCID^{γnull} (NSG) or NSG-SGM3 (NSGS, JAX stock# 013062) mice (J000106134), respectively. Upon confirmation of engraftment, mice were randomized into experimental groups (n=5 each group) and dosed accordingly with Cytarabine and/or FC531 starting on Study Day (SD) 0. Tumor burden was monitored once weekly by flow cytometry on whole blood samples collected *via* retro-orbital bleed. The flow cytometry panel included mouse CD45, human CD45, human CD3, human CD33, human CD11b, viability dye, and absolute counting beads. All animals were monitored for up to 12 weeks following the last dose of therapy prior to sacrifice or euthanized by CO₂ asphyxiation when moribund.

Immunohistochemistry, Digital Imaging and Analysis

All mouse tissue samples were collected following a detailed Laboratory Animal Resource Center (LARC) approved protocol. Human BM samples were obtained from 9 AML patients. Slides were stained with H&E, CA IX and CA XII for pathologic evaluation. All tissue sections were scanned at 20x magnification, unless indicated otherwise. Antigen retrieval was performed by immersing the slides in Target Retrieval Solution (DAKO; Agilent Technologies, Santa Clara, CA) for 20 min at 90°C. Subsequent staining steps were performed on the DAKO Immunostainer. Primary antibodies included anti-mouse CA IX (Novus NB100-47) and anti-mouse CA XII (Abcam ab244309). The Aperio Scan Scope CS system (Leica Biosystems, Wetzlar, Germany) was used for imaging. The Positive Pixel Count algorithm on Aperio ImageScope (Leica Biosystems) was used to quantify the amount of a specific stain present in a scanned slide image.

Statistical analysis

Statistical significance of differences was determined by Student's t-test. Difference was considered statistically significant when p-value was less than 0.05. Data is presented as mean ± standard error of the mean (SEM) unless stated otherwise. Kaplan–Meier survival curve

estimators were reported for each condition. The Cox proportional hazard model was used to test the difference of the time-to-event among different conditions.

Results

Hypoxic stress leads to induction of CA IX and/or CA XII in AML cells.

Previous work on cancer cells derived from patients with a broad spectrum of solid tumors has shown that hypoxia leads to the induction of complex signaling networks such as the hypoxia-inducible factor 1 α (HIF-1 α) and its downstream targets and transcriptional regulators, including carbonic anhydrases (CAs). While these findings have established hypoxia as a compelling target in the treatment of solid cancers, data about hypoxic responses in hematologic neoplasms are lacking. Almost 2 decades ago, Leppilampi et al. reported that CA II is expressed on leukemic blasts in 62% of patients with AML(40). Aside from the work by these authors, there is paucity of information about the etiological connection between CAs and AML. To investigate whether CAs are expressed in AML cells under hypoxic stress conditions we exposed a diverse panel of AML cell lines to 21% and 1% O₂ for 48h and thereafter assessed the expression of several CAs. Since out of 16 CA isoforms only CA I and II (cytosolic) have previously been reported to be expressed in the hematopoietic system, whereas CA IX and XII (membrane bound) have been linked to solid neoplasms(41), we focused our analysis on these 4 CAs. Using real-time quantitative PCR analysis, we found that CA IX and/or CA XII, less so CA I and/or CA II, were highly expressed under hypoxic stress in THP-1 and OCI-AML3 as well as in the FLT3/ITD mutated (FLT3/ITD⁺) cell lines Molm13 and Molm14 (**Figure 1A**). Next, we extended our experiments to include primary samples derived from FLT3/ITD⁺ AML patients with ND (n=5) and R/R (n=3) disease. Our PCR data revealed that, similar to our findings in cell line studies, CA IX and XII, but not CA I and II, were strongly induced under 1% compared to 21% O₂ conditions (**Figure 1B**). Of note, FLT3/ITD⁺ AML represents one of the most aggressive forms of blood cancer and carries a dismal prognosis due to short remission durations and high relapse rates(42). The dynamics associated with FLT3/ITD⁺ AML indicate that distinct mechanisms of resistance and MRD are operative in this disease, thus making it an ideal model to study the effects of novel therapeutic approaches. Although established as an effective drug target in AML, previous data has shown that FLT3 is downregulated in response to hypoxic stress(43),

indicating that other signaling pathways influence the ability of AML cells to escape cell death and to proliferate in hypoxic environments.

CA IX and/or CA XII is expressed in Cytarabine-residual FLT3/ITD⁺ AML cells in vivo.

Following our experiments aimed at assessing CA I, II, IX and XII mRNA expression in AML cells to low O₂ stress *in vitro*, we decided to corroborate our findings in xenograft studies. Using Molm14 xenografts, we administered a 7-day course of Cytarabine and sacrificed mice 24h after the last dose in order to assess immediate drug responses *in vivo*. As expected, immunohistochemistry (IHC) staining in untreated animals revealed a hypercellular marrow with collapse of the vascular channels. The vast majority of cells seen in the marrow were large myeloid, leukemic blasts consistent with the development of frank AML. The immunostaining for CA IX was multifocal and localized on the cell membrane (**Figure 2A**). Consistent with our *in vitro* findings, treatment with Cytarabine reduced the leukemic burden but CA IX staining was enhanced in residual blasts (**Figure 2B**). Similar findings were obtained in the spleen. In untreated animals, the spleen was enlarged with marked expansion of the red pulp and large, myeloid leukemic blasts replacing most of the normal architecture (**Figure 2C**). The spleen was smaller with less leukemic blasts in the red pulp compared to the untreated group in animals treated with Cytarabine. Residual blasts in the spleen showed enhanced CA-IX staining (**Figure 2D**). Of note, IHC did not reveal relevant CA XII staining which was consistent with low CA XII mRNA expression of Molm14 cells in PCR assays (**Figure 1A**). If CA IX and CA XII are involved in the development of AML drug resistance, then patients failing induction chemotherapy as evidenced by an interim BM assessment routinely performed 14-21 days after the initiation of therapy should show persistent or enhanced CA IX and/or CA XII staining when compared to the diagnostic marrow. We therefore stained BM samples from patients with FLT3 mutated AML (n=4) who had residual disease on their day 14 or day 21 marrow assessment. As shown in **Figures 3A-L**, 4 out of 4 patients showed increased CA IX and/or CA XII staining in leukemic blasts remaining after induction chemotherapy when compared to the diagnostic marrow.

Dual CA IX/ XII inhibition selectively kills FLT3/ITD⁺ AML cells under hypoxic conditions in vitro.

In accordance to our findings described above, CA IX and CA XII emerged as promising targets for AML-directed therapy. To investigate the anti-leukemic activity of dual CA IX/ XII inhibition, we exposed primary AML samples derived from patients with ND (n=5-6; **Figures 4A and B**) and R/R (n=3; **Figures 4C and D**) FLT3 mutated AML to the dual CA IX/ XII inhibitors FC531, SLC0111 and CA912 (**Supplemental Figure 1**), as well as to Cytarabine and the highly selective FLT3 inhibitor Quizartinib. After 48h, we performed MTT assays to measure cell proliferation and reduction in cell viability. In accordance to previously published data by Andreucci et al.(44), a dose range of 50-200 μ M was selected for all three CA inhibitors. As shown in **Figures 4A-D**, FC531, CA912 and SLC0111 were significantly more effective than Cytarabine and Quizartinib at clinically achievable doses under both 1% and 21% O₂. The ability of cancer cells to maintain neutral intracellular pH levels under hypoxic stress represents a critical requirement for their survival. Given the central role of CA IX and CA XII in intracellular pH regulation and its druggability as a trans-membranous protein, we hypothesized that pharmacologic targeting of CA IX and CA XII will result in strong intracellular acidification and cytotoxicity under low O₂ conditions. We therefore analyzed intracellular pH levels in hypoxia exposed Molm14 cells following treatment with dual CA IX/ CA XII inhibition. Because FC531 yielded the greatest effects among the three CA-targeted agents, we focused on this compound to further investigate the mechanisms of action of dual CA IX/ XII inhibition. Using the pHrodo Red AM fluorescent pH indicator, we found that treatment with FC531 for 48h led to a significant decrease in intracellular pH levels under hypoxic but not normoxic conditions (**Figure 4E**, **Table 2**). Utilizing annexin-V/PI staining we further demonstrated that FC531 substantially induced apoptosis in M14 cells after 48h under 1% but not 21% O₂, whereas induction of apoptosis was attenuated by Cytarabine at 1% O₂ (**Figures 4F and G**). In line with this observation, MTT assays showed that FC531 exhibited dose dependent, growth inhibitory effects under 1% but not 21% O₂ in Molm14 cells (IC₅₀ [1%O₂] = 4.04 μ M, 48h), **Figure 4H**), and was more effective than Cytarabine in this respect. Similar results were obtained in Molm13 cells (IC₅₀=2.85 μ M; *data not shown*). Remarkably, FC531 displayed synergistic toxicity against Molm14 cells when combined with Cytarabine at clinically achievable doses (combination index [CI]: 0.78, 48h; *data not shown*). We next determined whether differentiation could be

contributing to the overall cytotoxic effects of FC531 against M14 cells. Because FC531 yielded the greatest magnitude of cytotoxicity at 1% O₂, we focused on this experimental condition and analyzed M14 cells for expression of cell surface markers of differentiation following treatment with FC531. Using decrease of density of CD33 and CD64, and higher expression of CD11b as markers of differentiation, we found that FC531 dose dependently induced the expression of differentiation markers after cells were exposed for 72h (**Figure 4I**).

The dual CA IX/ XII inhibitor FC531 is well tolerated and confers anti-leukemic activity against FLT3/ITD⁺ AML cells in vivo

Next, we sought to assess the anti-leukemic activity of FC531 in patient derived xenograft (PDX) models(45). As shown in **Table 3**, mice were treated with single agent Cytarabine 30mg/kg IP (days 1-5 and 8-12), single agent FC531 30mg/kg IP (days 1-5 and 8-12), or Cytarabine (days 1-5) combined with FC531 (days 8-12, sequential therapy). Mice were monitored for leukemic burden in peripheral blood and survival over a course of 82 days. Leukemic burden was assessed via human (h)CD33 positivity per flow cytometry (**Figure 5A**) and FLT3/ITD mutant drops as detected per ddPCR (**Figure 5B**) within 24h after the last drug dose. Consistent with our *in vitro* observation, single agent FC531 (Group 4) significantly reduced tumor burden from 51.5±3.4 % [untreated, Group 1] to 30.3±3.9% hCD33⁺ (p=.003; n=5). Combined treatment with Cytarabine (Group 3) led to further reduction in tumor burden (0.5±0.03% hCD33⁺, p<.01; n=5). Although single agent Cytarabine (Group 2) was similarly effective against AML cells *in vivo* (0.7±0.2% hCD33⁺, p<.01; n=5), Cytarabine exposure induced multiple signs of illness, including lethargy, hunched posture and scruffy coat in all animals after 10 days of therapy. In contrast, FC531 was well tolerated in single agent mode (Group 4) and showed only minimal and transient toxicity when combined with a 5-day course of Cytarabine (Group 3). As demonstrated in **Figure 5C**, all (5/5) mice in the untreated group had died by day 82 (median survival 63 days). In contrast, combined treatment with FC531 and Cytarabine greatly improved survival with all (5/5) mice surviving for the 82-day experimental period (p<.01 vs. untreated, n=5). More than half of the mice (3/5) remained alive in the single agent FC531 and Cytarabine treated groups with a trend towards statistically improved survival when mice were treated with FC531 (p=.1). Our results demonstrate that FC531 confers anti-

leukemic activity against AML cells *in vivo*, is well tolerated in single agent mode and when combined with chemotherapy and improves survival in PDX models of AML thereby supporting the further investigation of FC531 therapy in clinical trials.

CA IX and/or CA XII is expressed in Cytarabine-residual non-FLT3 mutated AML cells in vivo.

We next assessed the CA IX and XII expression status in non-FLT3 mutated AML. We therefore stained BM samples from a diverse panel of AML patients (n=5) who had residual disease on their day 14 marrow exam. As shown in **Figures 6A-O**, 4 out of 5 patients showed significantly increased CA IX and/or CA XII staining in leukemic blasts that escaped chemotherapeutic elimination strongly suggesting that dual CA IX/XII inhibition may be of value as an adjunct to chemotherapy in the management of AML.

Discussion

Several studies have shown that hypoxia is a critical determinant of drug resistance and disease progression in a wide spectrum of cancers. However, most of the literature in this evolving field of research relies on studies carried out in solid tumors(46). The impact of O₂ deprivation on hematologic malignancies, particularly in AML, is therefore under-studied. While in solid neoplasms such as breast, pancreatic and renal cell cancers, hypoxia results from a mismatch in supply and consumption of O₂, a much different mechanism forms the basis of hypoxia in AML. In AML, BM derived neoplastic cells disseminate into the peripheral blood (PB) where they are exposed to a broad oxygenation window within multiple organs and the vascular system (7, 8, 47). With the intent to achieve a cure, traditional AML-directed treatments consist of an induction phase, aimed at clearing circulating blasts from the PB and marrow, and a consolidation phase to eliminate residual leukemia cells and prevent relapse(1). While effective debulking is frequently achieved, current treatment protocols mostly fail to eliminate residual cells from hypoxic BM niches. Innovative treatment concepts to effectively target drug resistant leukemia cells that reside in O₂-deprived “sanctuaries” therefore represent an unmet need and demand a deeper understanding of the mechanisms involved in this process. It has previously been acknowledged that a major contributor to the slow therapeutic progress in AML(48) is the difficulty of studying the disease *ex vivo* and the use of un-physiologic cell culture

techniques(49). As AML originates from a population of transformed hematopoietic stem and progenitor cells in the BM, culturing techniques for AML samples have been widely adapted from standardized protocols for hematopoietic stem cell culture, usually carried out in ambient air (normoxia, 21% O₂). Traditional culture techniques are therefore hyperoxic and not consistent with physiological conditions. In this work, we hypothesized that an in-depth understanding of hypoxic signaling pathways, and the functional consequences of cytotoxic therapy under hypoxic conditions in particular, holds the key for the identification of therapeutic vulnerabilities in AML. In the present study, we explored the molecular responses of FLT3/ITD⁺ AML cells to Cytarabine under O₂-controlled conditions *in vitro*. Taking a transcriptomic and proteomic approach, we found that CA IX and XII are induced in AML cells under hypoxic stress conditions. Intriguingly, CA IX and/or CA XII remained strongly expressed in Cytarabine-residual cells, as evidenced per IHC staining in M14 xenograft models and in primary samples obtained from AML patients failing induction chemotherapy. To our knowledge, this is the first report describing the induction of CA IX and XII in AML cells when exposed to low O₂ levels such as those encountered by leukemic blasts in clinical settings. Consistent with our observations, some studies have linked the expression of CA IX and XII to the development of drug resistance and poor outcomes(29, 50-52). Specifically, in a study of advanced non-small cell lung cancer, patients who showed positive CA IX expression levels per IHC after induction chemo-radiotherapy demonstrated poor survival(53). Similarly, Kopecka et al. reported that CA XII expression increased during the acquisition of chemoresistance in colorectal cancer cells and that chemosensitivity could be restored by pharmacological inhibition of CA XII(19). As at least CA IX has been reported to be expressed in very low amounts in only a few normal tissues, such as the gastric mucosa(25), CA IX inhibition may show relatively few side effects compared to standard anticancer drugs that interact with their target in both healthy and normal tissues. Accordingly, clinical data from early phase CA IX inhibitor trials have shown little toxicity(54). We therefore decided to visit the concept of dual CA IX/ XII inhibition in AML. Our screening of three different, dual CA IX/ XII inhibitors showed dose dependent activity against a panel of primary FLT3/ITD⁺ AML cells from ND and R/R samples, irrespective of the O₂ concentration used in the *in vitro* setting. FC531 was more effective than SLC-0111 and CA912, and exerted its cytotoxic activity via inhibition of cell growth, induction of apoptosis and differentiation. Intriguingly, at the doses tested, the anti-leukemic activity of FC531 against

Molm14 cells was only observed under hypoxic and not under normoxic conditions. These observations are reminiscent of the studies carried out by Pastorekova and colleagues, who inhibited CA IX/ XII enzyme activity with sulfonamides and found that the fluorescent inhibitor only accumulated in hypoxic but not in normoxic tumor cells(55, 56). The authors explained these observations as consequence of the PG domain of the CA protein, which is open under hypoxic and closes under normoxic conditions. Although higher FC531 doses were used in primary AML cells, the anti-leukemic activity of all three dual CA IX/ XII inhibitors at 21% O₂ was surprising. One potential explanation to reconcile this finding is that primary AML cells might retain the hypoxic signature acquired in the O₂ deprived BM niche, thereby preserving their susceptibility to dual CA IX/ XII inhibition even under normoxic conditions. Similar findings were observed by Msaki et al., who found that disseminated tumor cell (DTC) tumors with a predilection to the hematopoietic stem cell niche displayed a distinctive hypoxic phenotype that was maintained after 2-4 ex vivo passages under normoxic conditions(57). This behavior indicates that at least in primary cells, the hypoxic signature is maintained by intrinsic features of the leukemic blasts (e.g. through long term epigenetic activation of hypoxia regulated genes), whereas in established cell lines, such as the Molm14 cells, which have been in culture for decades and are thus well adapted to standard culture conditions, the hypoxic phenotype can be imposed by the O₂-deprived environment and is lost when these cells are cultured in ambient air. The significantly decreased tumor burden and improved survival of PDX mice in the single agent and combined treatment arm indicates that FC531 might potentially have a curative effect in AML. Importantly, FC531 treated animals showed minimal to no side effects, which strongly suggests that higher doses and longer treatment courses (e.g. maintenance therapy) might be tolerated in the clinical setting. In support of this concept, a first in human Phase 1 study of SLC-0111 in patients with advanced solid tumors demonstrated excellent safety and tolerability(54). No dose limiting toxicities were reported at doses \leq 1,000mg/d administered over a course of 28 days per treatment cycle. In conclusion, our preclinical data indicates that FC531 should be evaluated in clinical trials to assess its activity and toxicity in patients with AML. Despite multiple several new drug approvals in AML since 2017, most agents are available to a subset of patients only(2). In addition, hypoxia-targeted strategies have largely been disappointing to date. For example, a phase 1/2 study of the hypoxia-activated prodrug in R/R AML only showed modest activity as reported by *Konopleva et al.*. In their study, only one patient achieved a

complete response. PR-104 was associated with higher-grade adverse events and one case of sepsis and death(29). While the study by Konopleva et al. clearly provide support for the further evaluation of hypoxia-targeted strategies, the authors acknowledged that PR-104 was associated with severe toxicity against hematopoietic stem and progenitor cells. Several clinical trials of PR-104 have been terminated (e.g. NCT00544674, NCT00862082, NCT00862134), in part due to the low probability of clinically significant results and/or toxicity. The unique mechanism of action of FC531 along with its tolerability suggests that this drug will be a suitable combination partner with traditional and recently approved agents, helping to target residual AML cells hiding in O₂ deprived niches, thereby decreasing the risk of disease relapse and increasing the chances of a cure.

Acknowledgement

This work was supported in part by the Leukemia & Lymphoma Society (LLS) New Idea Award # 8006-17 to and the IU Simon Comprehensive Cancer Center/Walther Cancer Foundation via an Oncology Physical Sciences & Engineering Research Embedding Program Award (to HK).

Conflict of interest: The authors confirm that there are no conflicts of interest.

References

1. Dohner H, Weisdorf DJ, Bloomfield CD. Acute Myeloid Leukemia. *N Engl J Med.* 2015;373(12):1136-52.
2. Green SD, Konig H. Treatment of Acute Myeloid Leukemia in the Era of Genomics-Achievements and Persisting Challenges. *Front Genet.* 2020;11:480.
3. Paietta E. Minimal residual disease in acute myeloid leukemia: coming of age. *Hematology Am Soc Hematol Educ Program.* 2012;2012:35-42.
4. Zhou HS, Carter BZ, Andreeff M. Bone marrow niche-mediated survival of leukemia stem cells in acute myeloid leukemia: Yin and Yang. *Cancer Biol Med.* 2016;13(2):248-59.
5. Nombela-Arrieta C, Pivarnik G, Winkel B, Canty KJ, Harley B, Mahoney JE, et al. Quantitative imaging of haematopoietic stem and progenitor cell localization and hypoxic status in the bone marrow microenvironment. *Nat Cell Biol.* 2013;15(5):533-43.

6. Nombela-Arrieta C, Silberstein LE. The science behind the hypoxic niche of hematopoietic stem and progenitors. *Hematology Am Soc Hematol Educ Program*. 2014;2014(1):542-7.
7. Mohyeldin A, Garzon-Muvdi T, Quinones-Hinojosa A. Oxygen in stem cell biology: a critical component of the stem cell niche. *Cell Stem Cell*. 2010;7(2):150-61.
8. Chow DC, Wenning LA, Miller WM, Papoutsakis ET. Modeling pO₂ distributions in the bone marrow hematopoietic compartment. II. Modified Kroghian models. *Biophys J*. 2001;81(2):685-96.
9. Spencer JA, Ferraro F, Roussakis E, Klein A, Wu J, Runnels JM, et al. Direct measurement of local oxygen concentration in the bone marrow of live animals. *Nature*. 2014;508(7495):269-73.
10. Xia Y, Choi HK, Lee K. Recent advances in hypoxia-inducible factor (HIF)-1 inhibitors. *Eur J Med Chem*. 2012;49:24-40.
11. Ma Z, Xiang X, Li S, Xie P, Gong Q, Goh BC, et al. Targeting hypoxia-inducible factor-1, for cancer treatment: Recent advances in developing small-molecule inhibitors from natural compounds. *Semin Cancer Biol*. 2020.
12. Benito J, Zeng Z, Konopleva M, Wilson WR. Targeting hypoxia in the leukemia microenvironment. *Int J Hematol Oncol*. 2013;2(4):279-88.
13. Konopleva M, Tabe Y, Zeng Z, Andreeff M. Therapeutic targeting of microenvironmental interactions in leukemia: mechanisms and approaches. *Drug Resist Updat*. 2009;12(4-5):103-13.
14. Rashidi A, DiPersio JF. Targeting the leukemia-stroma interaction in acute myeloid leukemia: rationale and latest evidence. *Ther Adv Hematol*. 2016;7(1):40-51.
15. Kung AL, Wang S, Klco JM, Kaelin WG, Livingston DM. Suppression of tumor growth through disruption of hypoxia-inducible transcription. *Nat Med*. 2000;6(12):1335-40.
16. Carmeliet P, Dor Y, Herbert JM, Fukumura D, Brusselmans K, Dewerchin M, et al. Role of HIF-1 α in hypoxia-mediated apoptosis, cell proliferation and tumour angiogenesis. *Nature*. 1998;394(6692):485-90.
17. Blouw B, Song H, Tihan T, Bosze J, Ferrara N, Gerber HP, et al. The hypoxic response of tumors is dependent on their microenvironment. *Cancer Cell*. 2003;4(2):133-46.

18. Vukovic M, Guitart AV, Sepulveda C, Villacreces A, O'Duibhir E, Panagopoulou TI, et al. Hif-1alpha and Hif-2alpha synergize to suppress AML development but are dispensable for disease maintenance. *J Exp Med*. 2015;212(13):2223-34.
19. Kopecka J, Campia I, Jacobs A, Frei AP, Ghigo D, Wollscheid B, et al. Carbonic anhydrase XII is a new therapeutic target to overcome chemoresistance in cancer cells. *Oncotarget*. 2015;6(9):6776-93.
20. Logsdon DP, Shah F, Carta F, Supuran CT, Kamocka M, Jacobsen MH, et al. Blocking HIF signaling via novel inhibitors of CA9 and APE1/Ref-1 dramatically affects pancreatic cancer cell survival. *Sci Rep*. 2018;8(1):13759.
21. Lou Y, McDonald PC, Oloumi A, Chia S, Ostlund C, Ahmadi A, et al. Targeting tumor hypoxia: suppression of breast tumor growth and metastasis by novel carbonic anhydrase IX inhibitors. *Cancer Res*. 2011;71(9):3364-76.
22. Pacchiano F, Carta F, McDonald PC, Lou Y, Vullo D, Scozzafava A, et al. Ureido-substituted benzenesulfonamides potently inhibit carbonic anhydrase IX and show antimetastatic activity in a model of breast cancer metastasis. *J Med Chem*. 2011;54(6):1896-902.
23. Mboge MY, Mahon BP, McKenna R, Frost SC. Carbonic Anhydrases: Role in pH Control and Cancer. *Metabolites*. 2018;8(1).
24. Swietach P, Vaughan-Jones RD, Harris AL. Regulation of tumor pH and the role of carbonic anhydrase 9. *Cancer Metastasis Rev*. 2007;26(2):299-310.
25. Supuran CT. Inhibition of carbonic anhydrase IX as a novel anticancer mechanism. *World J Clin Oncol*. 2012;3(7):98-103.
26. Supuran CT, Winum JY. Carbonic anhydrase IX inhibitors in cancer therapy: an update. *Future Med Chem*. 2015;7(11):1407-14.
27. Dubois L, Peeters SG, van Kuijk SJ, Yaromina A, Lieuwes NG, Saraya R, et al. Targeting carbonic anhydrase IX by nitroimidazole based sulfamides enhances the therapeutic effect of tumor irradiation: a new concept of dual targeting drugs. *Radiother Oncol*. 2013;108(3):523-8.
28. Duivenvoorden WC, Hopmans SN, Gallino D, Farrell T, Gerdes C, Glennie D, et al. Inhibition of carbonic anhydrase IX (CA9) sensitizes renal cell carcinoma to ionizing radiation. *Oncol Rep*. 2015;34(4):1968-76.

29. Konopleva M, Thall PF, Yi CA, Borthakur G, Covelev A, Bueso-Ramos C, et al. Phase I/II study of the hypoxia-activated prodrug PR104 in refractory/relapsed acute myeloid leukemia and acute lymphoblastic leukemia. *Haematologica*. 2015;100(7):927-34.
30. Viikila P, Kivela AJ, Mustonen H, Koskensalo S, Waheed A, Sly WS, et al. Carbonic anhydrase enzymes II, VII, IX and XII in colorectal carcinomas. *World J Gastroenterol*. 2016;22(36):8168-77.
31. Chien MH, Ying TH, Hsieh YH, Lin CH, Shih CH, Wei LH, et al. Tumor-associated carbonic anhydrase XII is linked to the growth of primary oral squamous cell carcinoma and its poor prognosis. *Oral Oncol*. 2012;48(5):417-23.
32. Ilie MI, Hofman V, Ortholan C, Ammadi RE, Bonnetaud C, Havet K, et al. Overexpression of carbonic anhydrase XII in tissues from resectable non-small cell lung cancers is a biomarker of good prognosis. *Int J Cancer*. 2011;128(7):1614-23.
33. Chen Z, Ai L, Mboge MY, Tu C, McKenna R, Brown KD, et al. Differential expression and function of CAIX and CAXII in breast cancer: A comparison between tumorgraft models and cells. *PLoS One*. 2018;13(7):e0199476.
34. Lounnas N, Rosilio C, Nebout M, Mary D, Griessinger E, Neffati Z, et al. Pharmacological inhibition of carbonic anhydrase XII interferes with cell proliferation and induces cell apoptosis in T-cell lymphomas. *Cancer Lett*. 2013;333(1):76-88.
35. Li G, Chen TW, Nickel AC, Muhammad S, Steiger HJ, Tzaridis T, et al. Carbonic Anhydrase XII is a Clinically Significant, Molecular Tumor-Subtype Specific Therapeutic Target in Glioma with the Potential to Combat Invasion of Brain Tumor Cells. *Onco Targets Ther*. 2021;14:1707-18.
36. Hsieh MJ, Chen KS, Chiou HL, Hsieh YS. Carbonic anhydrase XII promotes invasion and migration ability of MDA-MB-231 breast cancer cells through the p38 MAPK signaling pathway. *Eur J Cell Biol*. 2010;89(8):598-606.
37. Ma J, Li X, Su Y, Zhao J, Luedtke DA, Epshteyn V, et al. Mechanisms responsible for the synergistic antileukemic interactions between ATR inhibition and cytarabine in acute myeloid leukemia cells. *Sci Rep*. 2017;7:41950.
38. Chen F, Wu X, Niculite C, Gilca M, Petrusca D, Rogozea A, et al. Classic and targeted anti-leukaemic agents interfere with the cholesterol biogenesis metagene in acute myeloid leukaemia: Therapeutic implications. *J Cell Mol Med*. 2020;24(13):7378-92.

39. Parkin B, Londono-Joshi A, Kang Q, Tewari M, Rhim AD, Malek SN. Ultrasensitive mutation detection identifies rare residual cells causing acute myelogenous leukemia relapse. *J Clin Invest*. 2017;127(9):3484-95.
40. Leppilampi M, Koistinen P, Savolainen ER, Hannuksela J, Parkkila AK, Niemela O, et al. The expression of carbonic anhydrase II in hematological malignancies. *Clin Cancer Res*. 2002;8(7):2240-5.
41. Supuran CT. Carbonic anhydrases: novel therapeutic applications for inhibitors and activators. *Nat Rev Drug Discov*. 2008;7(2):168-81.
42. Konig H, Levis M. Targeting FLT3 to treat leukemia. *Expert Opin Ther Targets*. 2015;19(1):37-54.
43. Sironi S, Wagner M, Kuett A, Drolle H, Polzer H, Spiekermann K, et al. Microenvironmental hypoxia regulates FLT3 expression and biology in AML. *Sci Rep*. 2015;5:17550.
44. Andreucci E, Ruzzolini J, Peppicelli S, Bianchini F, Laurenzana A, Carta F, et al. The carbonic anhydrase IX inhibitor SLC-0111 sensitises cancer cells to conventional chemotherapy. *J Enzyme Inhib Med Chem*. 2019;34(1):117-23.
45. Hidalgo M, Amant F, Biankin AV, Budinska E, Byrne AT, Caldas C, et al. Patient-derived xenograft models: an emerging platform for translational cancer research. *Cancer Discov*. 2014;4(9):998-1013.
46. Muz B, de la Puente P, Azab F, Azab AK. The role of hypoxia in cancer progression, angiogenesis, metastasis, and resistance to therapy. *Hypoxia (Auckl)*. 2015;3:83-92.
47. Carreau A, El Hafny-Rahbi B, Matejuk A, Grillon C, Kieda C. Why is the partial oxygen pressure of human tissues a crucial parameter? Small molecules and hypoxia. *J Cell Mol Med*. 2011;15(6):1239-53.
48. Estey E. Why Is Progress in Acute Myeloid Leukemia So Slow? *Semin Hematol*. 2015;52(3):243-8.
49. Griessinger E, Anjos-Afonso F, Pizzitola I, Rouault-Pierre K, Vargaftig J, Taussig D, et al. A niche-like culture system allowing the maintenance of primary human acute myeloid leukemia-initiating cells: a new tool to decipher their chemoresistance and self-renewal mechanisms. *Stem Cells Transl Med*. 2014;3(4):520-9.

50. Pastorekova S, Gillies RJ. The role of carbonic anhydrase IX in cancer development: links to hypoxia, acidosis, and beyond. *Cancer Metastasis Rev.* 2019;38(1-2):65-77.
51. Mujumdar P, Kopecka J, Bua S, Supuran CT, Riganti C, Poulsen SA. Carbonic Anhydrase XII Inhibitors Overcome Temozolomide Resistance in Glioblastoma. *J Med Chem.* 2019;62(8):4174-92.
52. Haapasalo J, Hilvo M, Nordfors K, Haapasalo H, Parkkila S, Hyrskyluoto A, et al. Identification of an alternatively spliced isoform of carbonic anhydrase XII in diffusely infiltrating astrocytic gliomas. *Neuro Oncol.* 2008;10(2):131-8.
53. Sowa T, Menju T, Chen-Yoshikawa TF, Takahashi K, Nishikawa S, Nakanishi T, et al. Hypoxia-inducible factor 1 promotes chemoresistance of lung cancer by inducing carbonic anhydrase IX expression. *Cancer Med.* 2017;6(1):288-97.
54. McDonald PC, Chia S, Bedard PL, Chu Q, Lyle M, Tang L, et al. A Phase 1 Study of SLC-0111, a Novel Inhibitor of Carbonic Anhydrase IX, in Patients With Advanced Solid Tumors. *Am J Clin Oncol.* 2020;43(7):484-90.
55. Svastova E, Hulikova A, Rafajova M, Zat'ovicova M, Gibadulinova A, Casini A, et al. Hypoxia activates the capacity of tumor-associated carbonic anhydrase IX to acidify extracellular pH. *FEBS Lett.* 2004;577(3):439-45.
56. Cecchi A, Hulikova A, Pastorek J, Pastorekova S, Scozzafava A, Winum JY, et al. Carbonic anhydrase inhibitors. Design of fluorescent sulfonamides as probes of tumor-associated carbonic anhydrase IX that inhibit isozyme IX-mediated acidification of hypoxic tumors. *J Med Chem.* 2005;48(15):4834-41.
57. Msaki A, Pasto A, Curtarello M, Arigoni M, Barutello G, Calogero RA, et al. A hypoxic signature marks tumors formed by disseminated tumor cells in the BALB-neuT mammary cancer model. *Oncotarget.* 2016;7(22):33081-95.

Figure legends

Figure 1: Hypoxic stress leads to the induction of CA IX and/or XII mRNA expression in AML cells. Focused quantitative RT-PCR assays for CA I, II, IX and XII were carried out in (A) a diverse panel of AML cell lines as well as (B) primary cells derived from FLT3/ITD⁺ AML

patients with newly diagnosed and relapsed/refractory disease after exposure to 21% and 1% O₂ for 48 hours. Results shown in (A) represent the mean ± SEM fold increase in mRNA expression versus the untreated control at 21% O₂ (n = 3). (B) Due to the limited availability of human tissue, primary cell culture experiments were only performed once for each patient sample.

Figure 2: CA IX and/or CA XII is expressed in Cytarabine-residual FLT3/ITD⁺ AML cells in vivo. (A) Representative tissue sections from untreated animals showed BM hypercellularity with collapse of the vascular channels, occasional small foci of normal erythroid and myeloid cells as well as few megakaryocytes. The vast majority of cells seen in the marrow consisted of large myeloid blasts filling most of the marrow space. The immunostaining for CA IX was multifocal and localized on the cell membrane. (B) Treatment of M14 xenografts with Cytarabine (12.5mg/kg BW) for 5 days led to a reduction in the leukemic burden with enhanced CA IX staining in blasts remaining after treatment with Cytarabine. (C) In untreated animals, the spleen showed marked expansion of the red pulp with large, myeloid blasts replacing most of the normal architecture. (D) In Cytarabine treatment animals, less leukemic blasts were observed in the red pulp compared to the untreated group. Similar to the findings in the BM, CA IX staining was multifocal and enhanced in blasts remaining after treatment with Cytarabine. The Positive Pixel Count algorithm on Aperio ImageScope (Leica Biosystems) was used to quantify the amount of CA IX and CA XII staining present in a scanned slide image. A range of color (range of hues and saturation) and three intensity ranges (weak, positive, and strong) were masked and evaluated. The analysis specific to this project required the exclusion of macrophages in the field of analysis. Macrophages stain intensely with CA-IX and CA-XII and were therefore excluded from the analysis. An FDA-approved algorithm was used to distinguish between brown and blue pixels. Corresponding H&E stained sections from the BM and spleen are shown in **Supplemental Figures 2A-D**.

Figure 3: CA IX and/or CA XII is expressed in FLT3/ITD⁺ AML patients failing induction chemotherapy. CA IX and XII staining of BM samples from patients with FLT3 mutated AML (n=4) who had residual disease on day 14 (pt#12, J-L) or day 21 (pt#9-11, A-I) marrow assessment. Consistent with data obtained from M14 xenograft studies, 4 out of 4 patients showed increased CA IX and/or CA XII staining in leukemic blasts remaining after induction

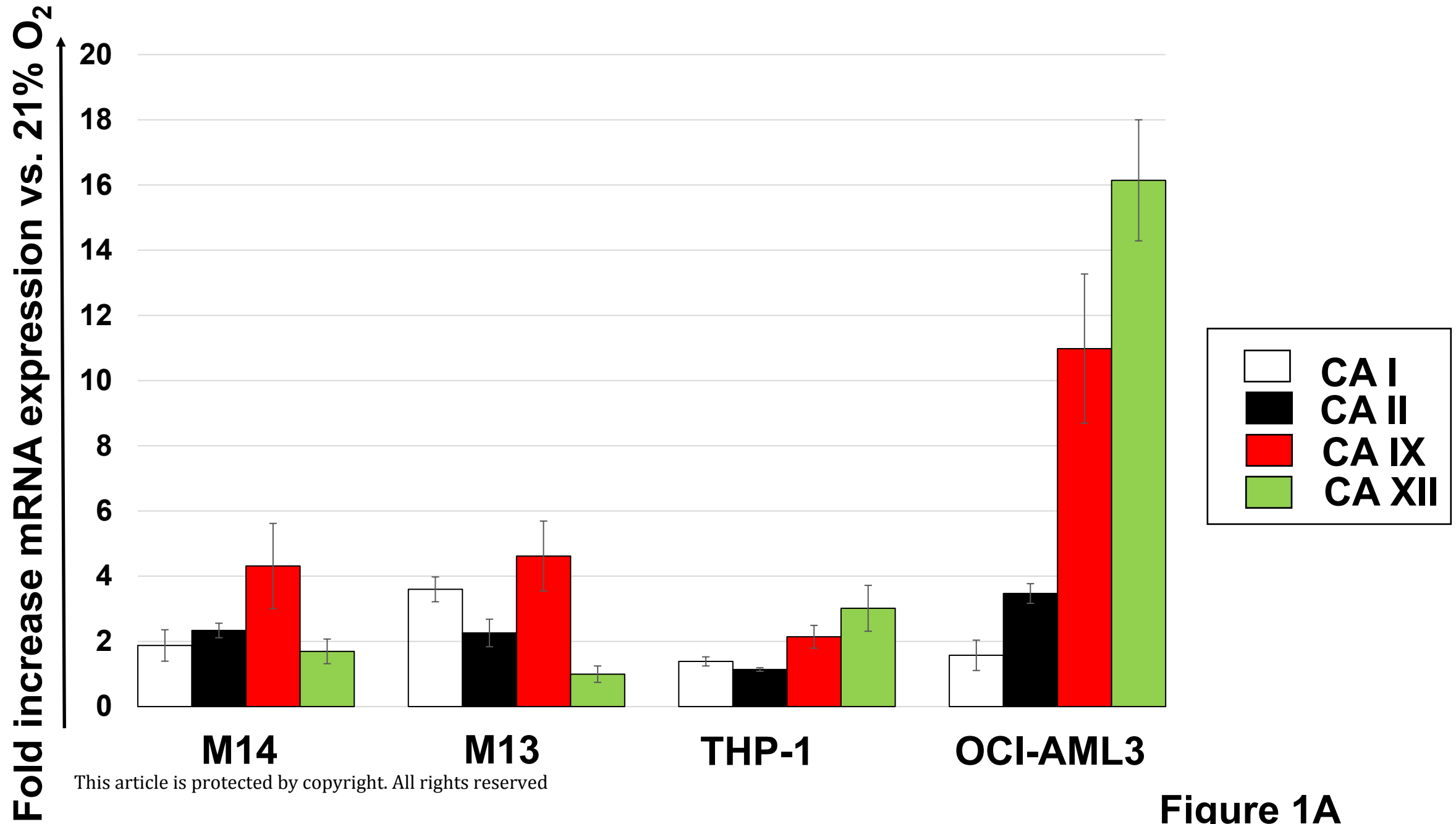
chemotherapy. Pts #9-11 were treated with an induction regimen consisting of “7+3” combined with the FLT3 inhibitor midostaurin. Pt #12 received induction chemotherapy with “7+3” only as treatment occurred prior to the approval of midostaurin. Results shown represent the mean \pm SEM % CA IX or XII positivity. Statistically significant changes in the percentage of CA staining are indicated (* $<$.05; ** $p <$.01; *** $p <$.001). Leukemic blast cell percentages were quantified per clinical flow cytometric immunophenotyping by the Indiana University Health Pathology Laboratory. Corresponding H&E stained sections from the BM are shown in **Supplemental Figures 3A-H**.

Figure 4: Dual inhibition of CA IX and XII in FLT3/ITD⁺ AML cells leads to intracellular acidification, induction of apoptosis and differentiation under hypoxic conditions. The dual CA IX/ XII inhibitors FC531, CA912 and SLC0111 confer growth inhibitory effects under ambient air and hypoxic cell culture conditions in newly diagnosed (New Dx) (A, B) and relapsed/refractory (C, D) primary AML patient samples. FC531-, CA912- and SLC-0111-induced growth inhibition occurred in a dose dependent fashion and was significantly greater than in response to clinically achievable concentrations of Cytarabine and Quizartinib, which only had mild to no effects in the high and low O₂ setting. Cells were incubated in the presence of Cytarabine, Quizartinib or dual CA IX/ XII inhibitors under 21% or 1% O₂ for 48h. Growth inhibition was assessed using MTT cell viability assays. The mean \pm SEM is based on replicate experiments (n = 5-6 [ND]), n=3 [R/R]). Statistically significant changes in the percentage of growth inhibition are indicated (* or † $p <$.05; ** or †† $p <$.01; *** or ††† $p <$.001). (E) Dual CA IX/ XII targeting with FC531 acidifies the intracellular pH in M14 cells in a dose dependent manner under hypoxic but not under ambient air conditions. The mean \pm SEM is based on replicate experiments (n = 3). Statistically significant changes in intracellular acidification are indicated (** $p <$.01; *** $p <$.001). (F) FC531 induces apoptosis in M14 cells at 1% O₂ and is significantly more effective than Cytarabine in this respect. Apoptosis was analyzed by FACS as the percentage of cells positively labeled by Annexin V-PE. The mean \pm SEM is based on replicate experiments (n = 3). Statistically significant changes in apoptosis induction (fold increase) are indicated (** $p <$.01; *** $p <$.001). (G) Representative data for apoptosis of Molm14 cells are shown. (H) FC531 potently inhibits M14 cell growth under 1% but not 21%

O₂. Growth inhibition was assessed using MTT cell viability assays. The mean ± SEM is based on replicate experiments (n = 3). Statistically significant changes in the percentage of growth inhibition are indicated (* $p < .05$; ** $p < .01$). (I) Treatment of M14 cells with FC531 under hypoxic conditions results in a dose dependent increase in CD11b expression. Representative data from flow cytometric analysis (n=2) is shown.

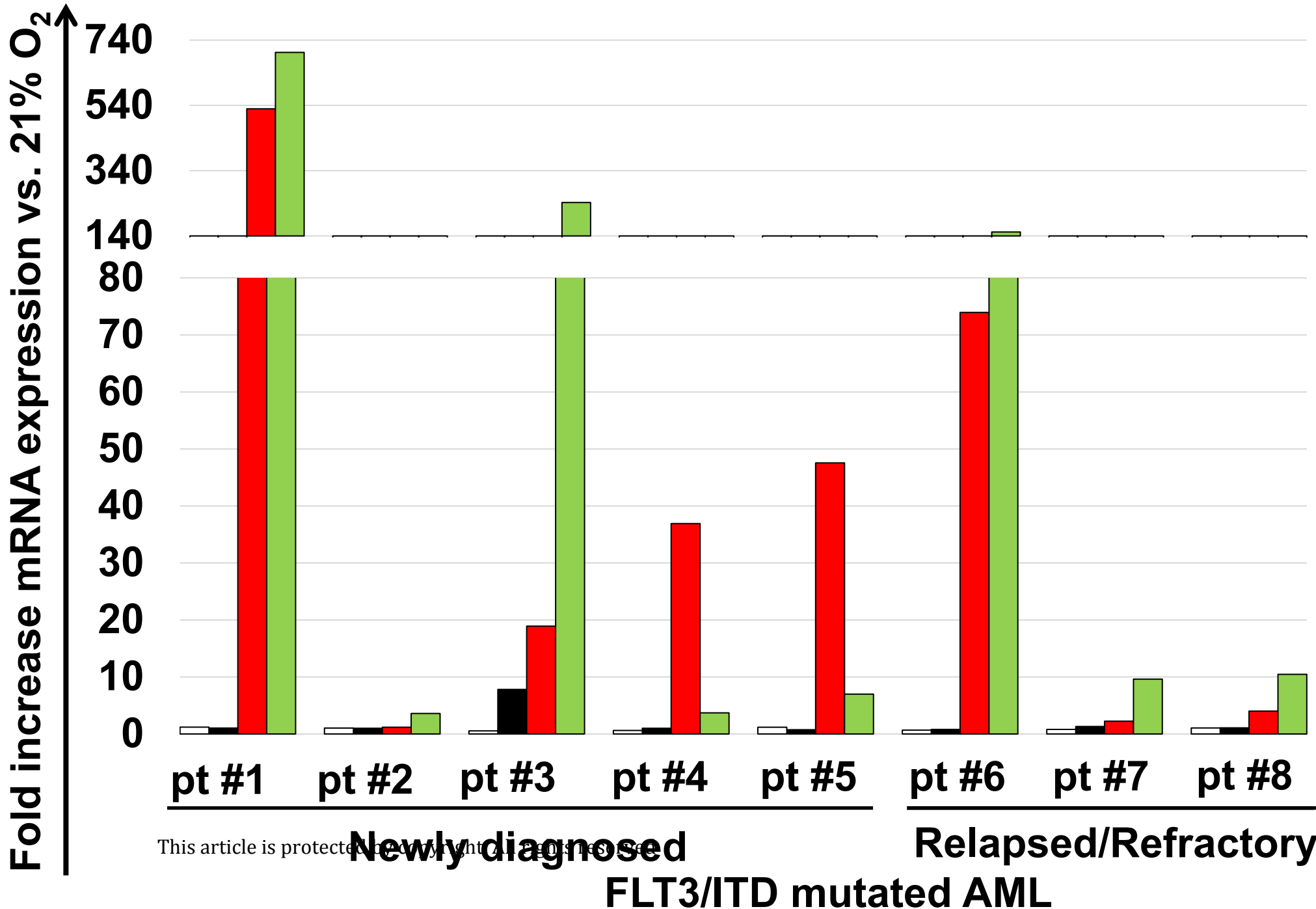
Figure 5: FC531 is well tolerated and confers anti-leukemic activity against FLT3/ITD⁺ AML cells in PDX models (JAX model J000106134). FC531 demonstrated single agent activity against AML cells in vivo as shown by a significant reduction of leukemic burden after 10 doses. Leukemic burden was assessed via (A) human (h)CD33 positivity per flow cytometry and (B) FLT3/ITD mutant drops as detected per highly sensitive ddPCR. The mean ± SEM is based on replicate experiments (n = 5). Statistically significant changes in the change of leukemic burden are indicated (** $P < .01$; *** $p < .001$). (C) Kaplan Meier analysis depicting the survival of mice treated with a 10 days course (days 1-5 and 8-12) of single agent Cytarabine, single agent FC531 or Cytarabine (days 1-5) followed by FC531 (days 8-12) (as outlined in **Table 3**). Only combined therapy resulted in statistically improved survival compared to untreated animals (p=.0018). FC531 only treated mice showed a trend towards improved survival (p=.1 vs. untreated).

Figure 6: CA IX and/or CA XII is expressed in non-FLT3 mutated AML patients failing induction chemotherapy. CA IX and XII staining of BM samples from a diverse panel of non-FLT3 mutated AML patients who had residual disease on their day 14 marrow assessment (A-O). Consistent with data obtained from AML xenograft studies, 4 out of 5 patients showed significantly increased CA IX and/or CA XII staining in leukemic blasts remaining after induction chemotherapy. All patients were treated with the “7+3” induction regimen. Results shown represent the mean ± SEM % CA IX or XII positivity. Statistically significant changes in the percentage of CA staining are indicated (* $< .05$; ** $p < .01$; *** $p < .001$). Leukemic blast cell percentages were quantified per clinical flow cytometric immunophenotyping by the Indiana University Health Pathology Laboratory. Corresponding H&E stained sections from the BM are shown in **Supplemental Figures 4A-H**.



This article is protected by copyright. All rights reserved

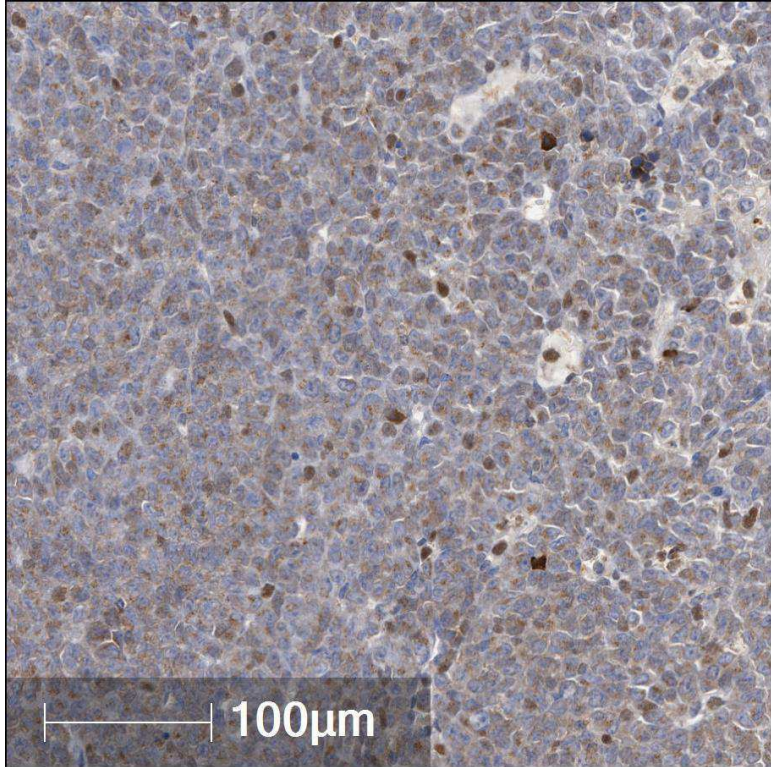
Figure 1A



This article is protected by copyright. See [https://doi.org/10.1182/blood-2018-08-858585](#)

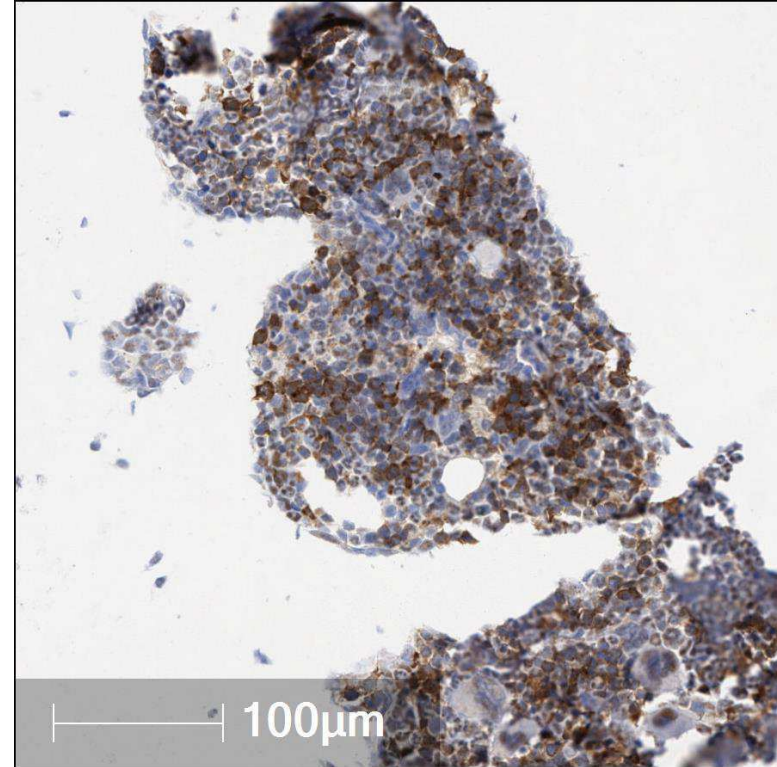
Figure 1B

A



untreated

B

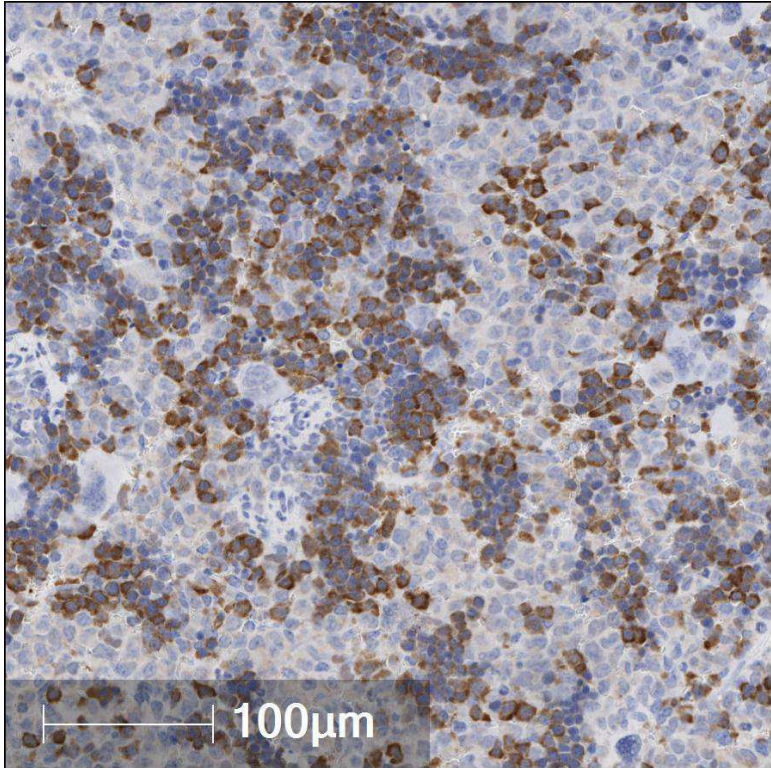


Cytarabine

Bone marrow

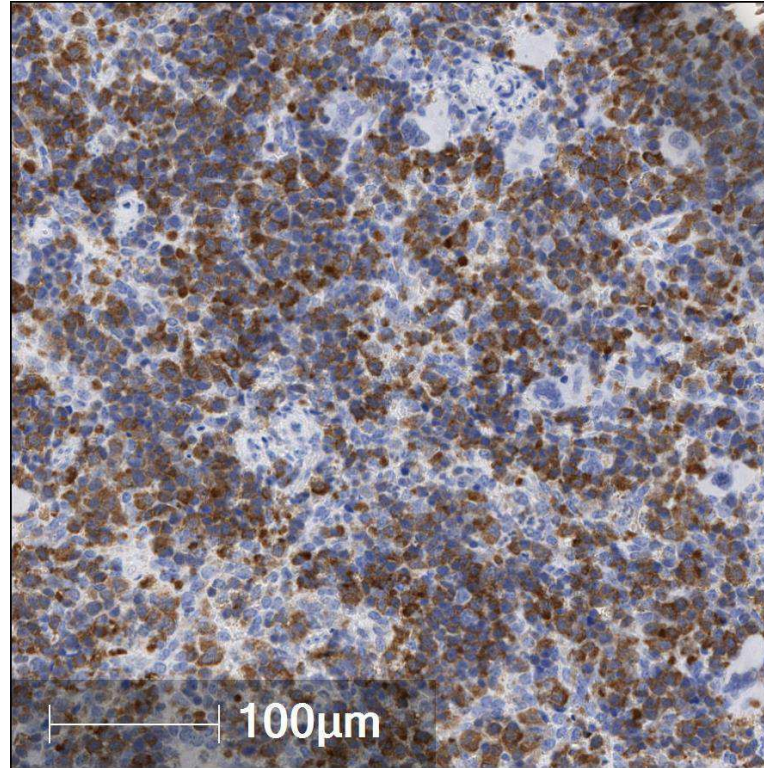
Figure 2

C



untreated

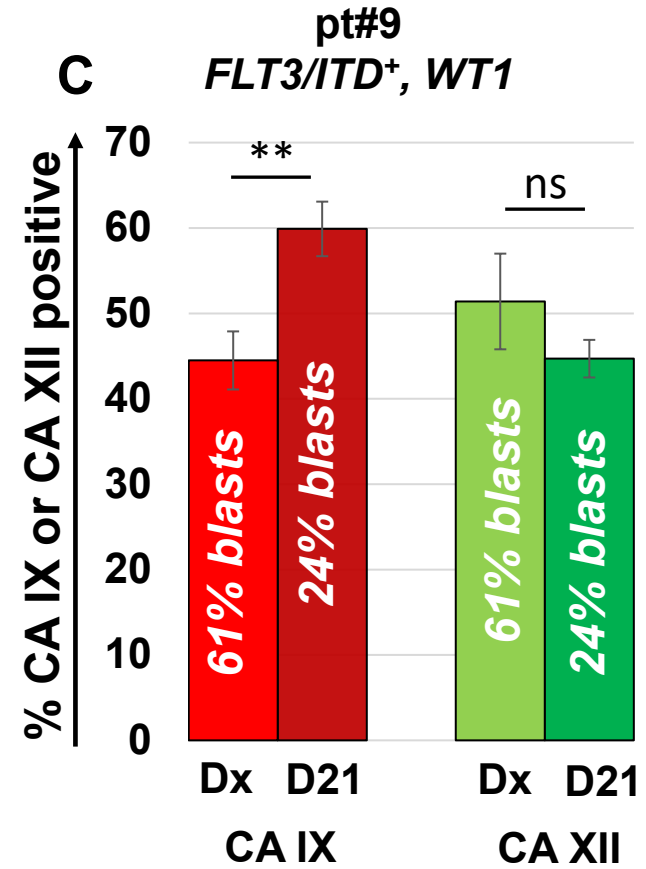
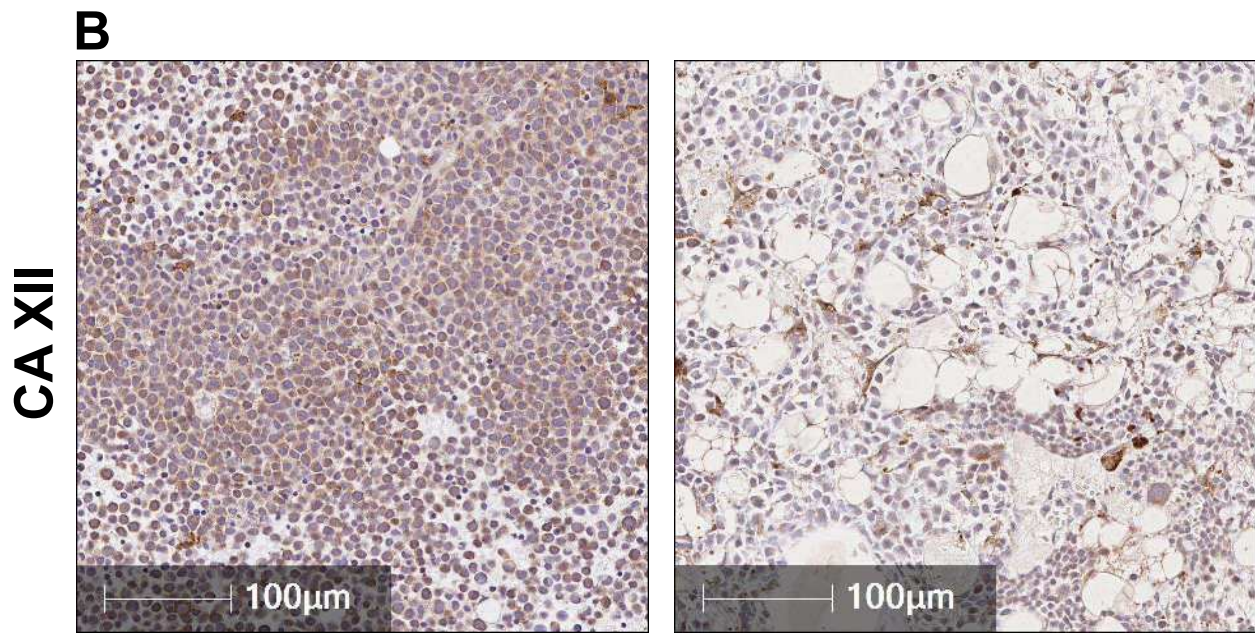
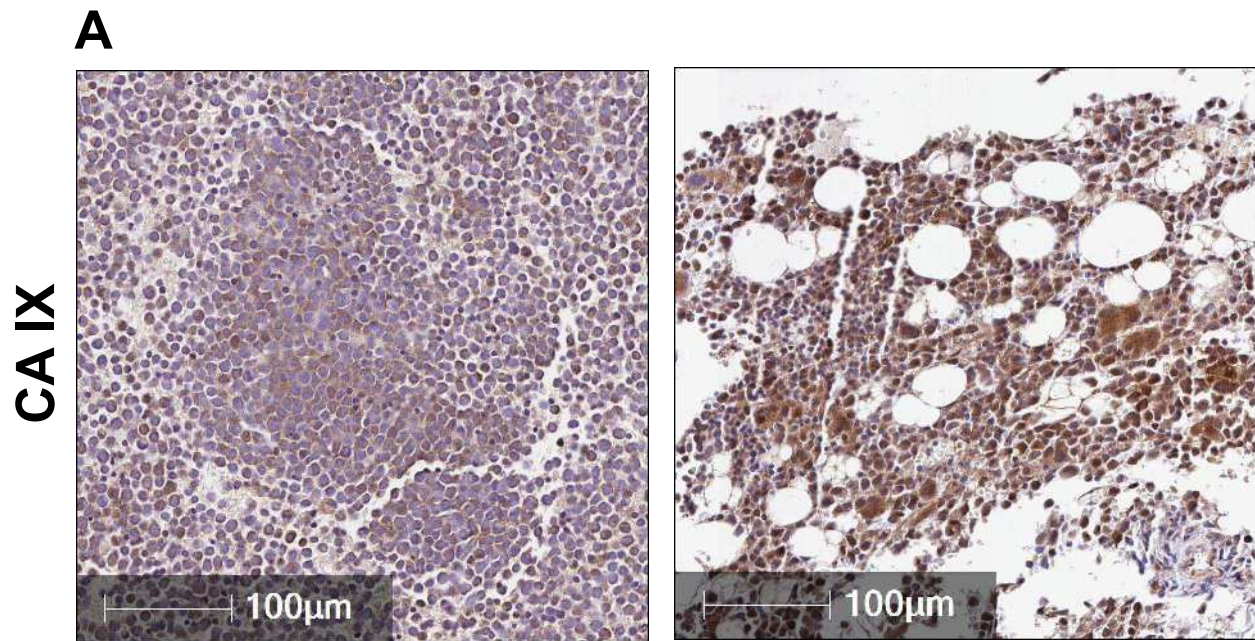
D



Cytarabine

Spleen

Figure 2



This article is protected by copyright. All rights reserved

Dx

Day 21

Figure 3

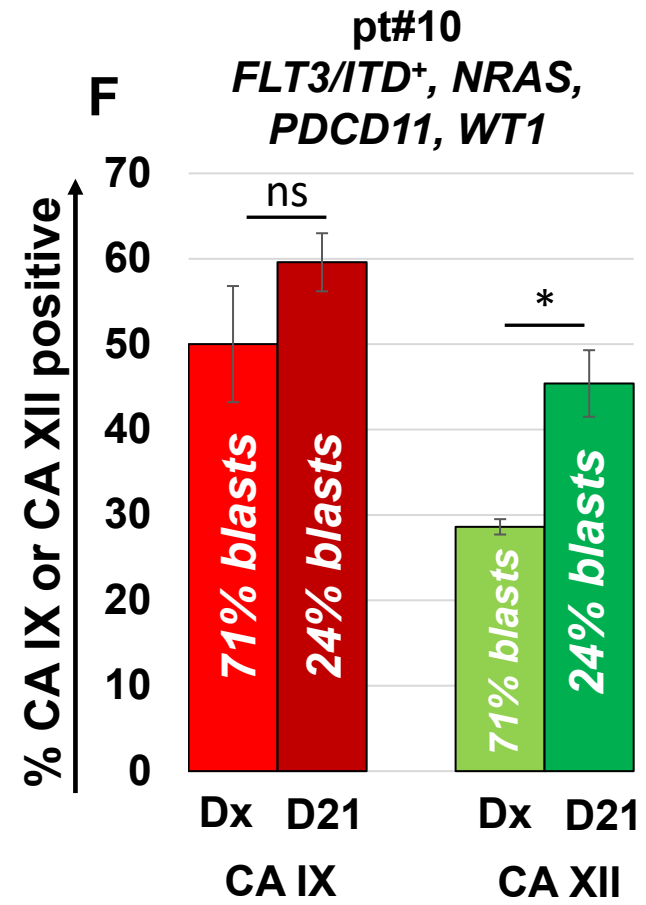
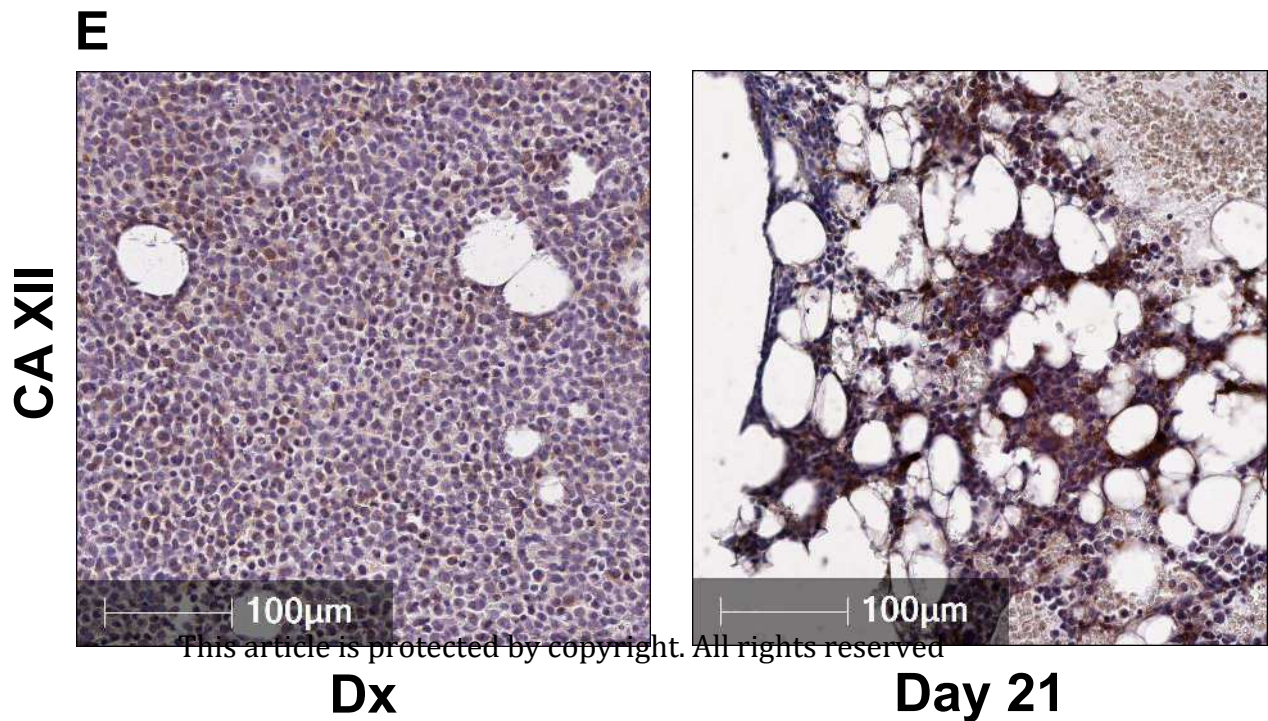
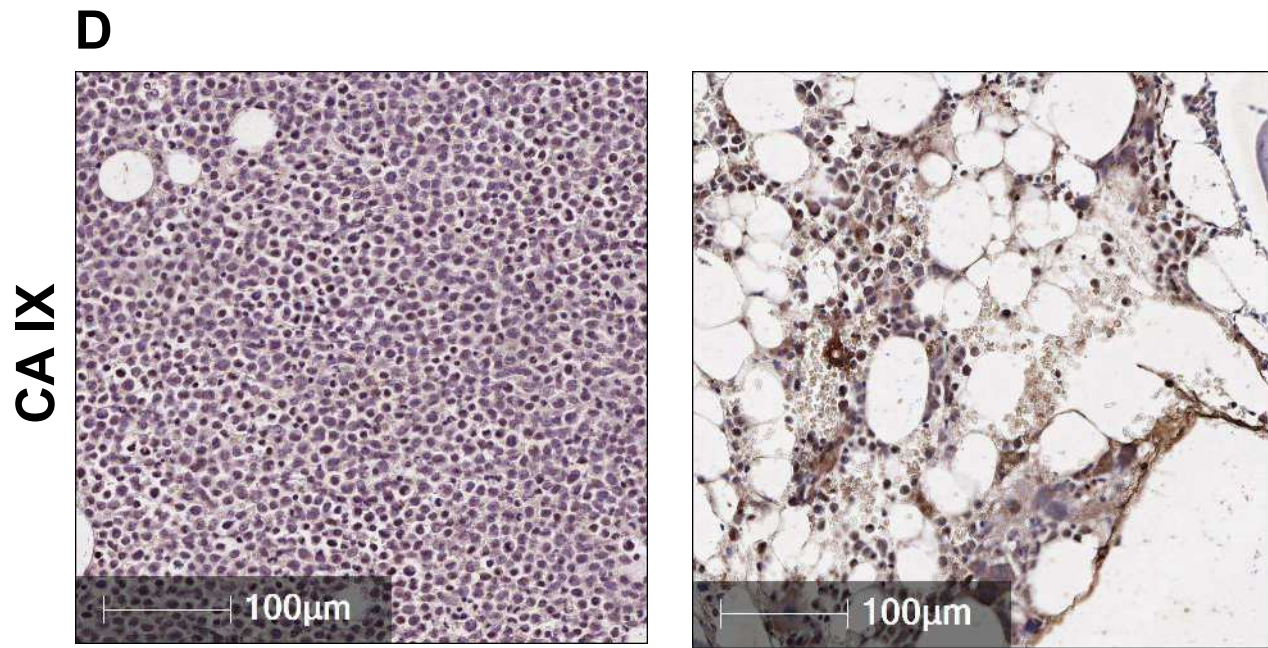
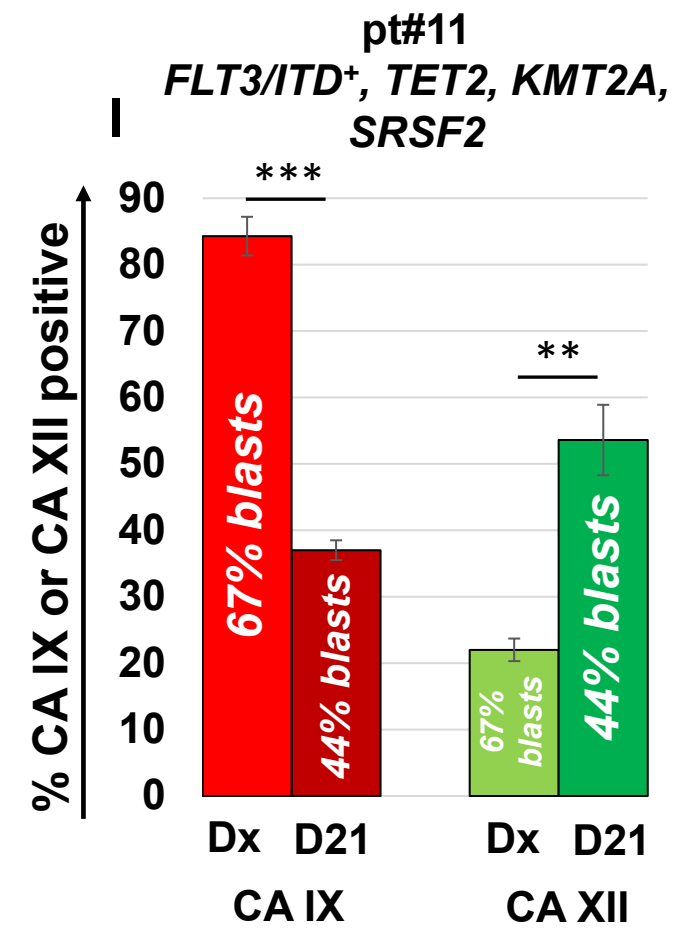
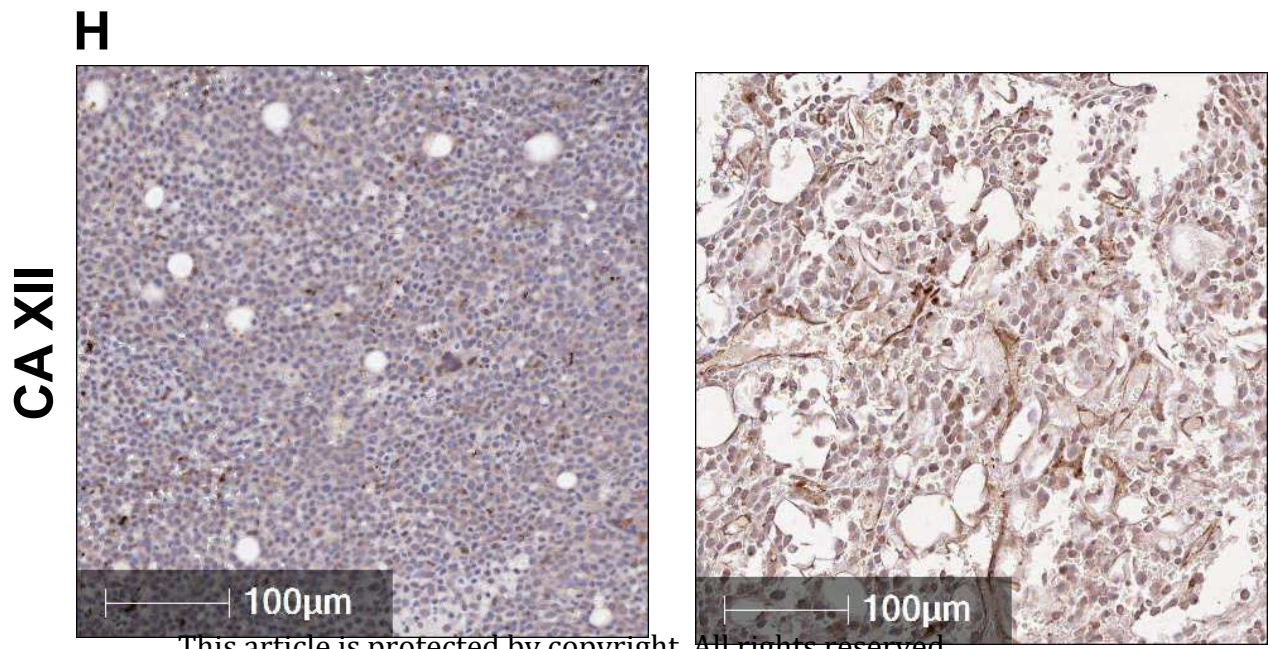
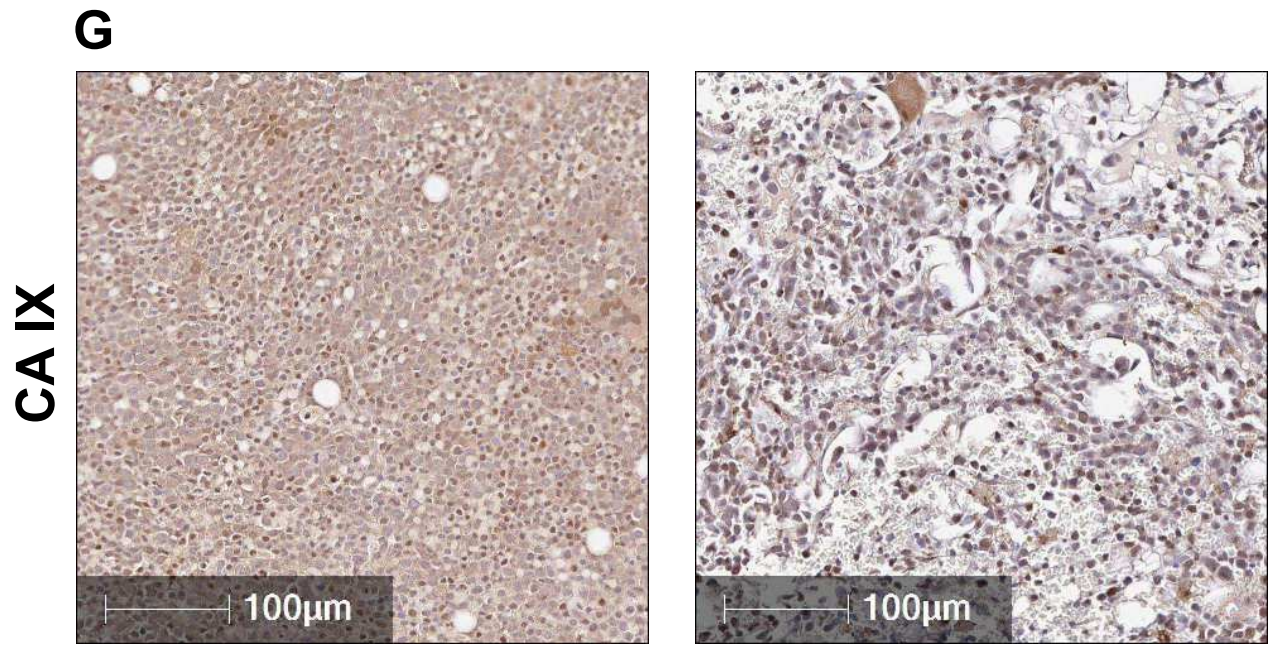


Figure 3

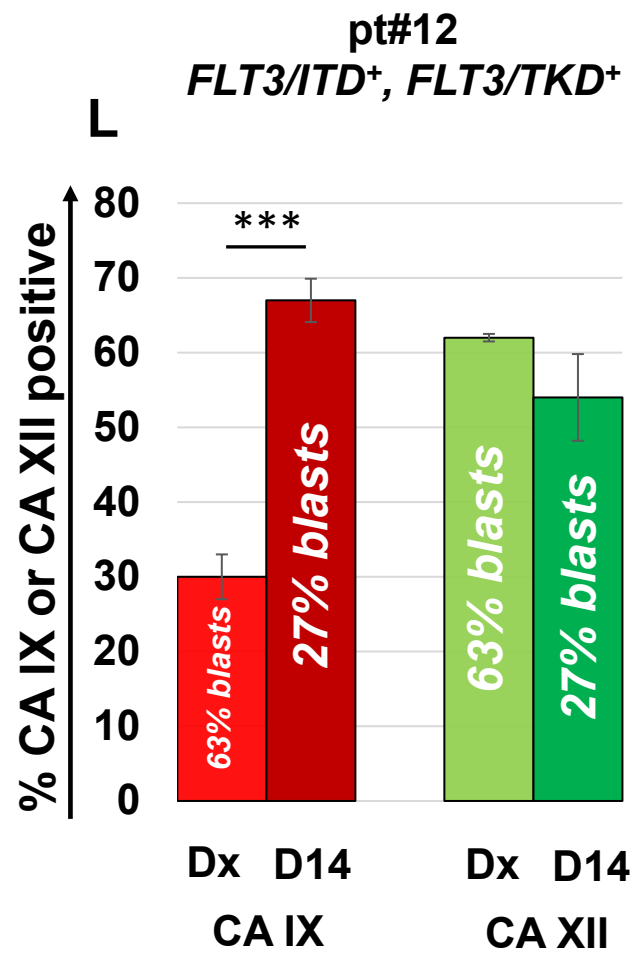
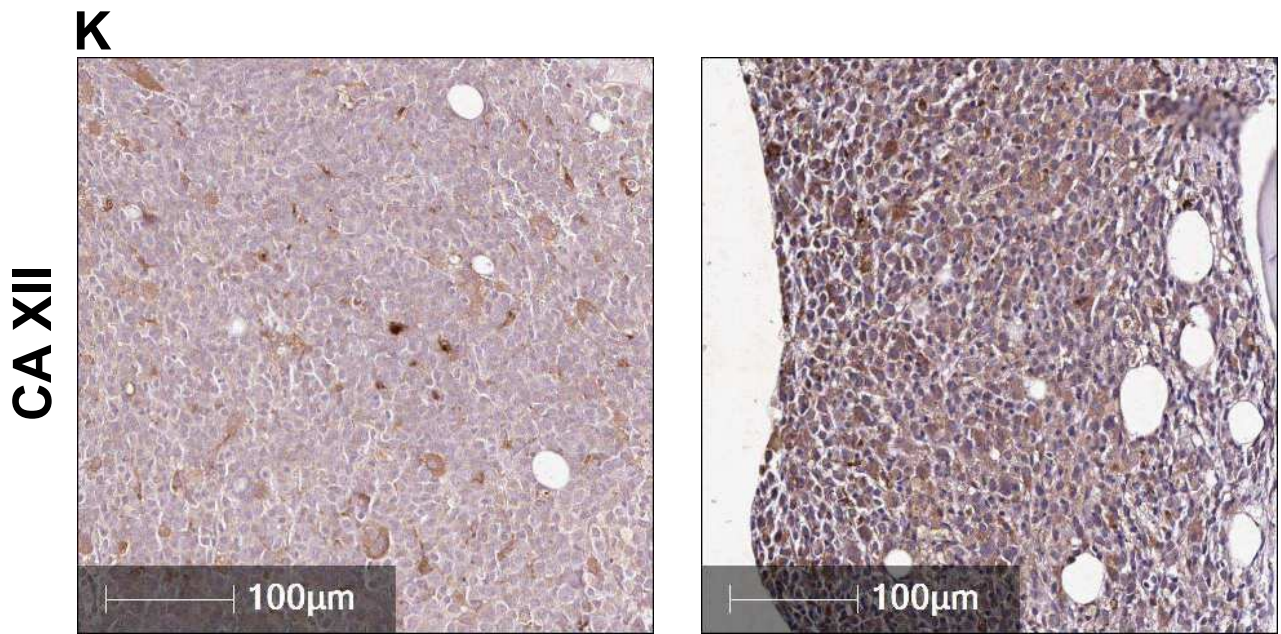
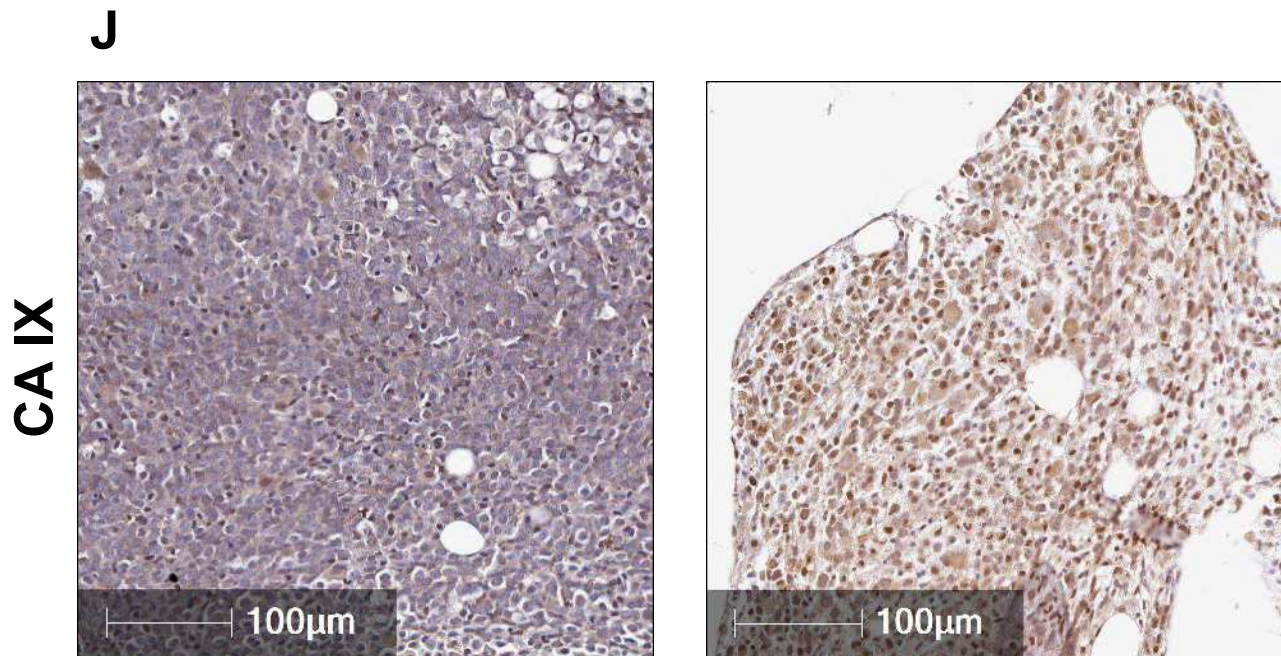


This article is protected by copyright. All rights reserved

Dx

Day 21

Figure 3



This article is protected by copyright. All rights reserved

Dx

Day 14

Figure 3

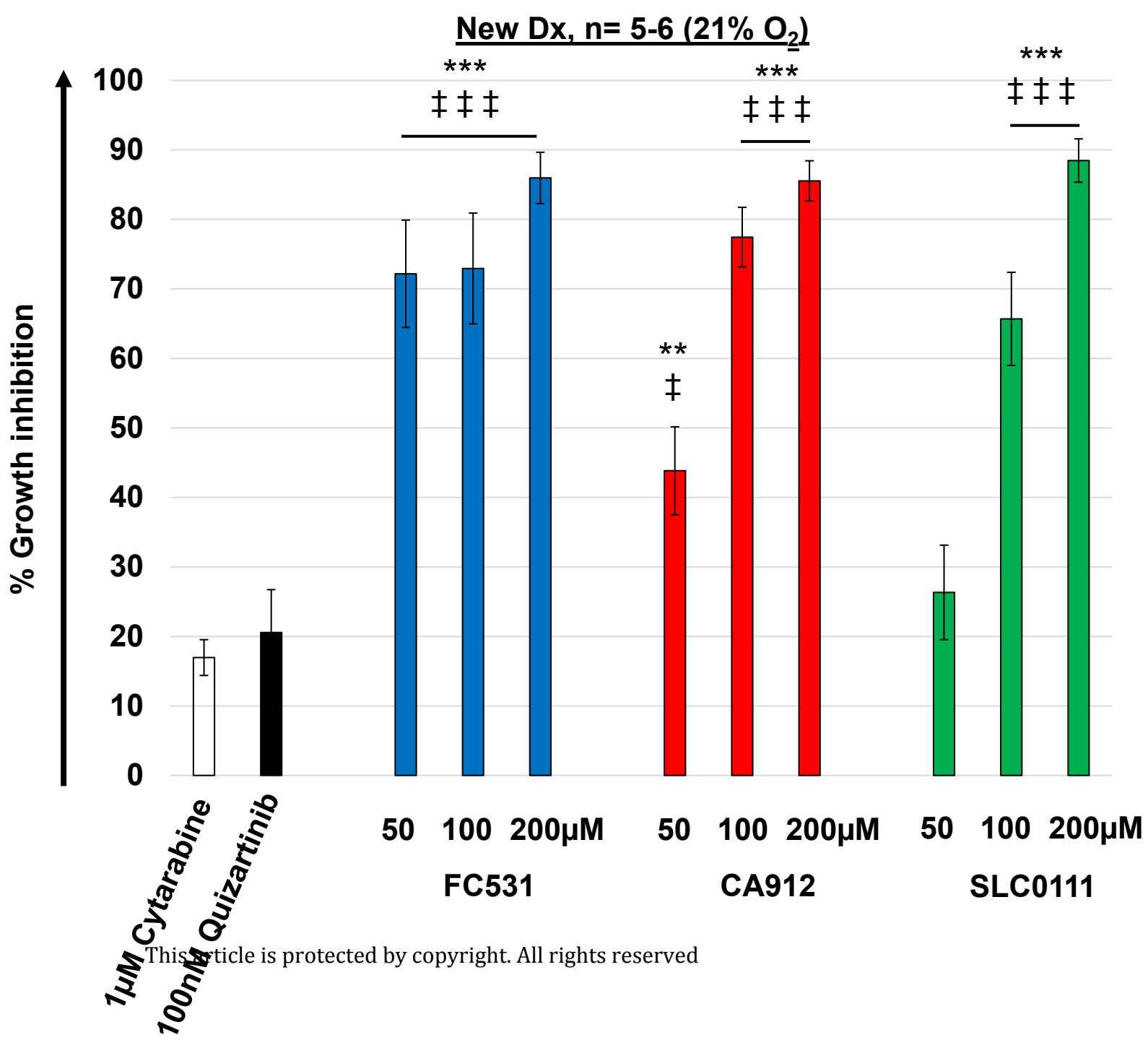
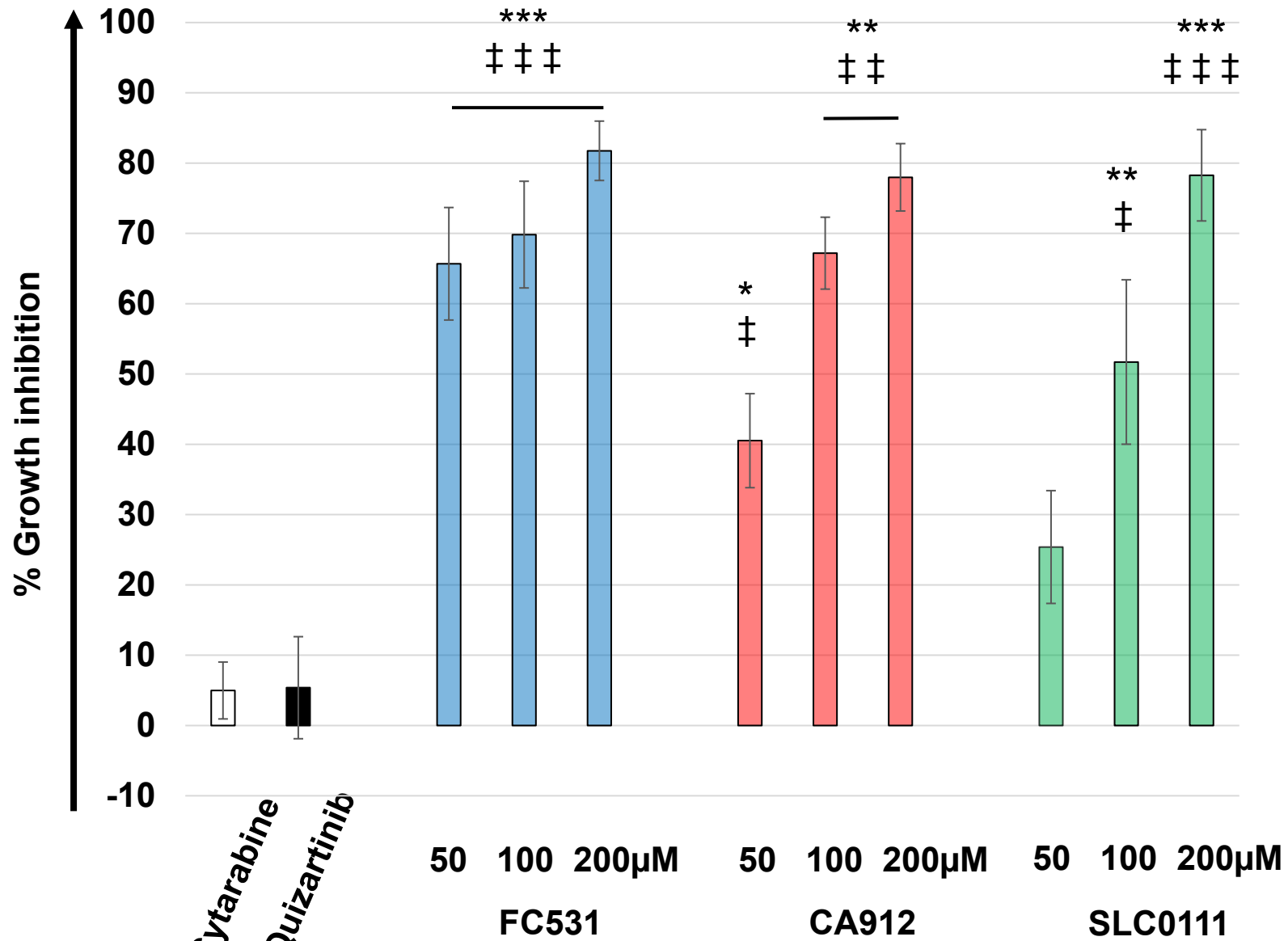


Figure 4A

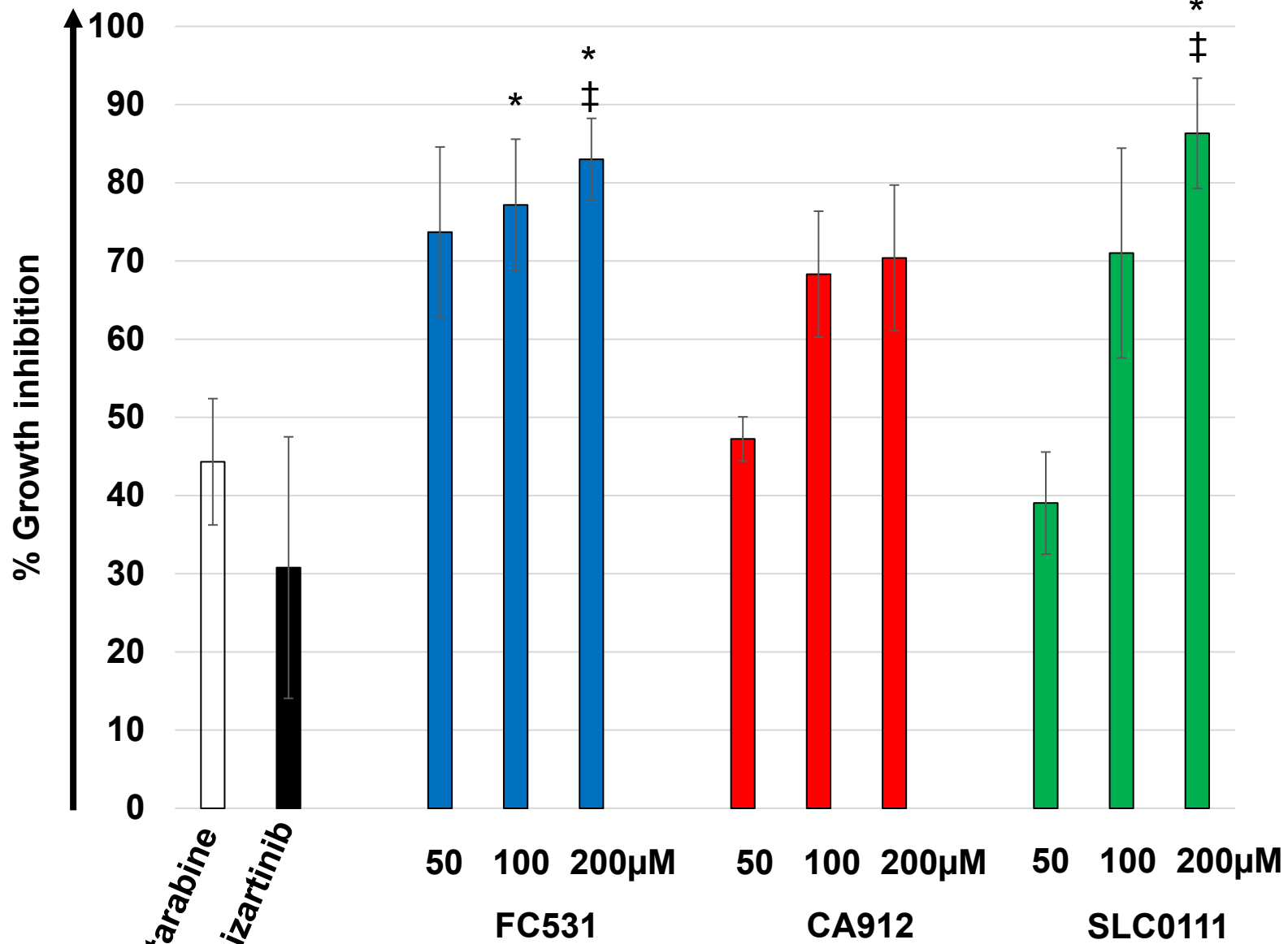
New Dx, n= 5-6 (1% O₂)



* vs. Cytarabine
‡ vs. Quizartinib

Figure 4B

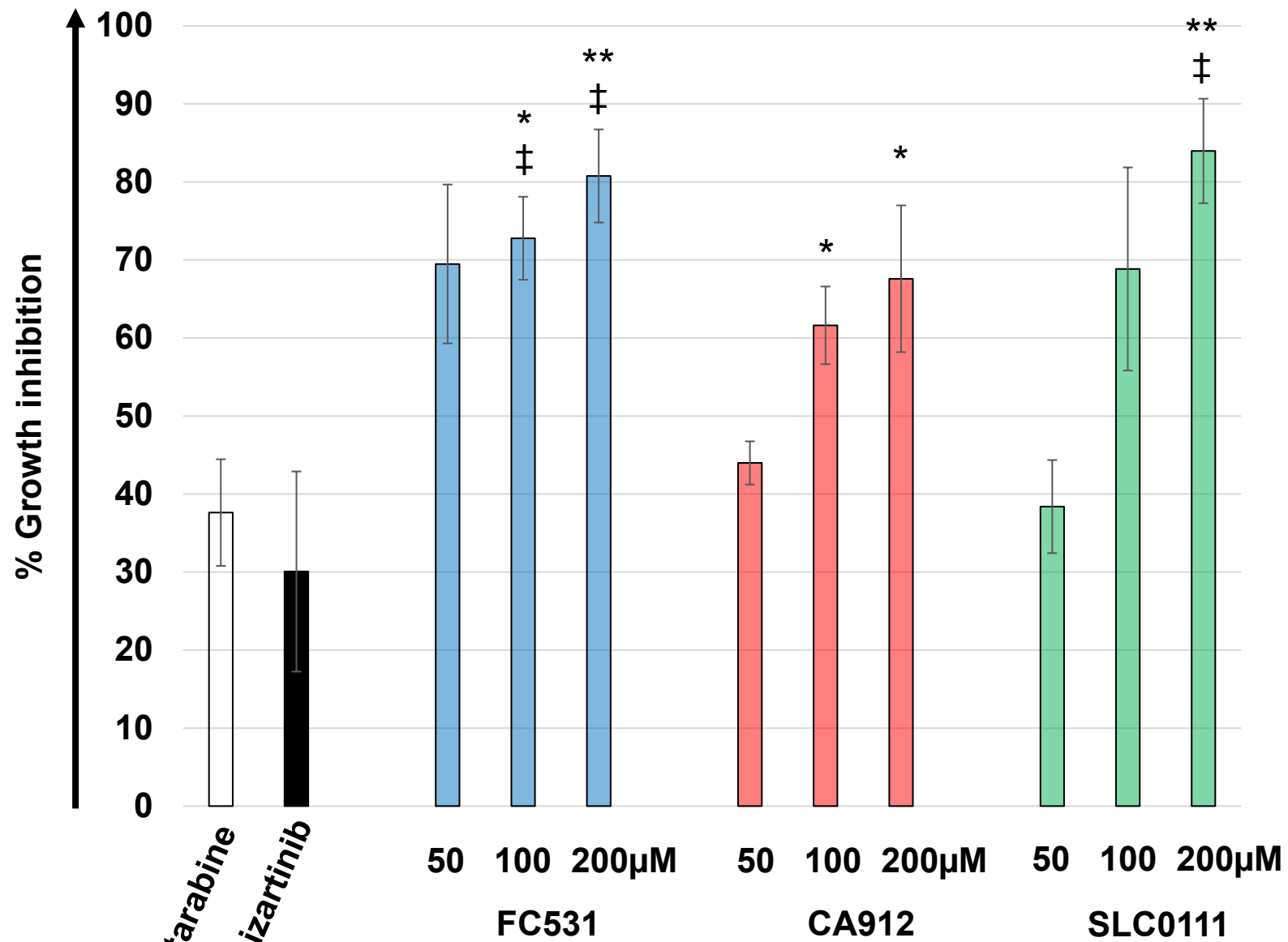
Relapsed/Refractory, n= 3 (21% O₂)



* vs. Cytarabine
‡ vs. Quizartinib

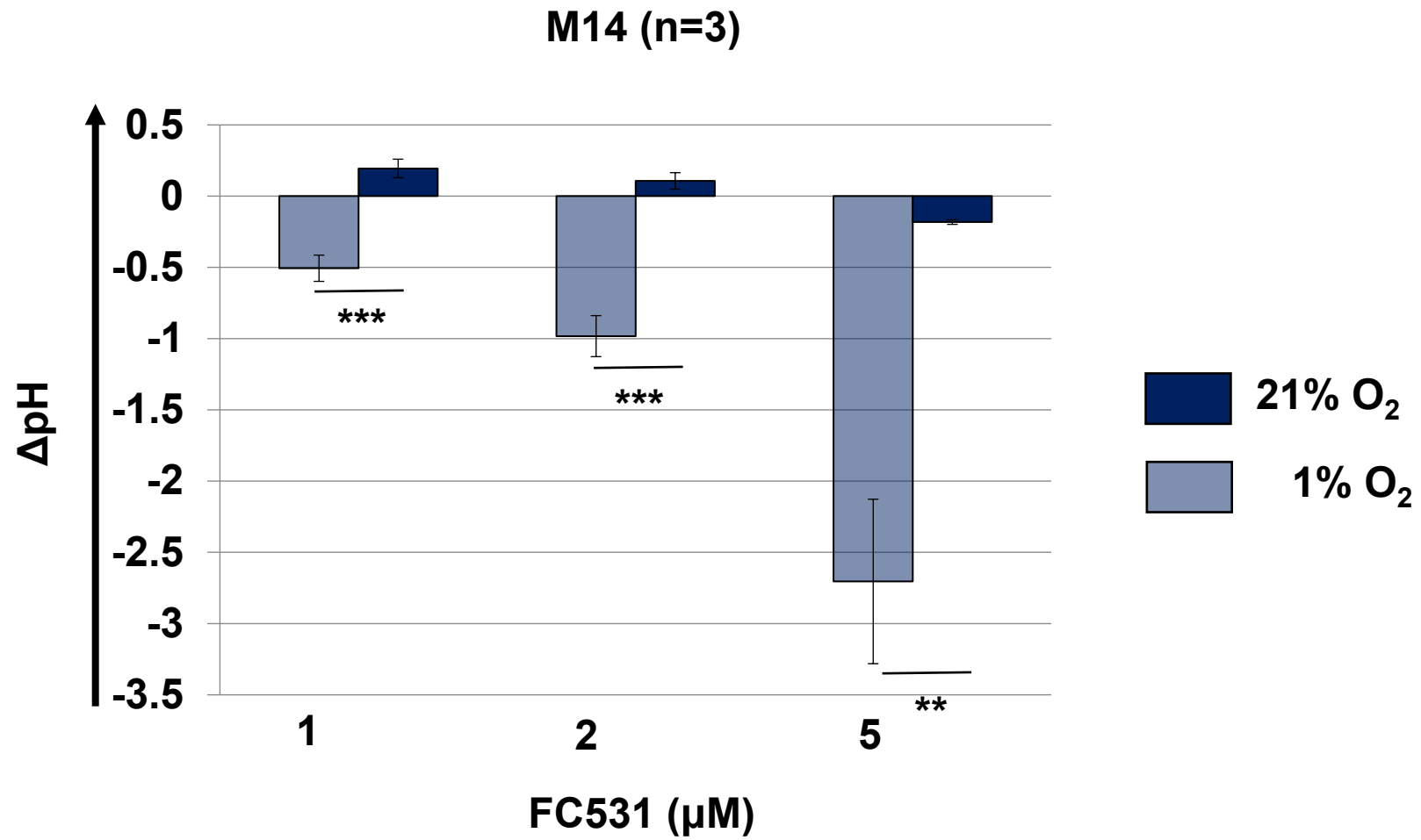
Figure 4C

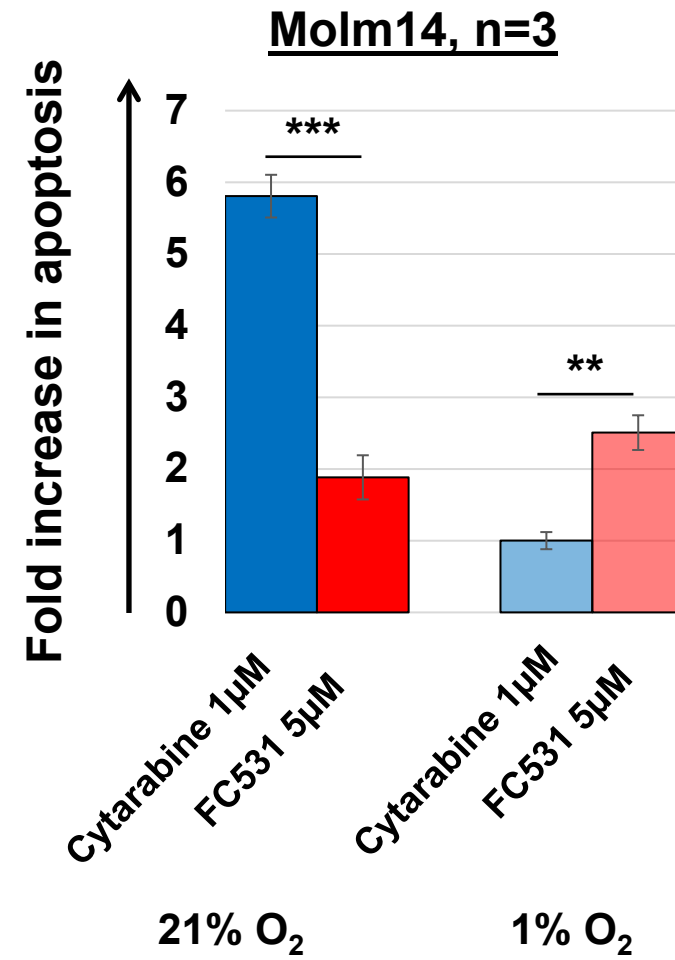
Relapsed/Refractory, n= 3 (1% O₂)



* vs. Cytarabine
† vs. Quizartinib

Figure 4D





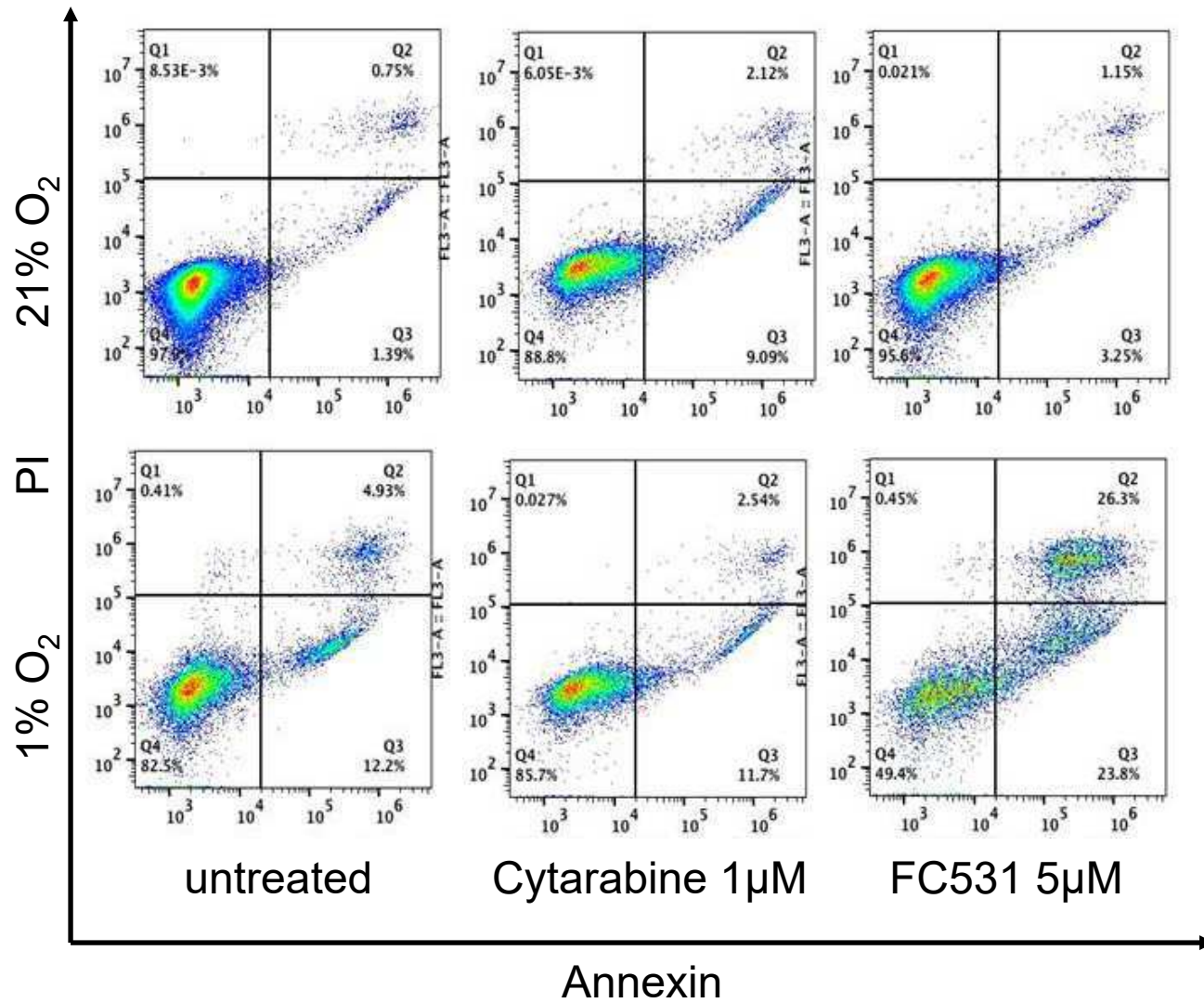


Figure 4G

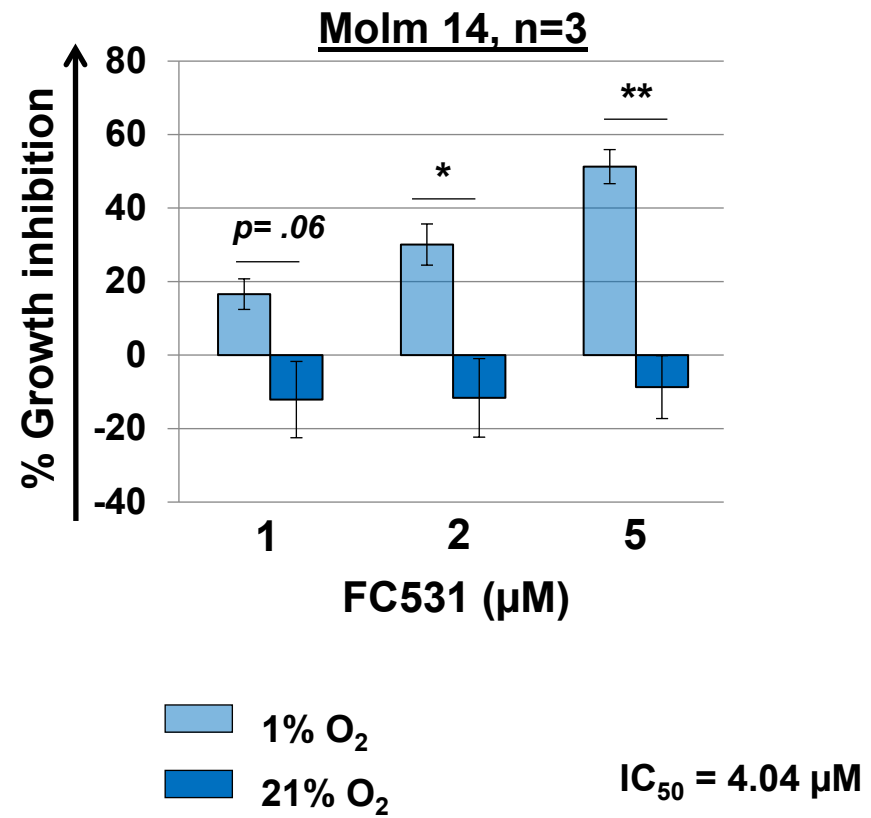
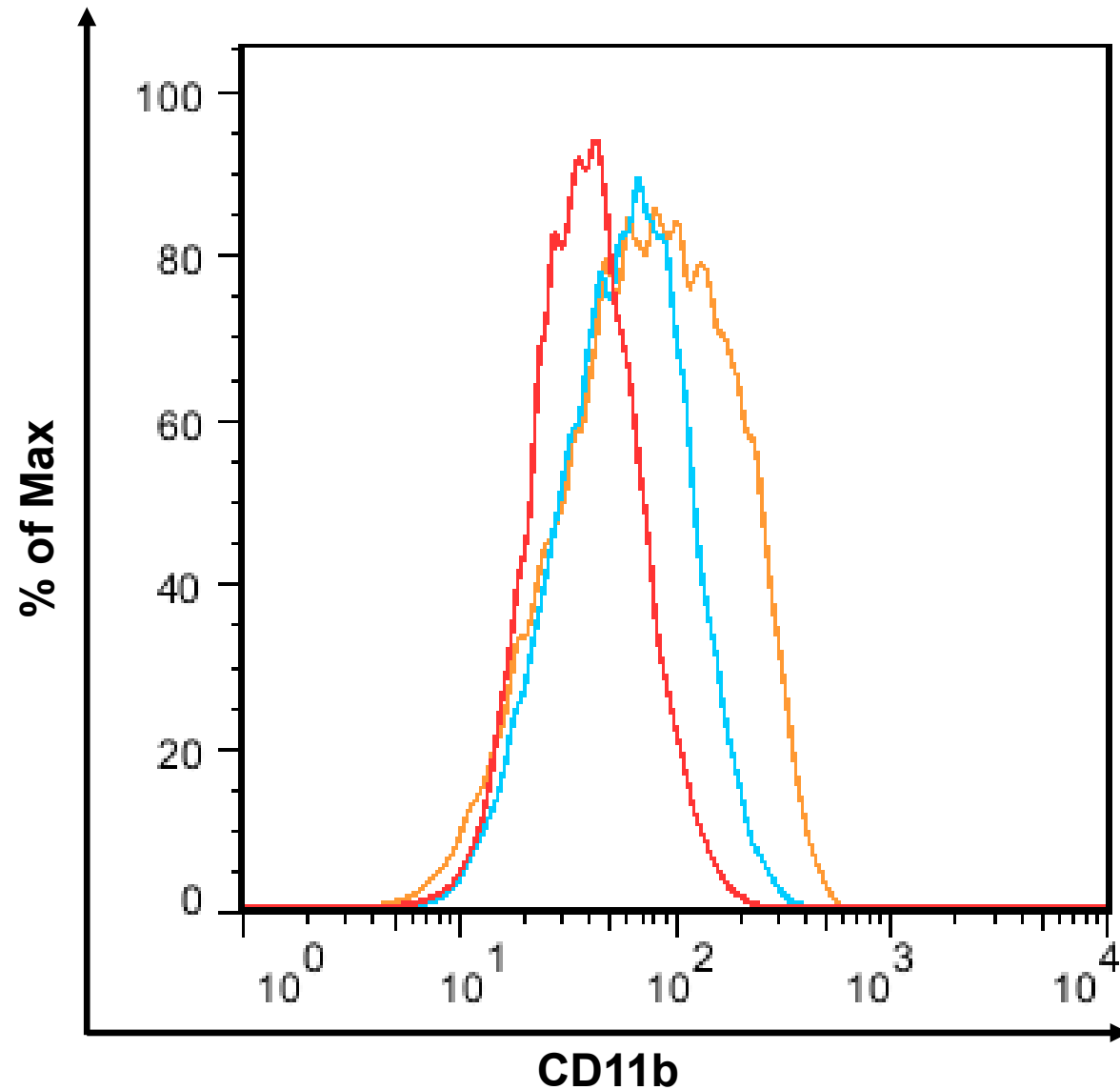


Figure 4H






	Sample Name
	M14_Specimen_001_untreated_001.fcs
	M14_Specimen_001_FC531 2uM_002.fcs
	M14_Specimen_001_FC531 5uM_003.fcs

Figure 4I

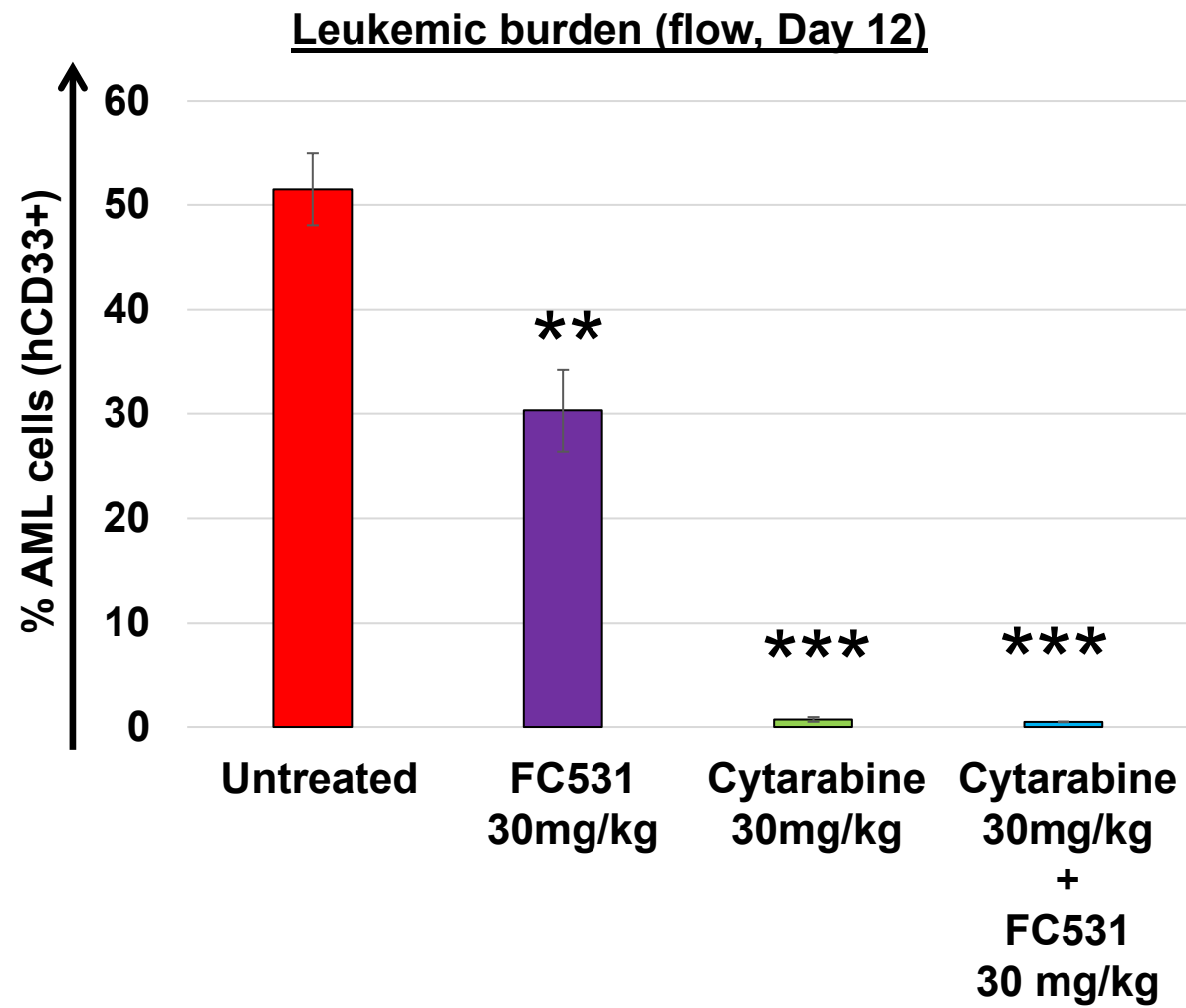


Figure 5A

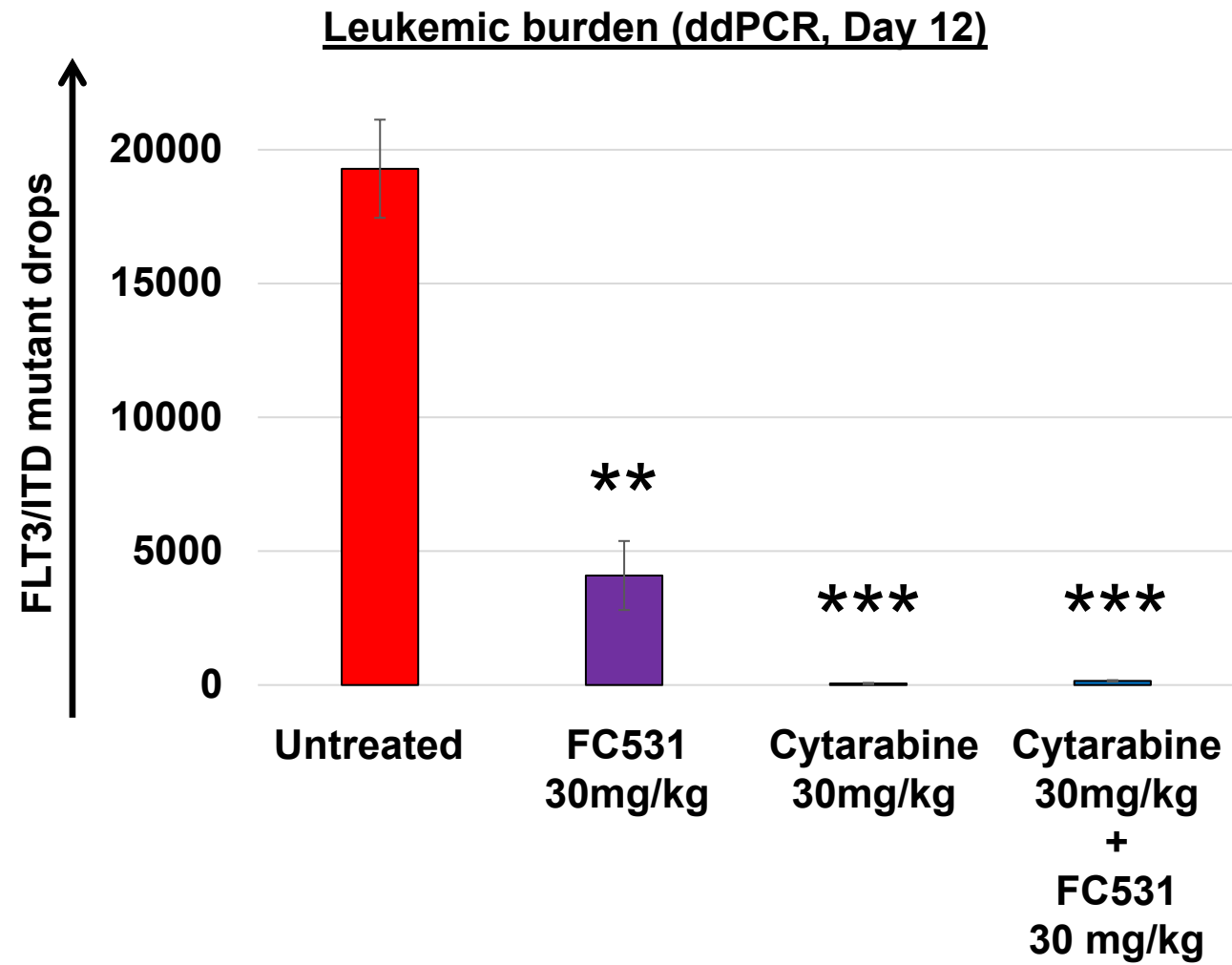
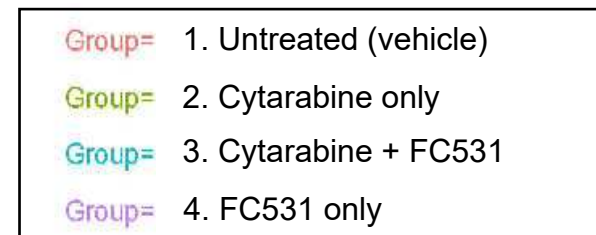
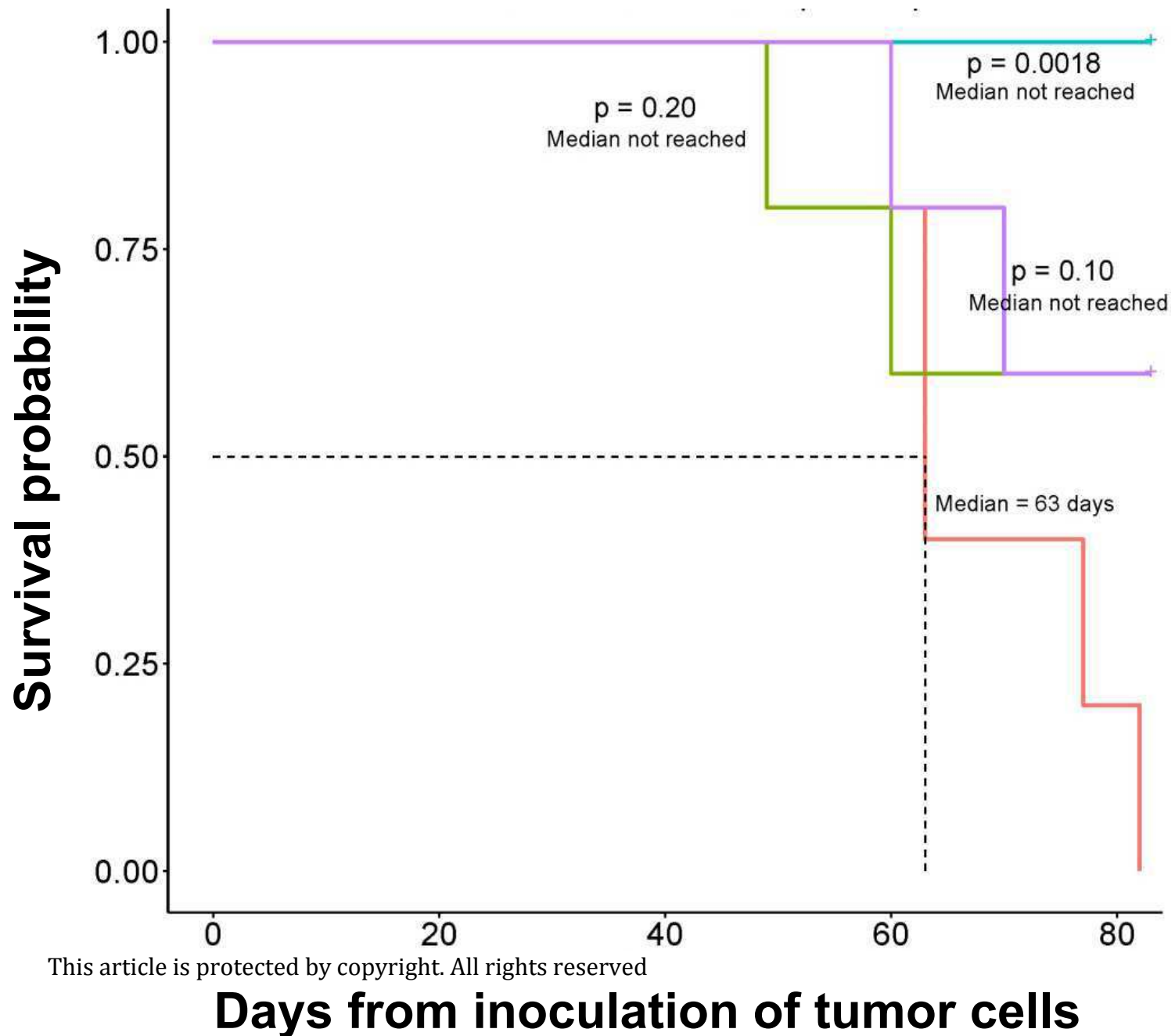


Figure 5B



This article is protected by copyright. All rights reserved

Figure 5C

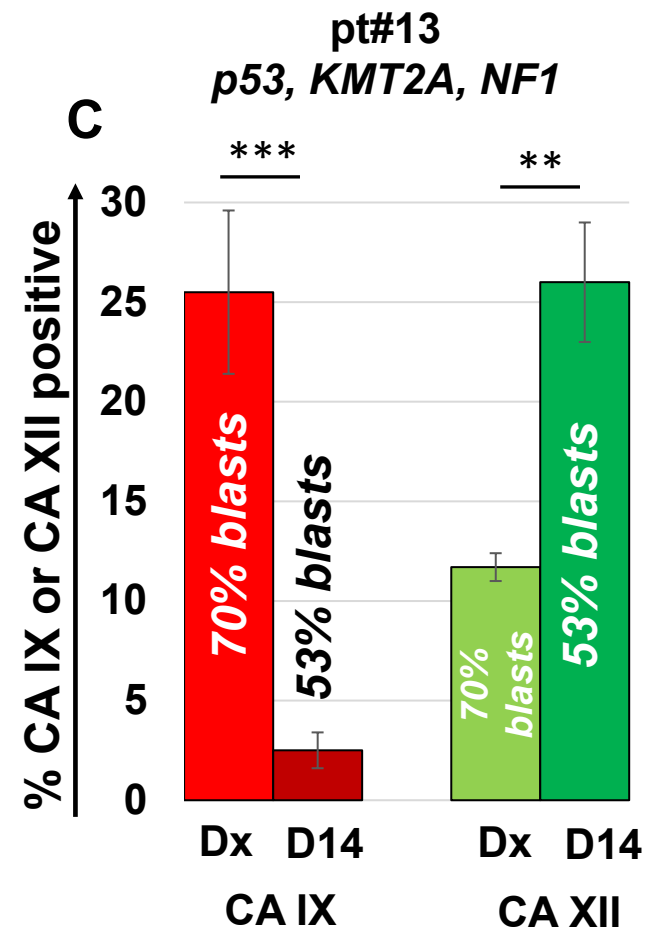
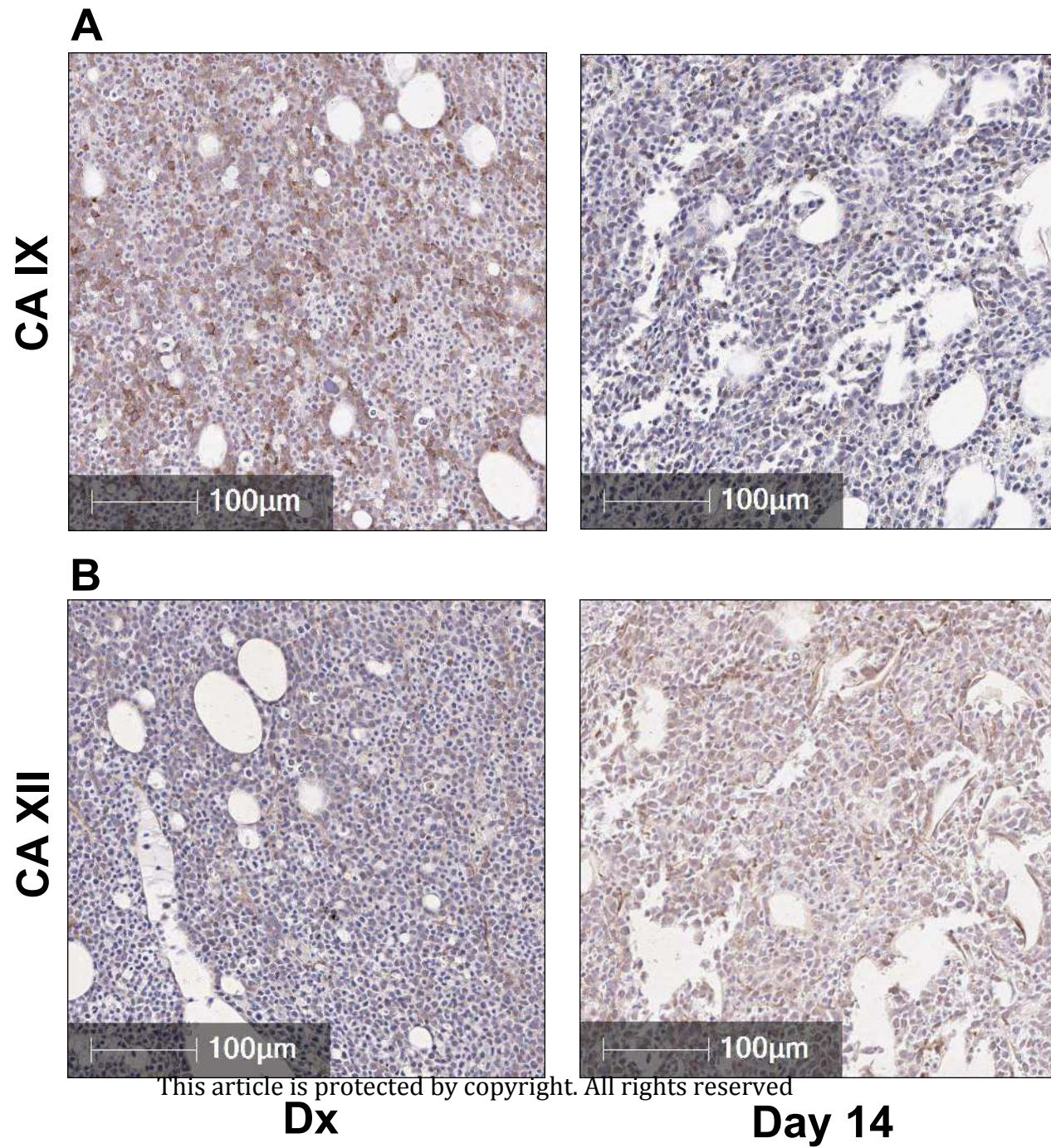
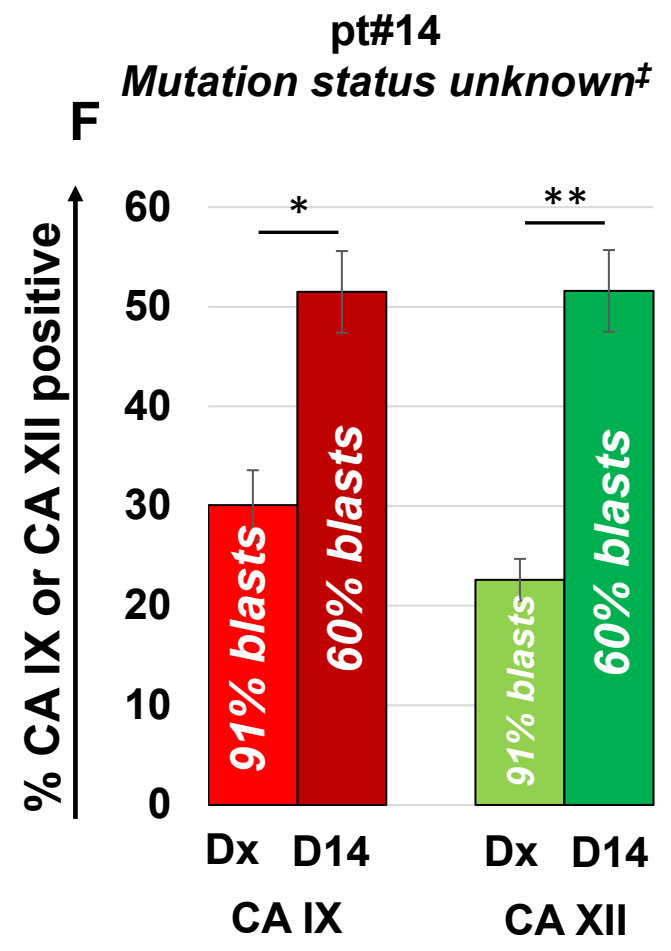
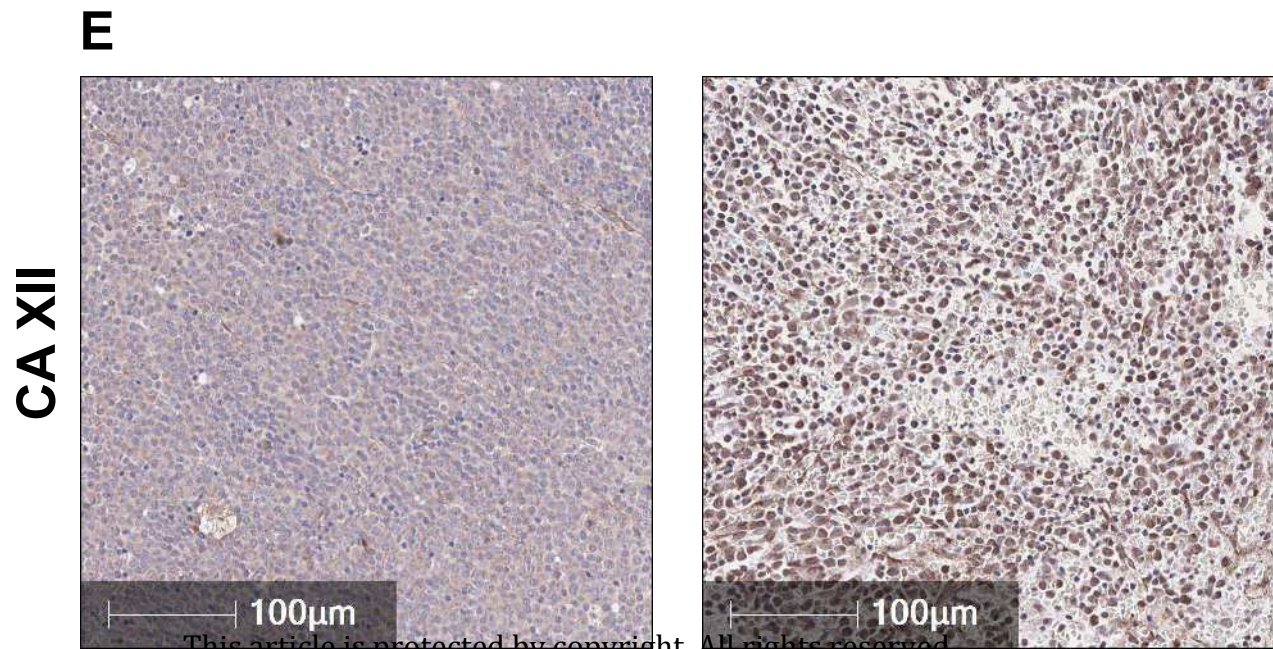
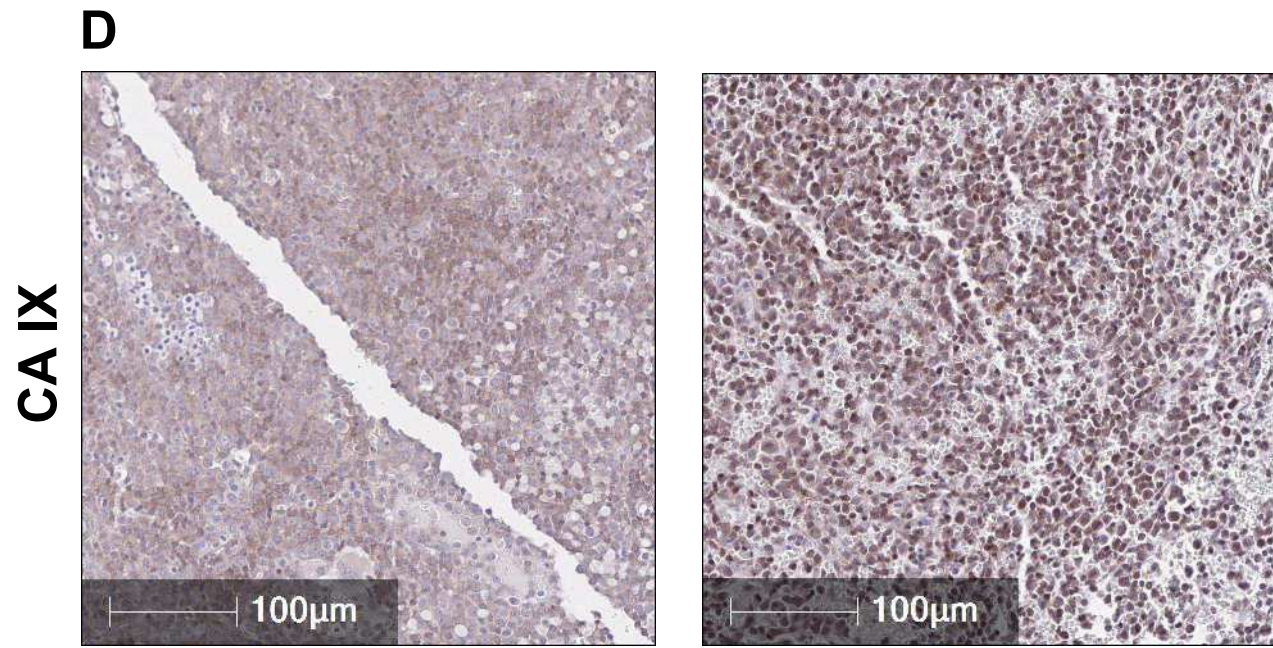


Figure 6



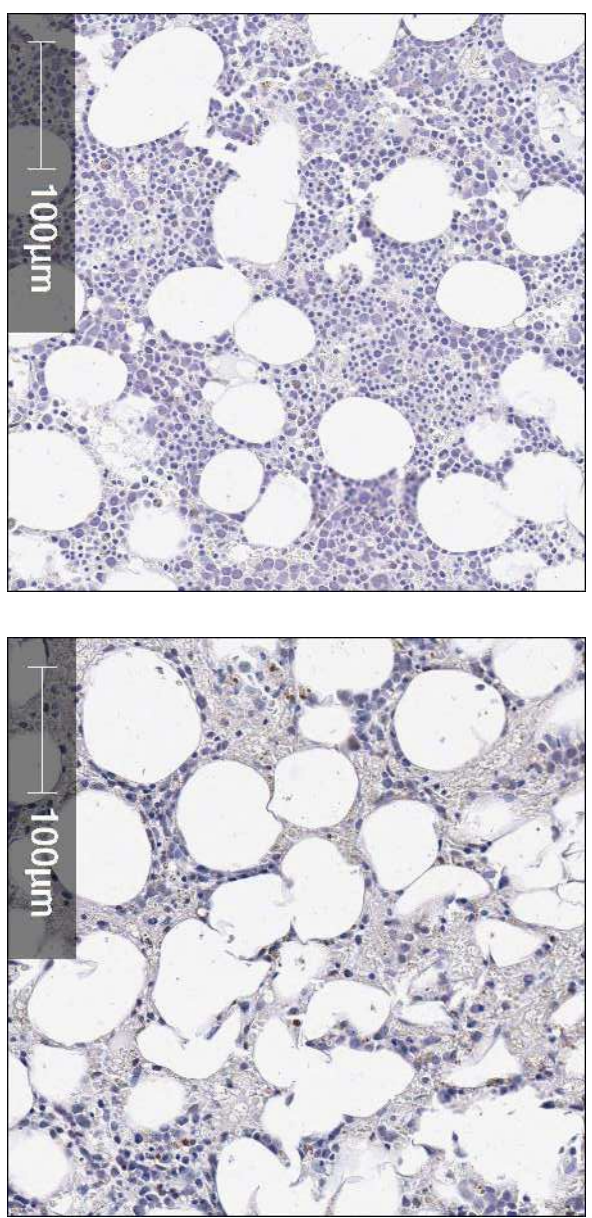
‡ NGS deferred by patient

This article is protected by copyright. All rights reserved

Dx **Day 14**

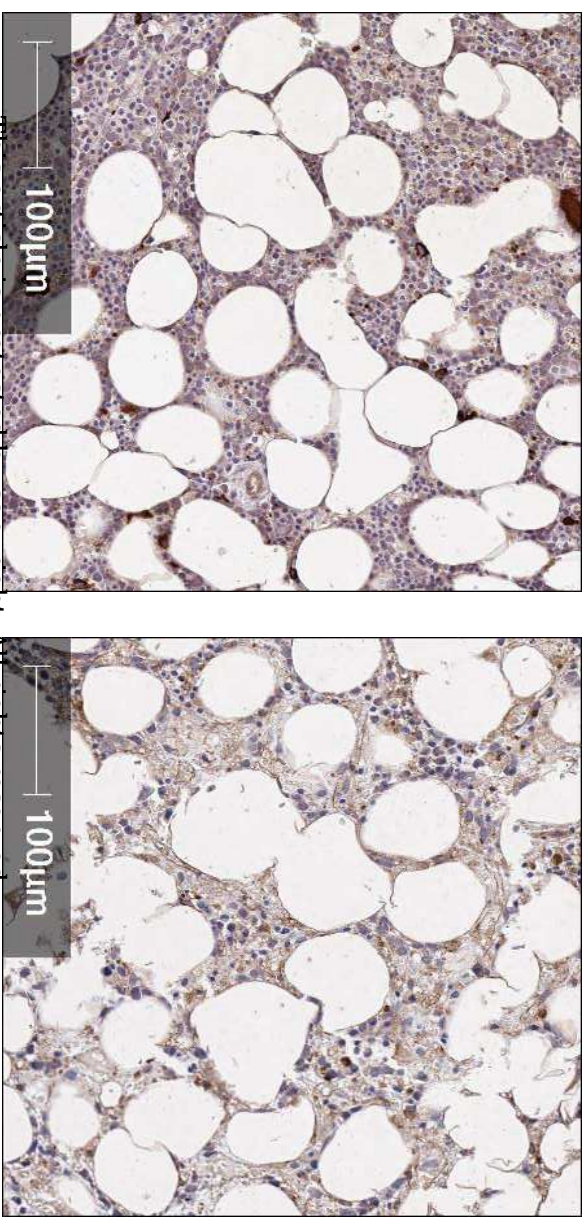
Figure 6

G



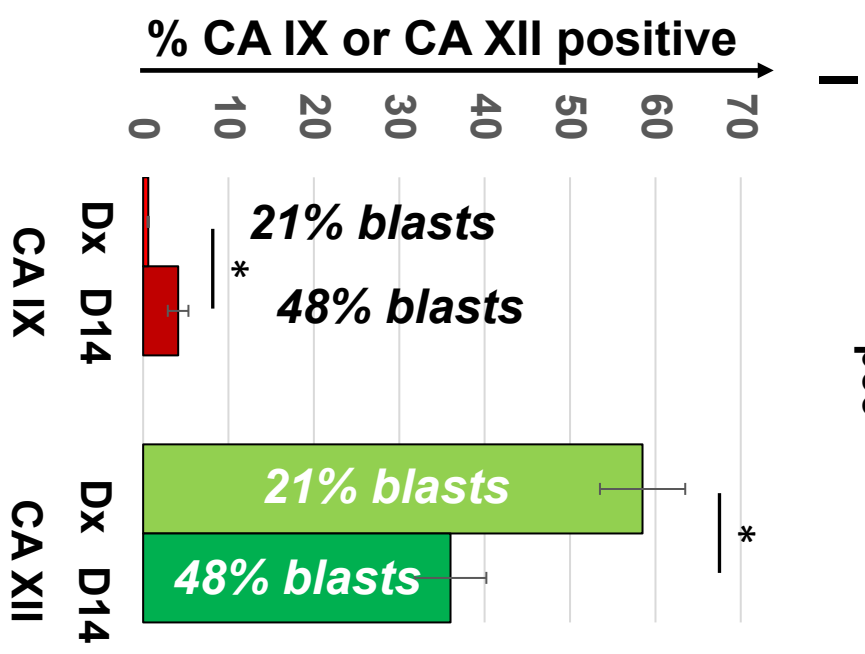
CA IX

H



CA XII

**pt#15
p53**

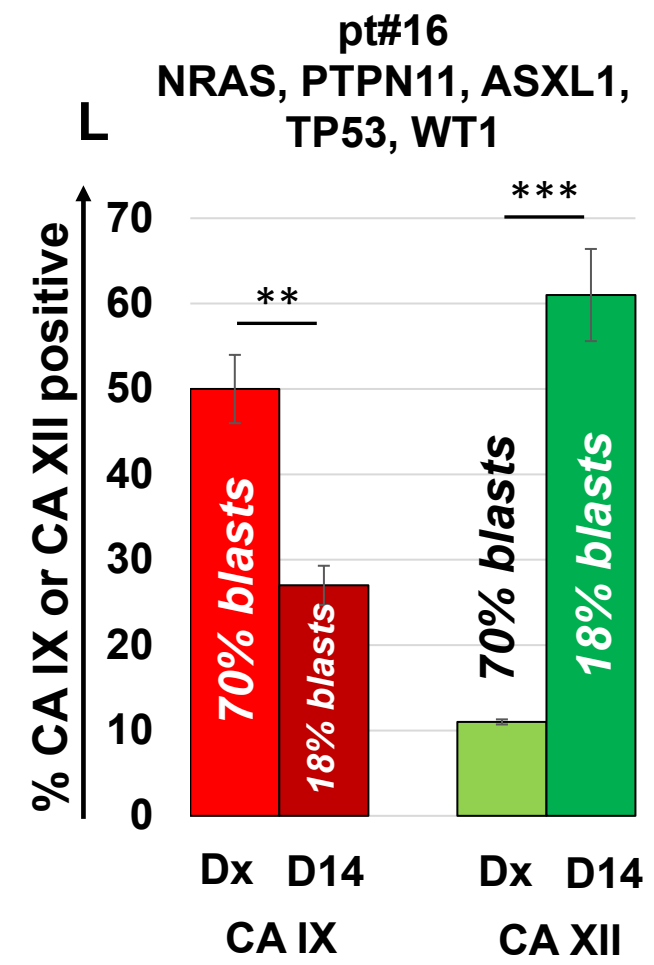
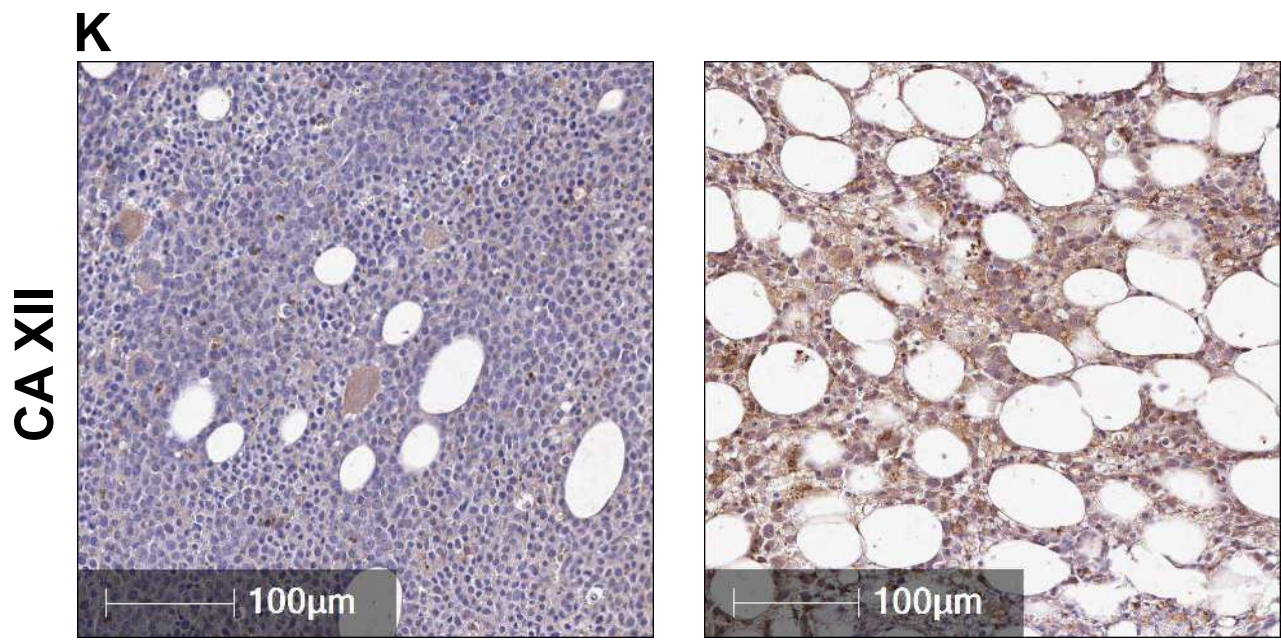
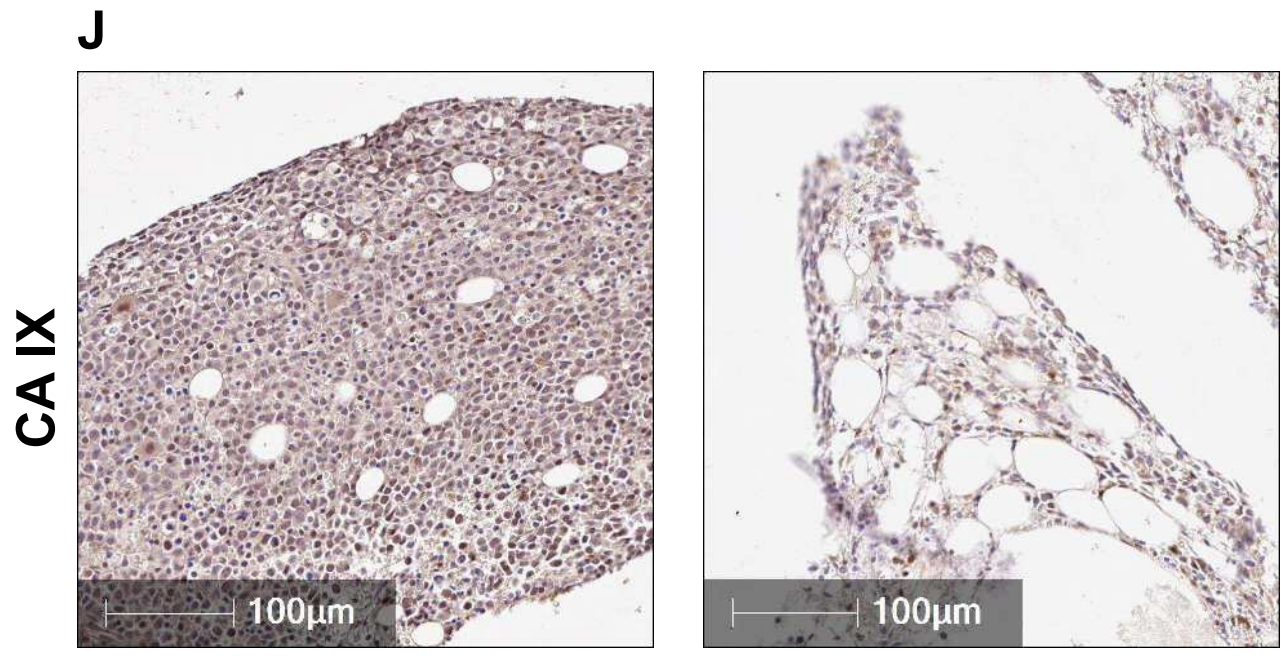


This article is protected by copyright. All rights reserved

Dx

Day 14

Figure 6



This article is protected by copyright. All rights reserved

Dx

Day 14

Figure 6

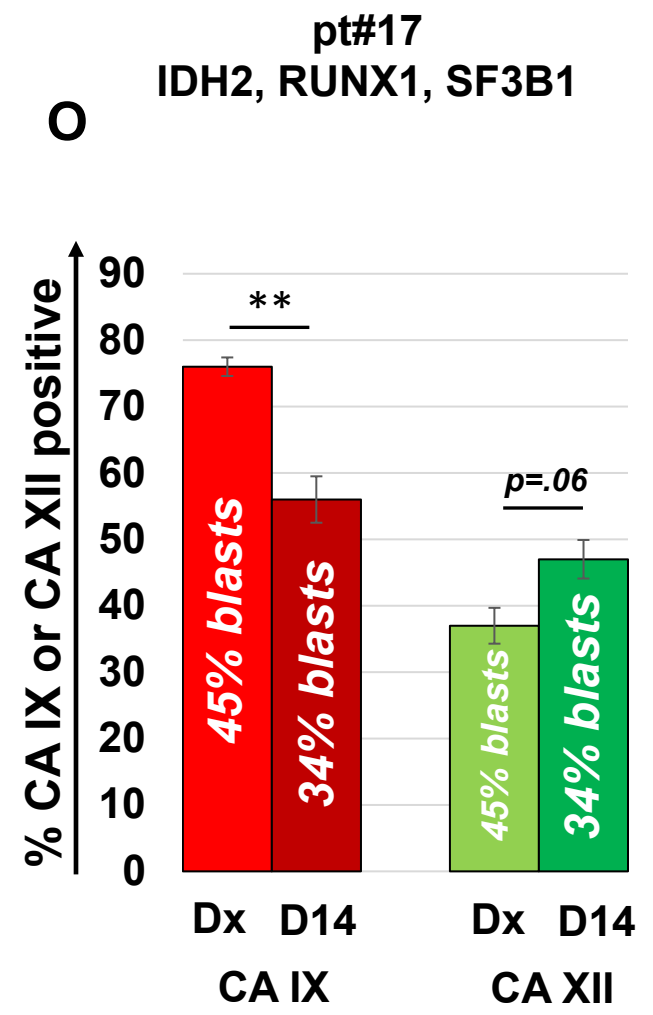
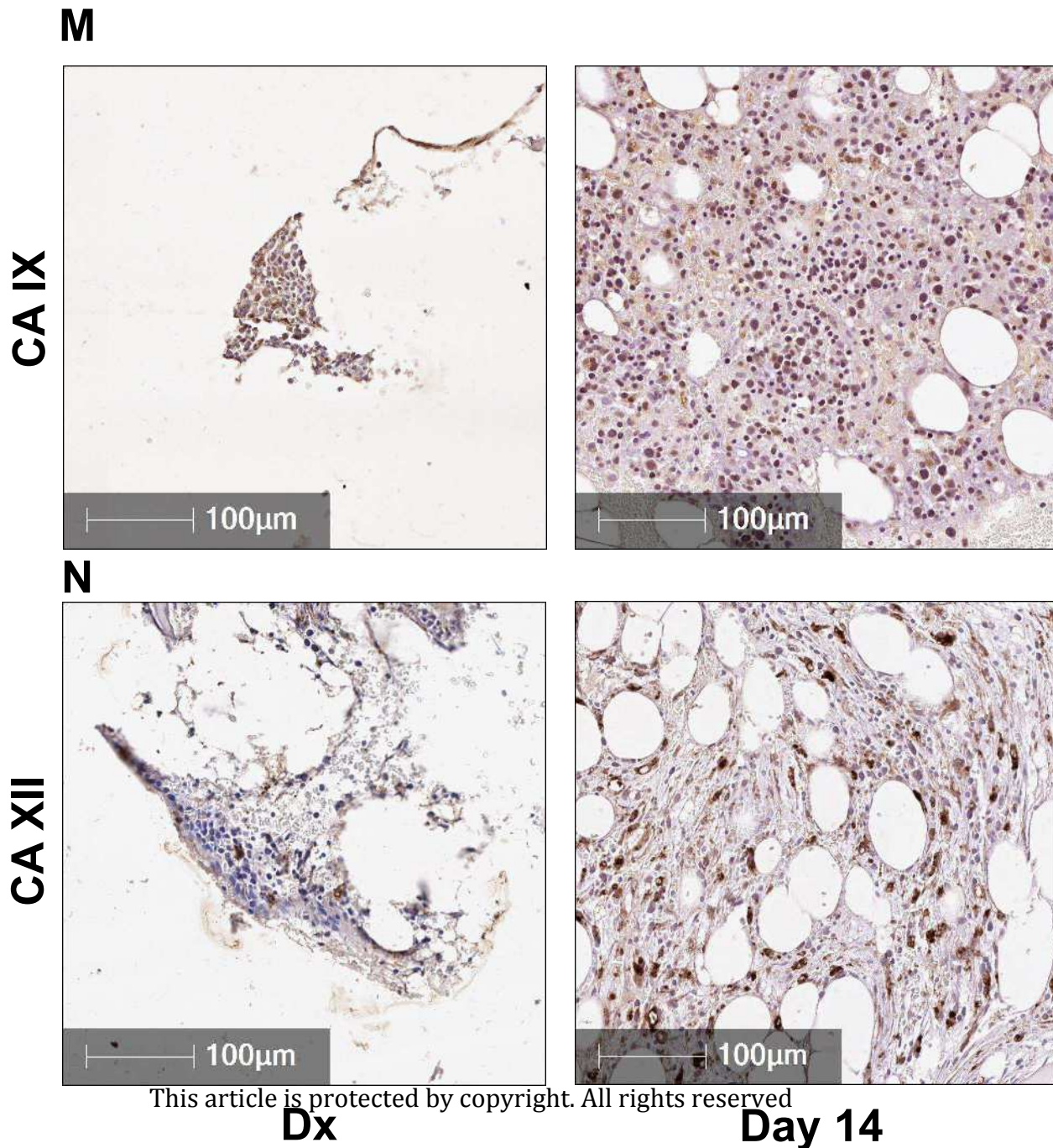


Figure 6

Patient No.	Age (y)	Gender, male (M)/ female (F)	Newly diagnosed (NDx), Relapsed/Refractory (R/R)	Cytogenetics	Molecular alterations identified
1	33	F	NDx	46,XX,inv(12) (p11.2q13)	FLT3/ITD, NPM1
2	75	F	NDx	46,XX	FLT3/ITD, NPM1
3	24	F	NDx	47, XX, +8	FLT3/ITD
4	56	M	NDx	46, XY	FLT3/ITD, ATRX, CCT6B, KMT2C (MLL3), NPM1, PTPN11, RAD21
5	50	F	NDx	46, XX	FLT3/TKD, IDH2, DNMT3A
6	35	F	R/R	46, XX	FLT3/ITD, NPM1
7	60	M	R/R	46, XY	FLT3/ITD
8	36	F	R/R	46, XX	FLT3/ITD, NPM1, ATRX, ASXL1, RUNX1, TET2
9	30	M	NDx	46, XY	FLT3/ITD, WT1
10	39	M	NDx	46,XY,t(5;22)(q35;q11.2)	FLT3/ITD, NRAS, PDCD11, WT1
11	46	M	NDx	47,XY,+11	FLT3/ITD, TET2, KMT2A, SRSF2
12	38	F	NDx	46, XX	FLT3/ITD, FLT3/TKD

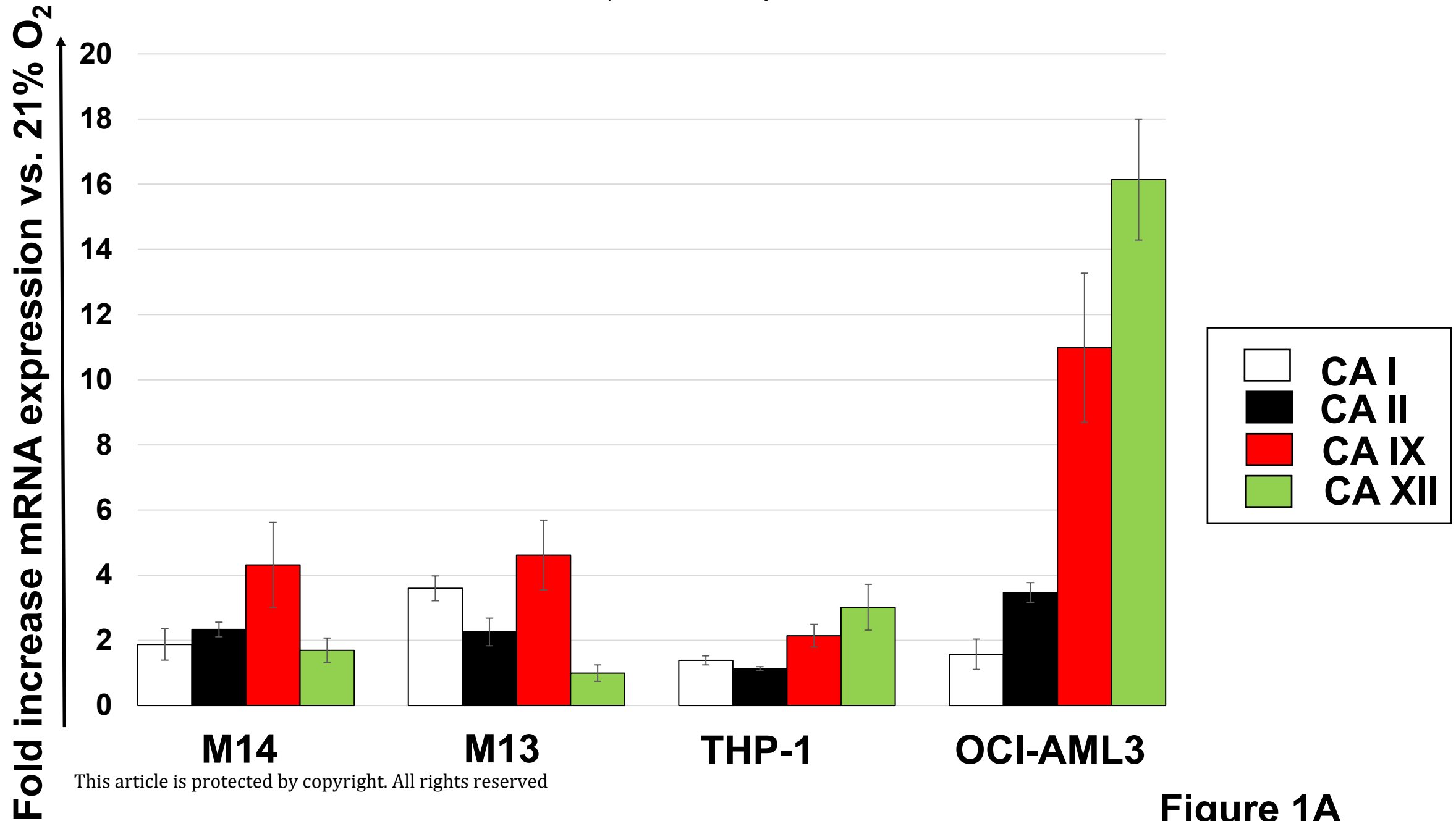
Patient No.	Age (y)	Gender, male (M)/ female (F)	Newly diagnosed (NDx), Relapsed/Refractory (R/R)	Cytogenetics	Molecular alterations identified
13	63	M	NDx	46,XY,del(20)(q11.2q13.3)[9]/46,sl,del(5)(q13q33),+7,der(7;17)(q10;q10),+8,add(11)(q23),18,3~6dmin[5]/47,sdl1,+6,3~20dmin[2]/46,sdl2,der(7;17),-8,5~12dmin[2]/46,XY[2]	P53, KMT2A, NF1
14	25	M	NDx	46, XY	Unknown*
15	65	M	NDx	45,XY,add(1)(p22),-2,-5,add(9)(p11), -12,-15, add(16)(q22), add(17)(p11.2), -18,+mar1, +mar4,+mar5,+mar8[7]/ 43~44,idem, -X,-3,-4,-7, -20,+mar2,+mar3, +mar6,+mar7[cp5]/ 46,XY[8]	P53
16	66	M	NDx	45,XX,add(5)(q1?3),add(14)(p12),add(17)(p11.2),-18[2]/45,sl,der(16)t(11;16)(q13;p13.3)[11]/ 46,sdl1,+8[5]/ 46,XX[3]	NRAS, PTPN11, ASXL1, TP53, WT1
17	60	F	NDx	92<4n>,XXXX[2]/ 46,XX[18]	IDH2, RUNX1, SF3B1

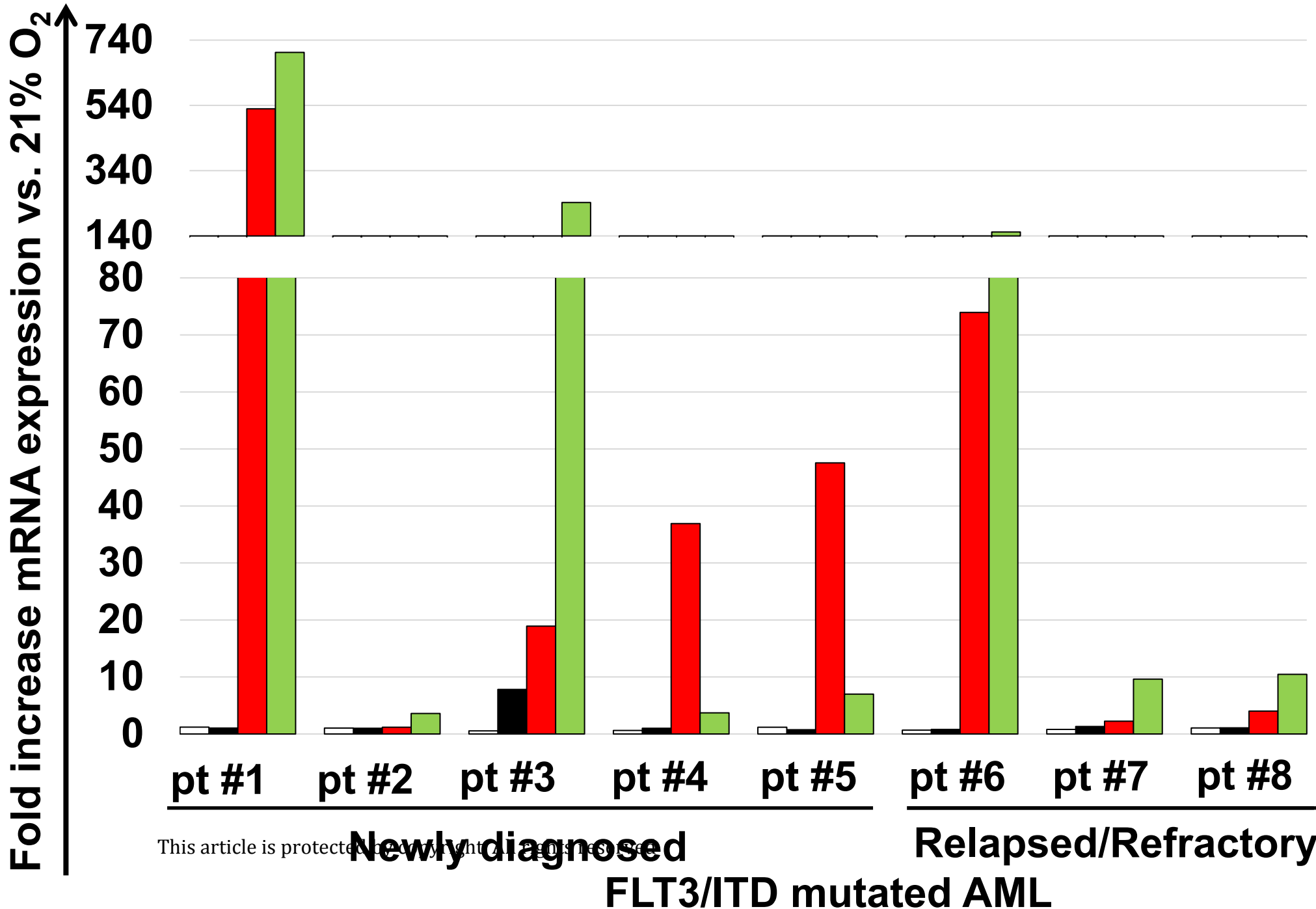
Intracellular pH		
O₂	21%	1%
Untreated	<i>7.40±0.26</i>	<i>7.31±0.51</i>
FC531 1µM	<i>7.59±0.30</i>	<i>6.80±0.42</i>
FC531 2µM	<i>7.50±0.23</i>	<i>6.32±0.57</i>
FC531 5µM	<i>7.21±0.42</i>	<i>4.60±1.03</i>

Table 2

PDX Group	d1-5	d8-12
1	<i>PBS (untreated)</i>	<i>PBS (untreated)</i>
2	<i>Cytarabine 30 mg/kg/d i.p.</i>	<i>Cytarabine 30 mg/kg/d i.p.</i>
3	<i>Cytarabine 30 mg/kg/d i.p.</i>	<i>FC531 30 mg/kg/d i.p.</i>
4	<i>FC531 30 mg/kg/d i.p.</i>	<i>FC531 30 mg/kg/d i.p.</i>

Table 3

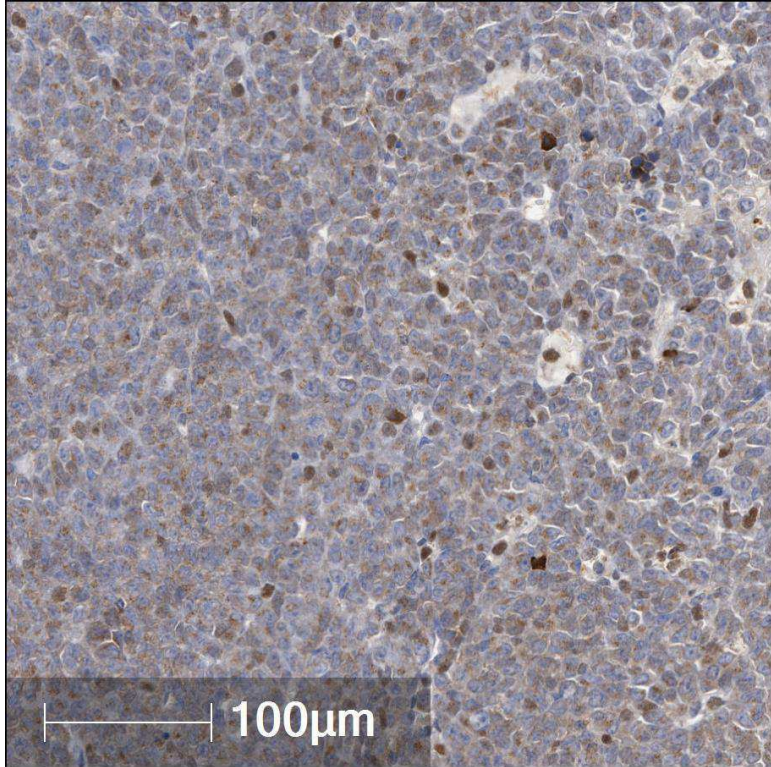




This article is protected by copyright. See [https://doi.org/10.1182/blood-2018-08-858888](#) for full text.

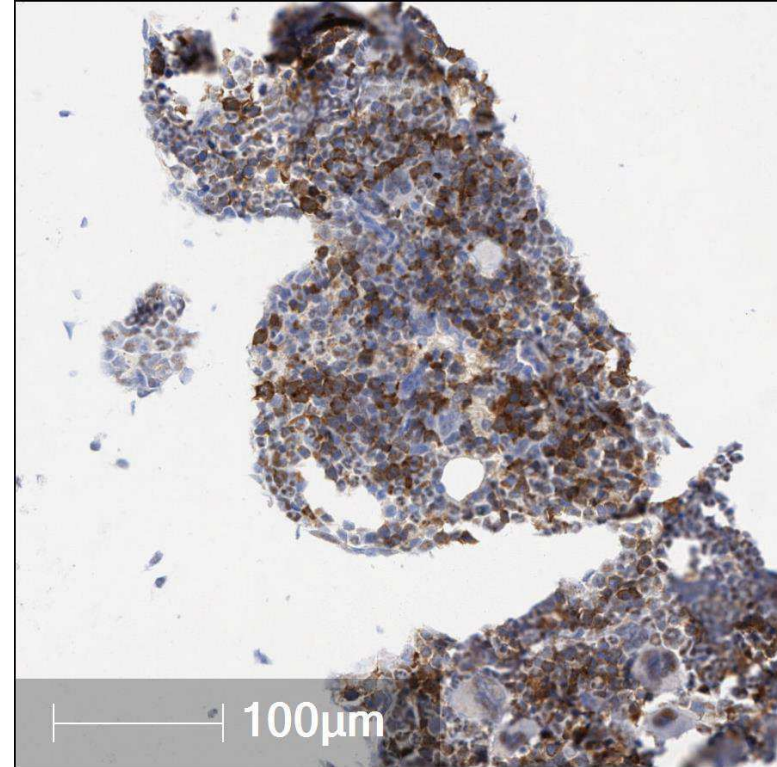
Figure 1B

A



untreated

B

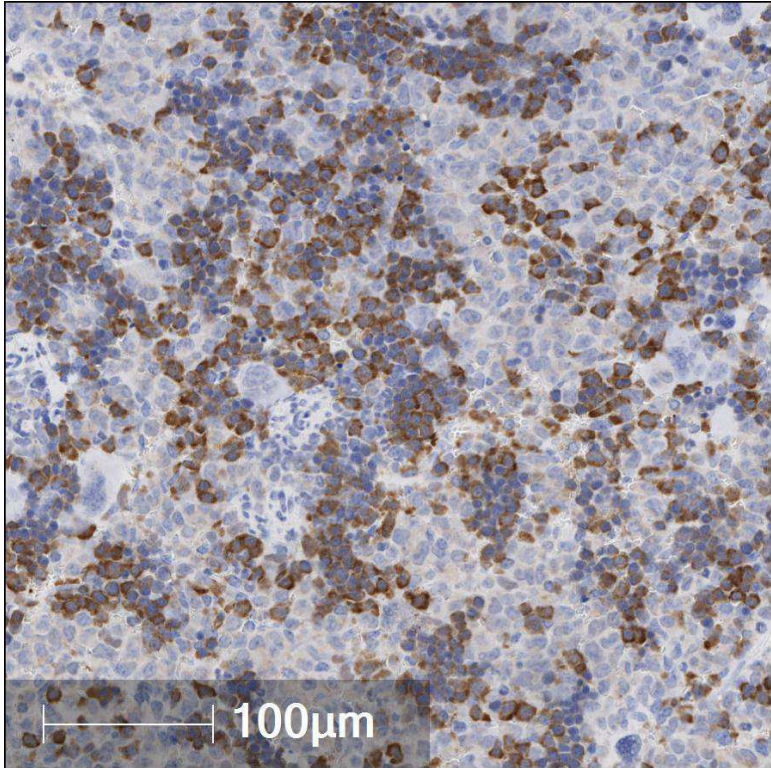


Bone marrow

Cytarabine

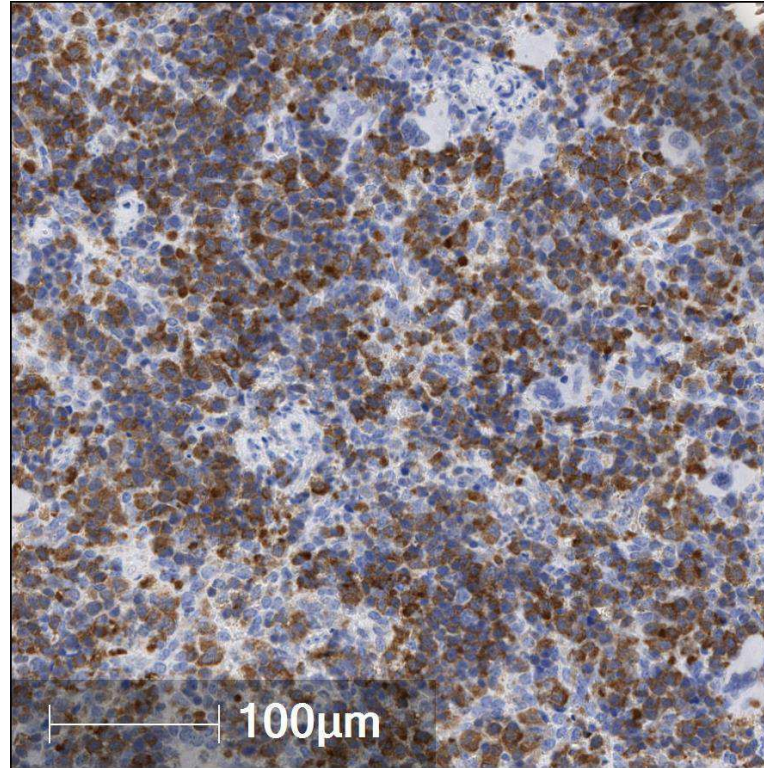
Figure 2

C



untreated

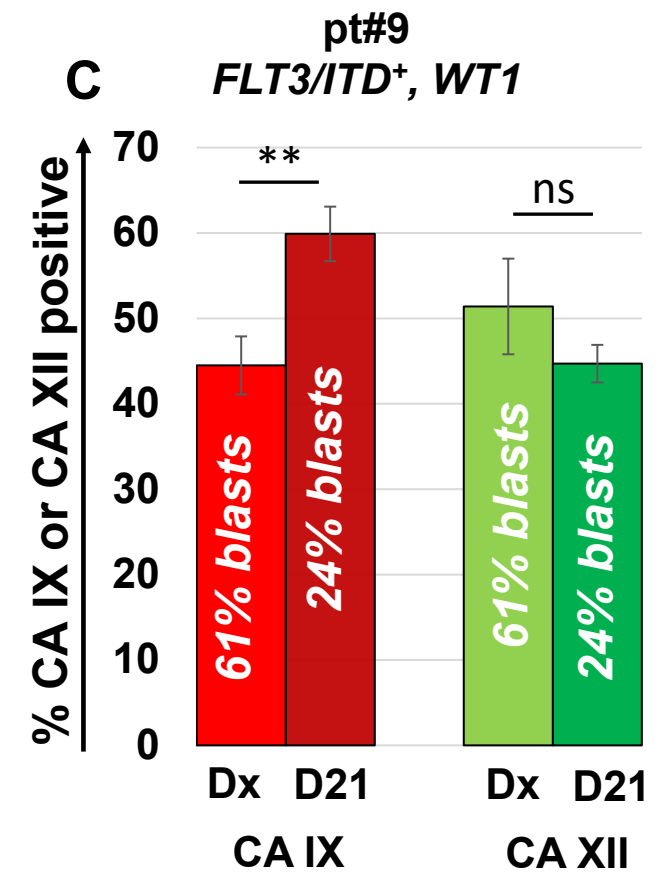
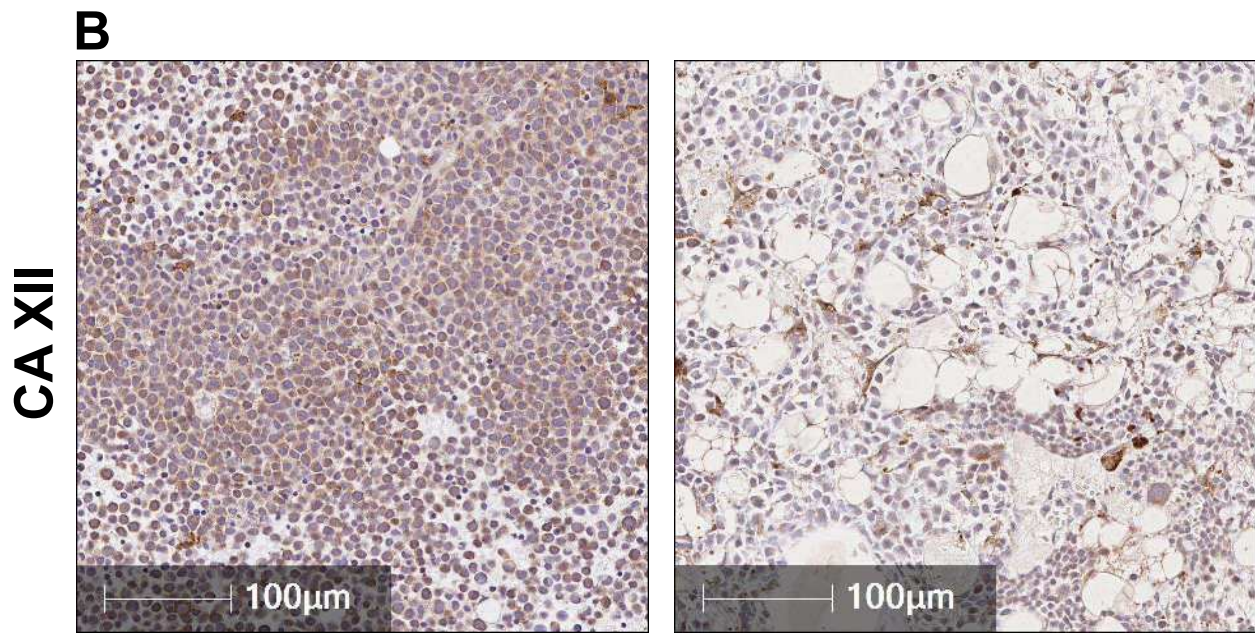
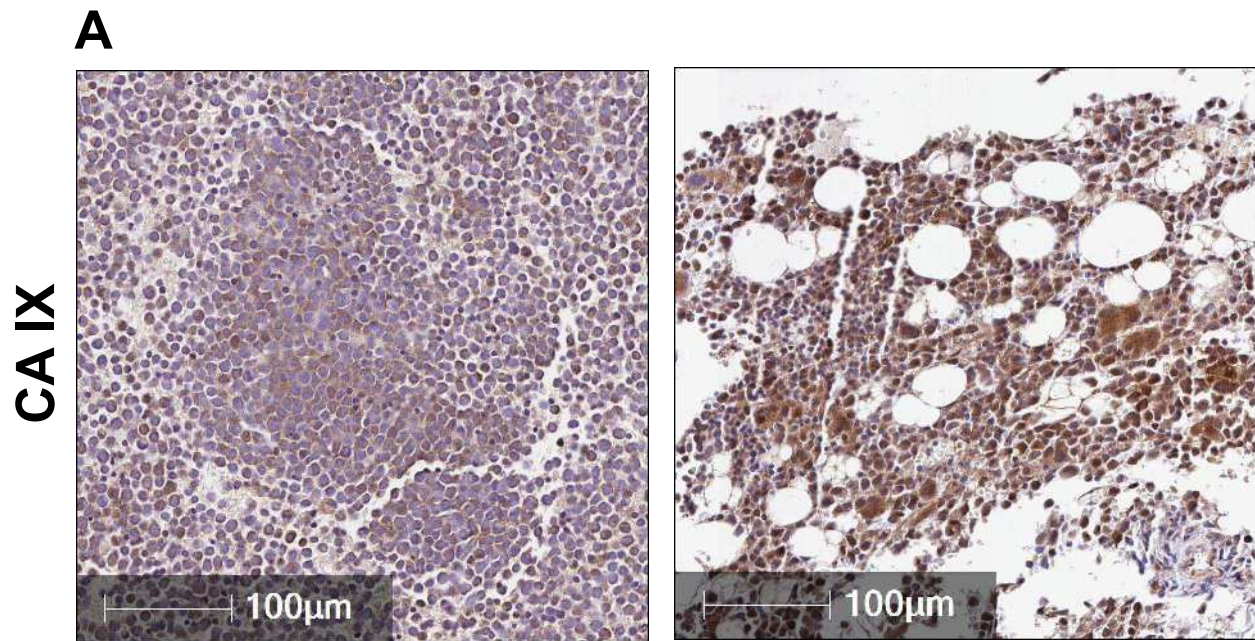
D



Cytarabine

Spleen

Figure 2



This article is protected by copyright. All rights reserved

Dx **Day 21**

Figure 3

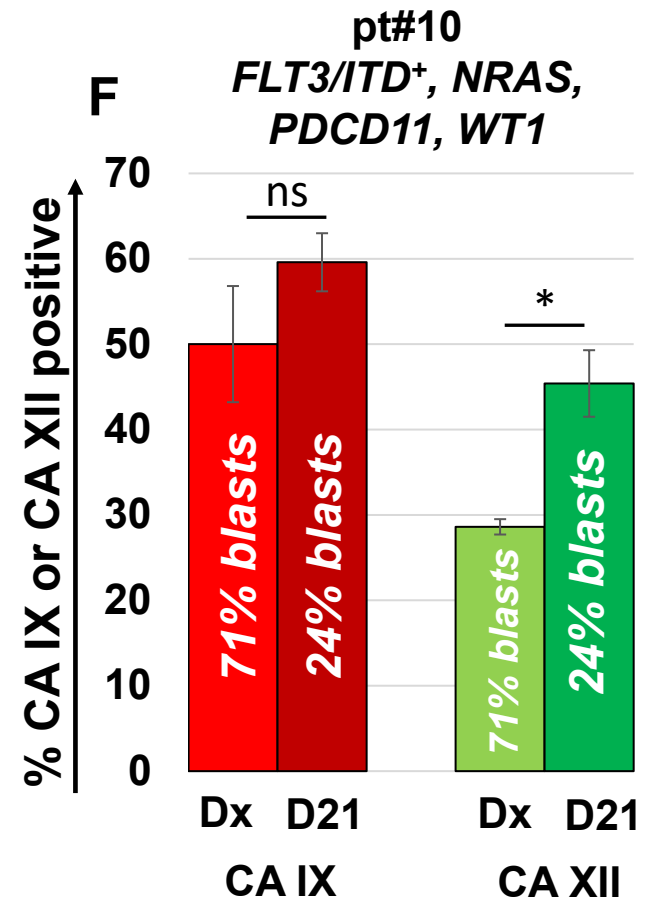
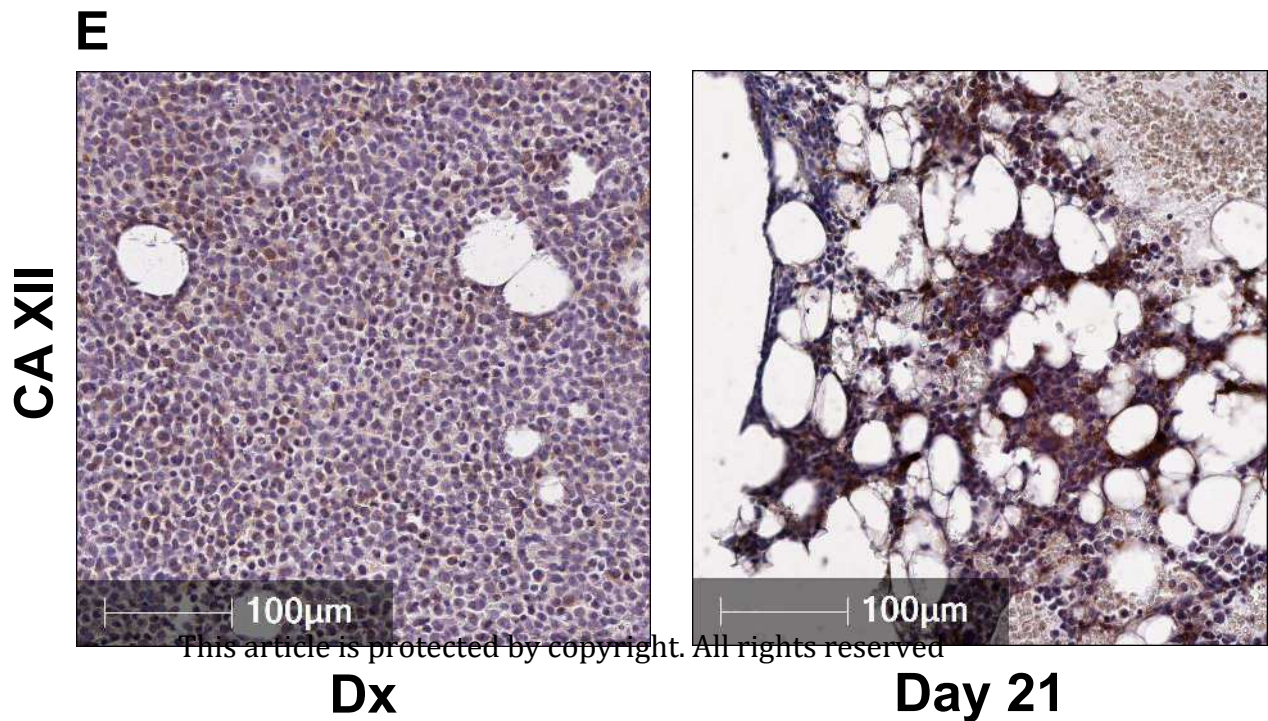
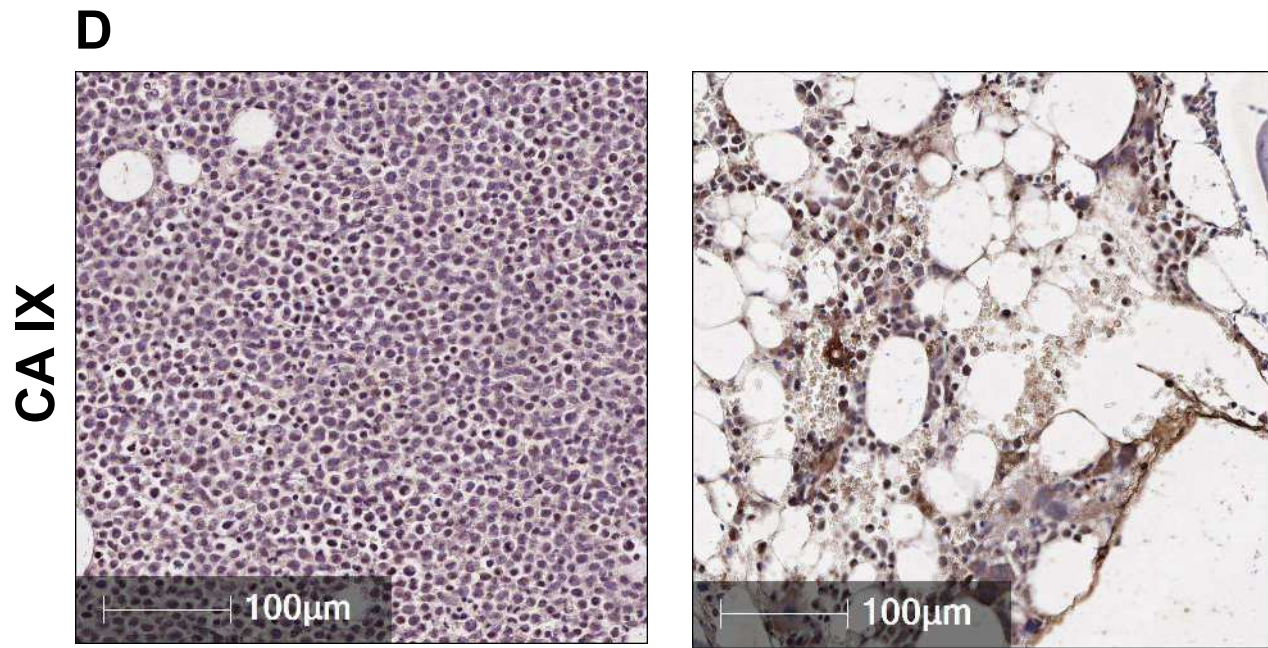
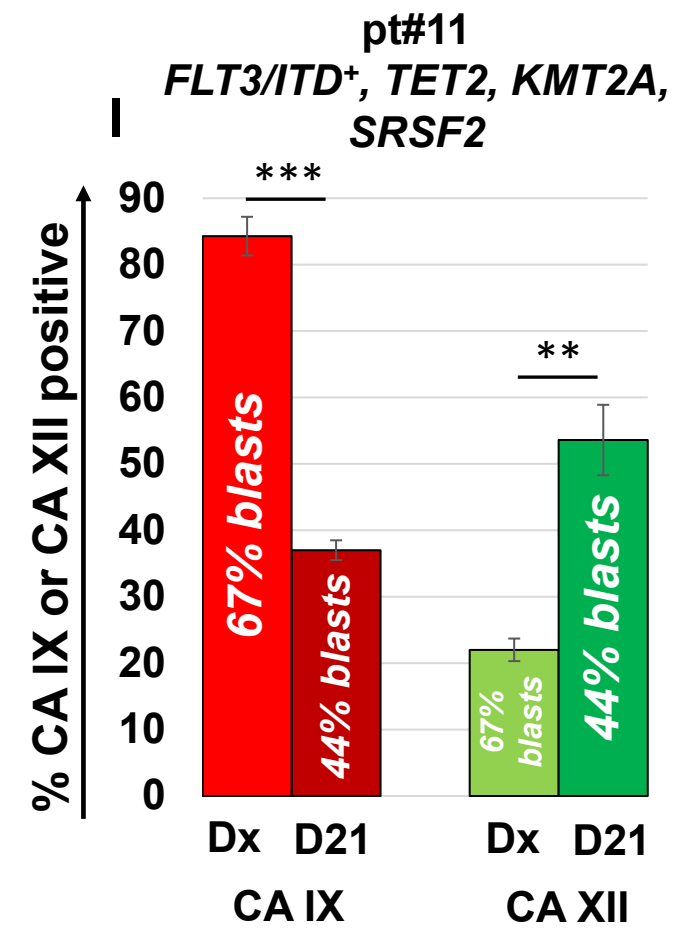
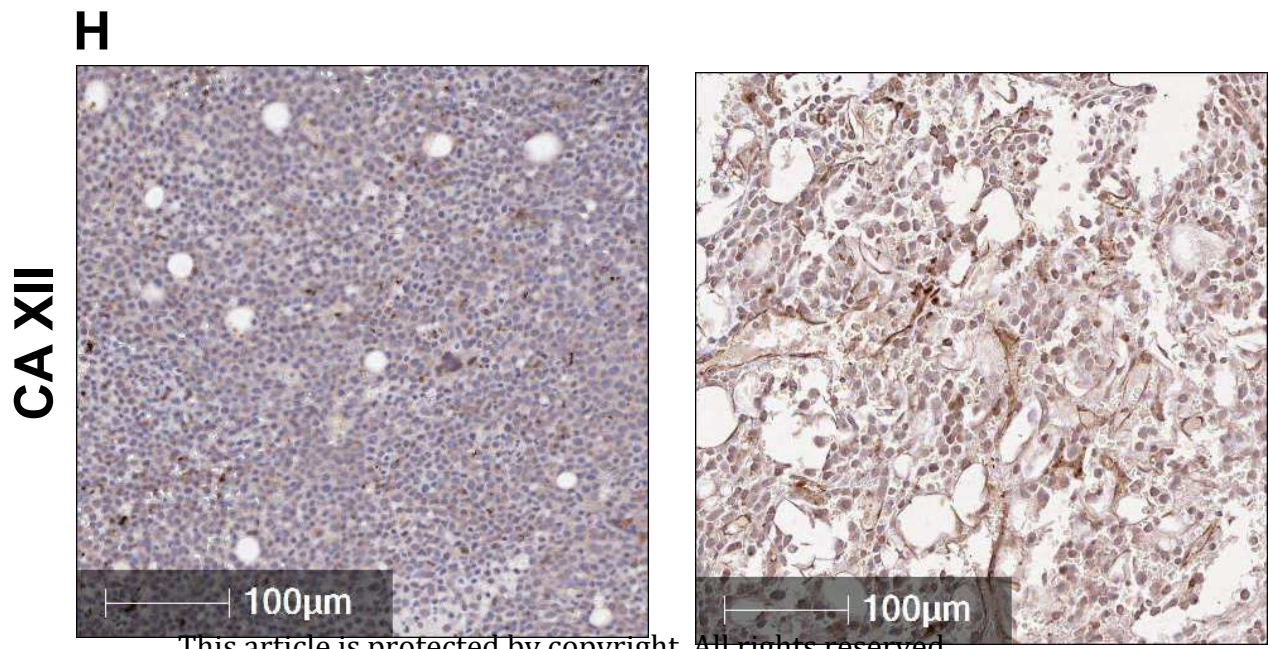
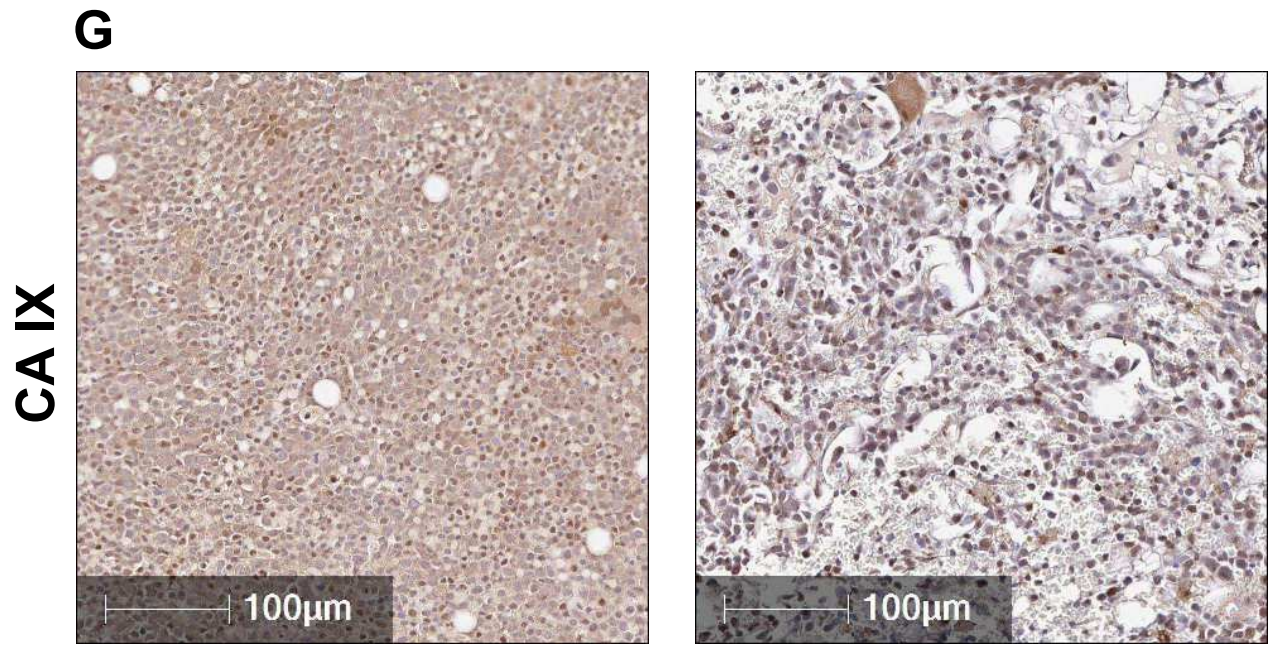


Figure 3



This article is protected by copyright. All rights reserved

Dx

Day 21

Figure 3

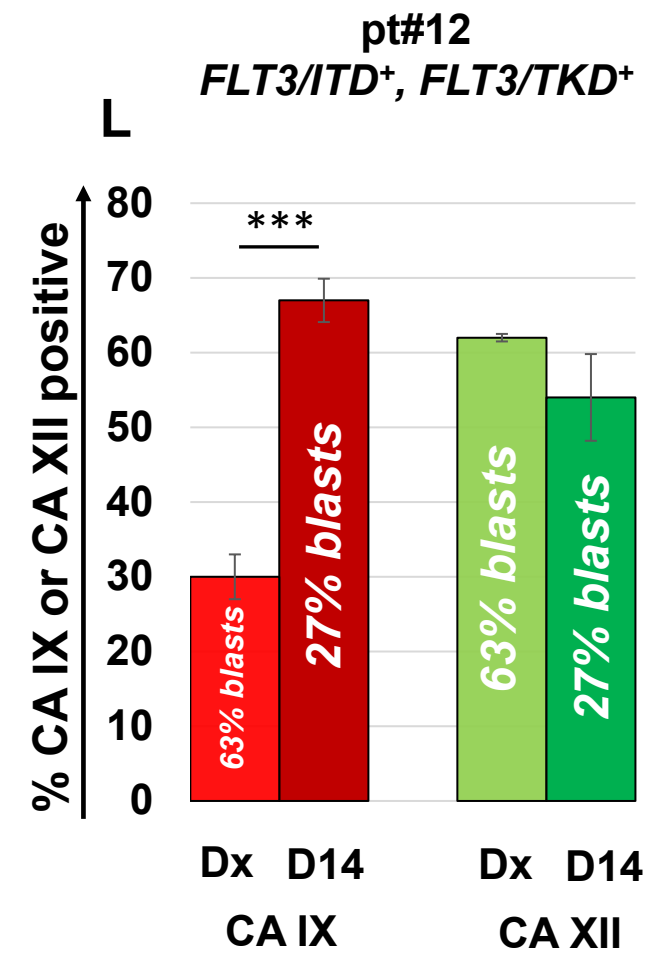
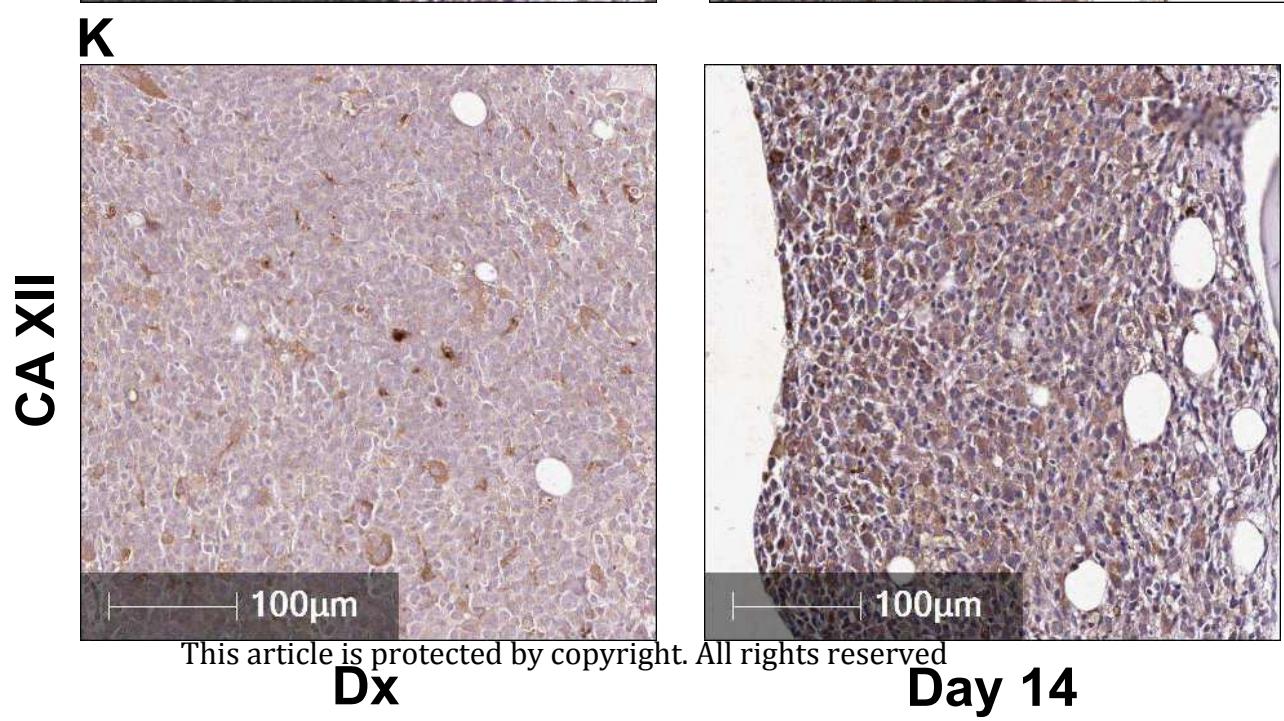
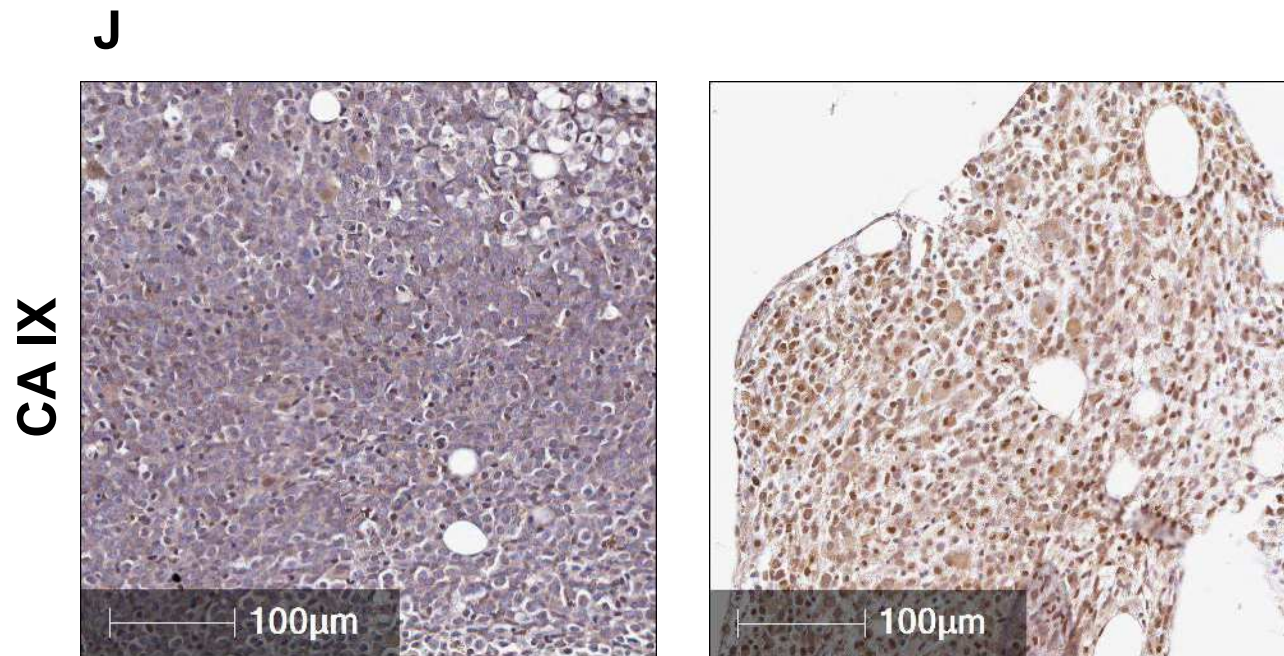


Figure 3

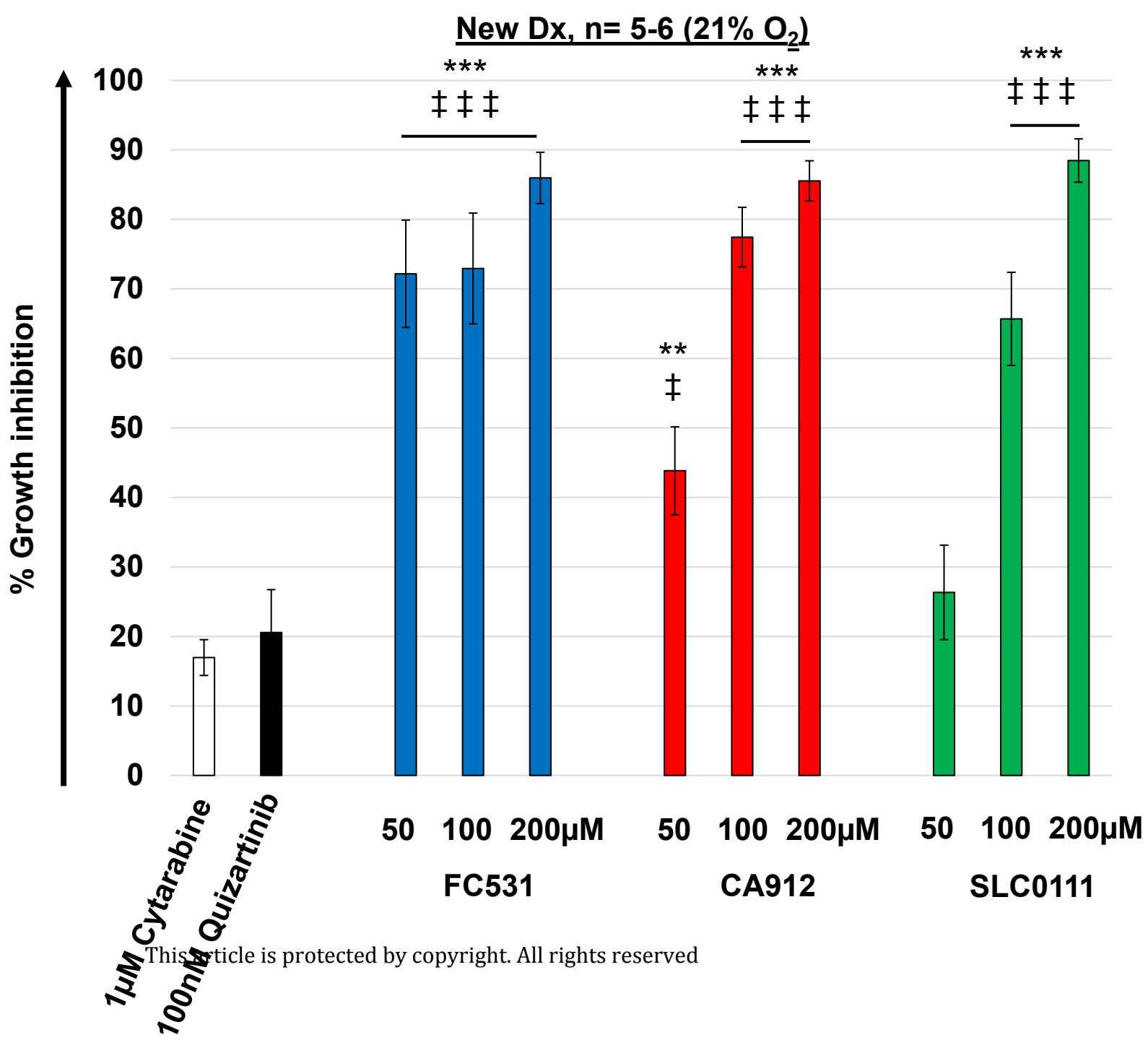
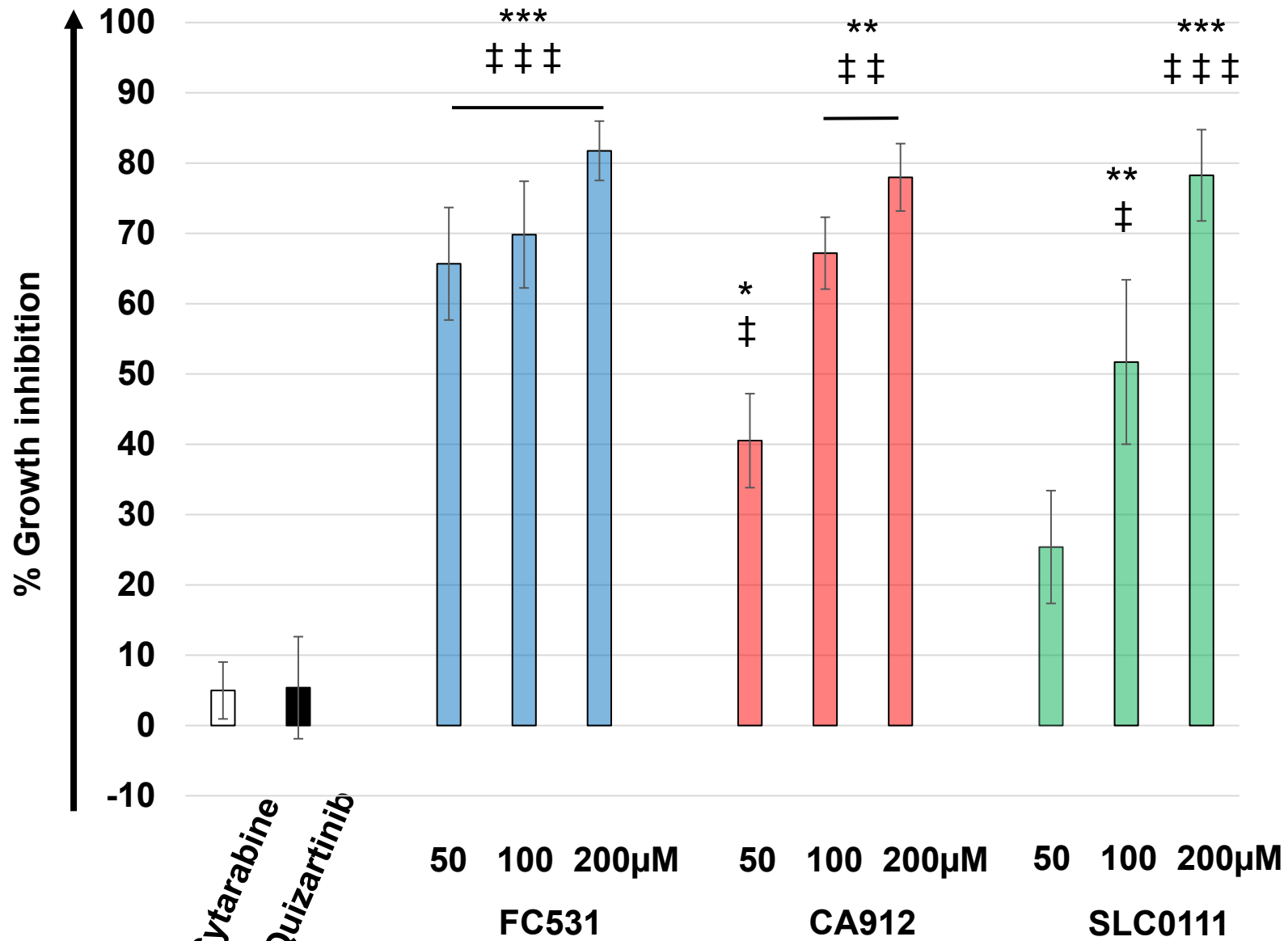


Figure 4A

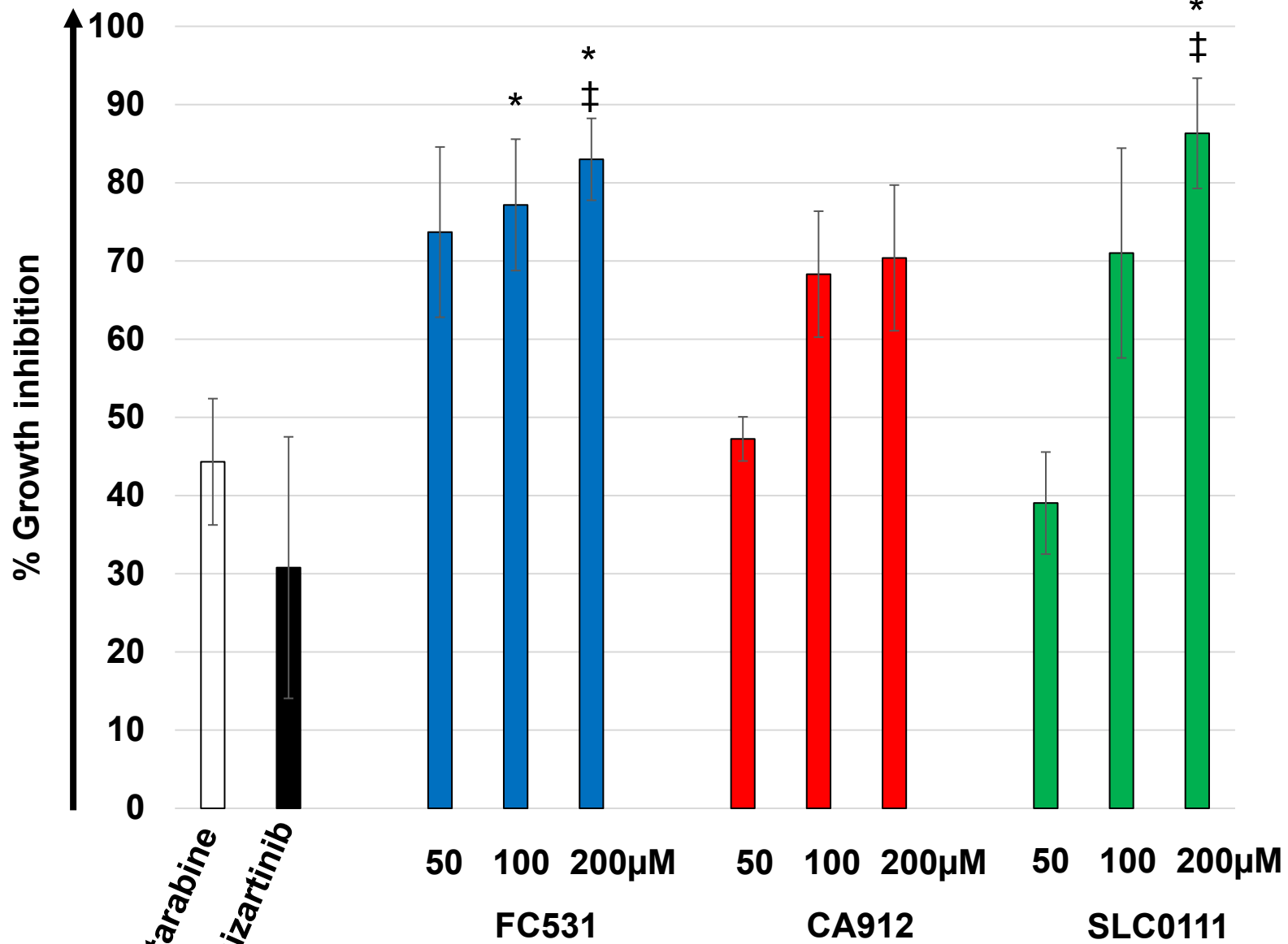
New Dx, n= 5-6 (1% O₂)



* vs. Cytarabine
‡ vs. Quizartinib

Figure 4B

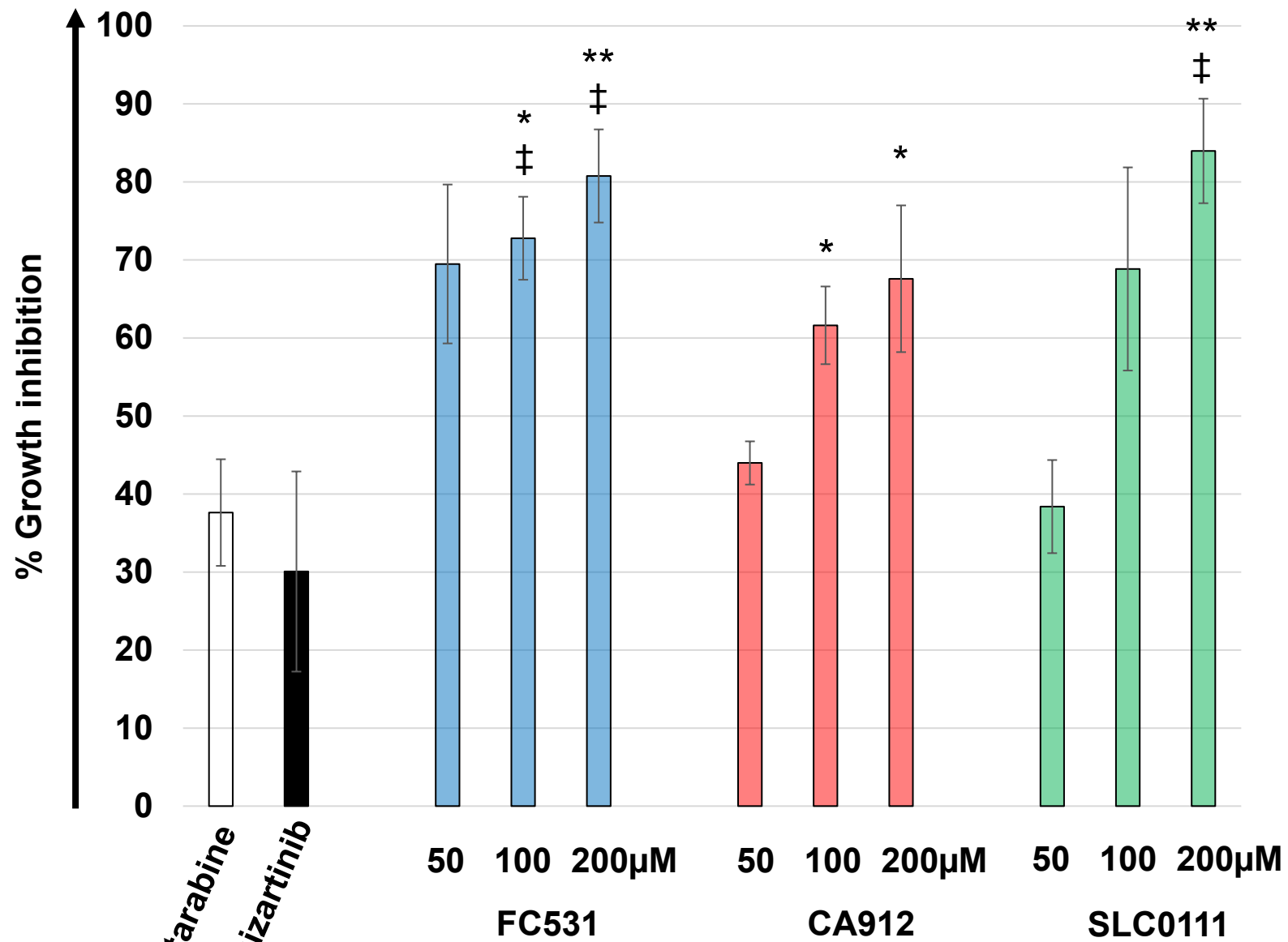
Relapsed/Refractory, n= 3 (21% O₂)



* vs. Cytarabine
‡ vs. Quizartinib

Figure 4C

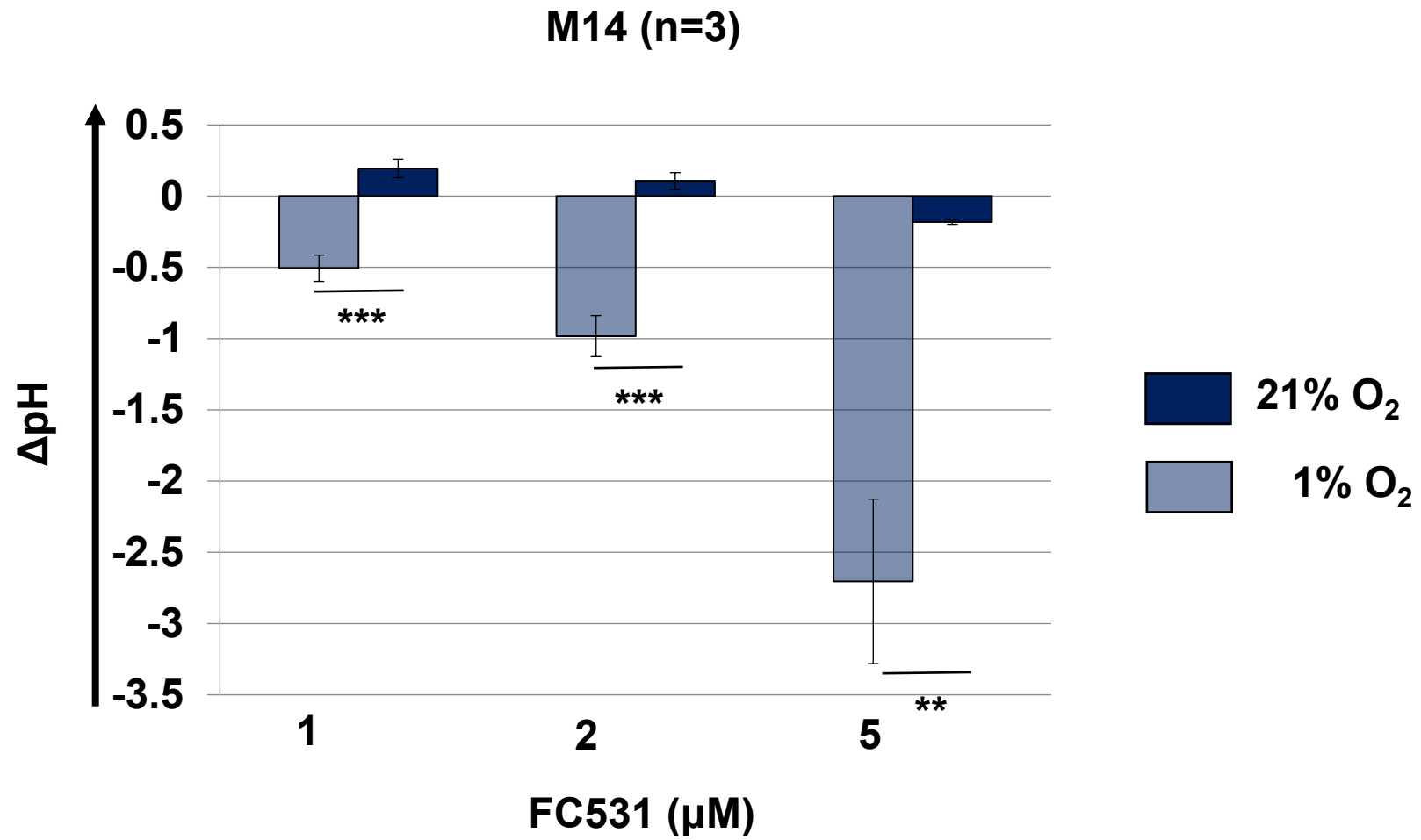
Relapsed/Refractory, n= 3 (1% O₂)

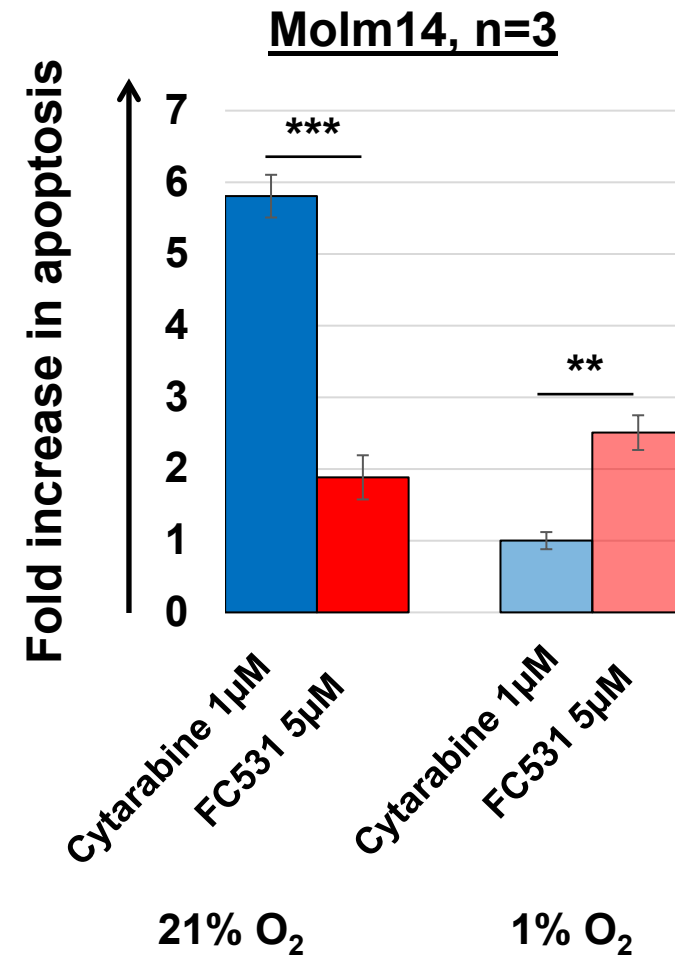


1 μM Cytarabine
100 nM Quizartinib

This article is protected by copyright. All rights reserved

Figure 4D





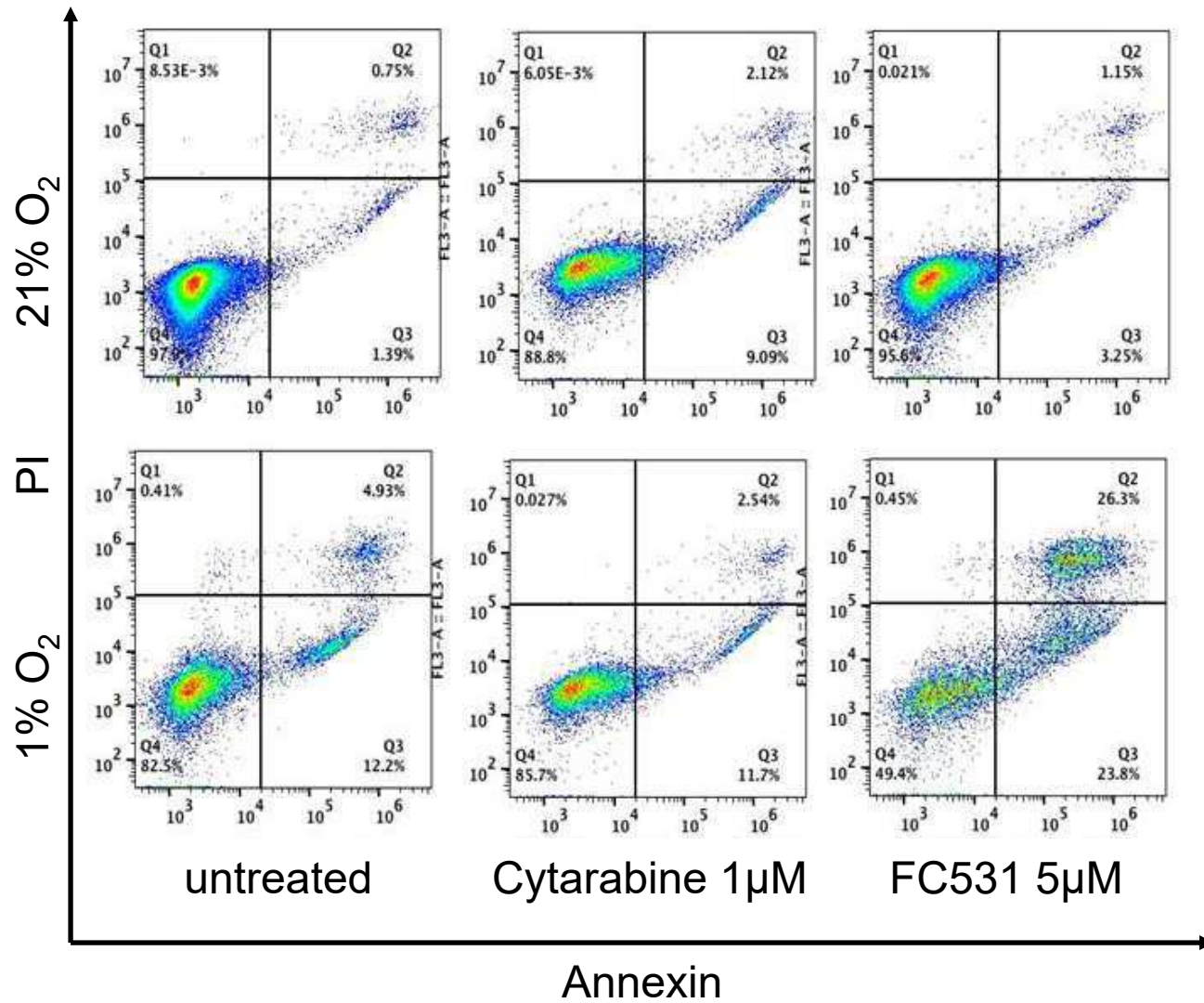


Figure 4G

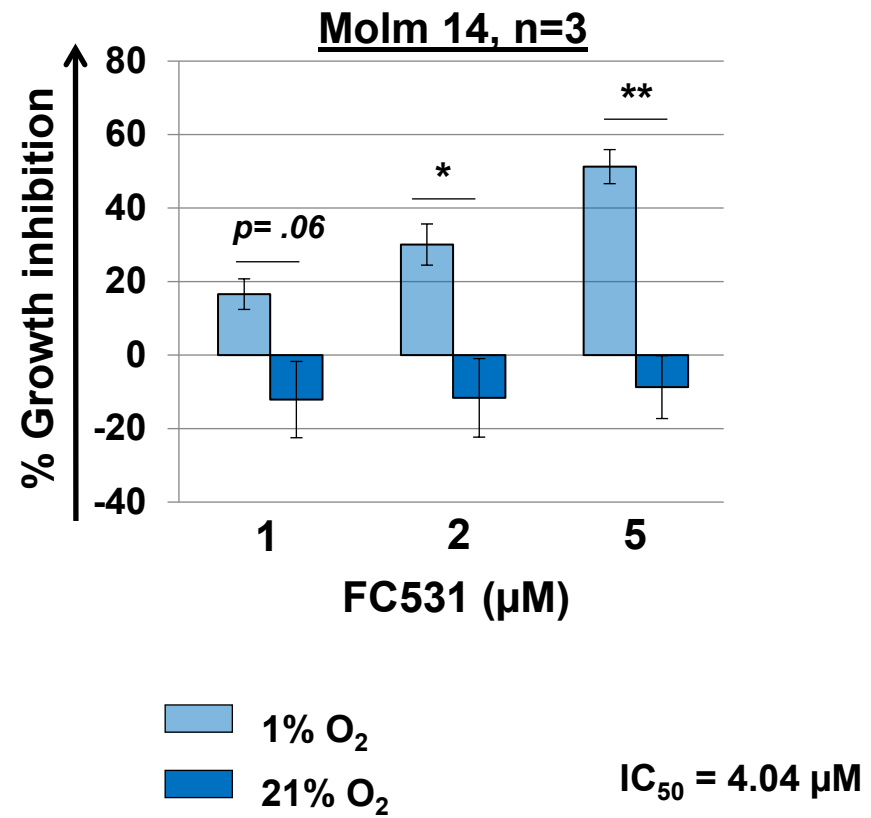
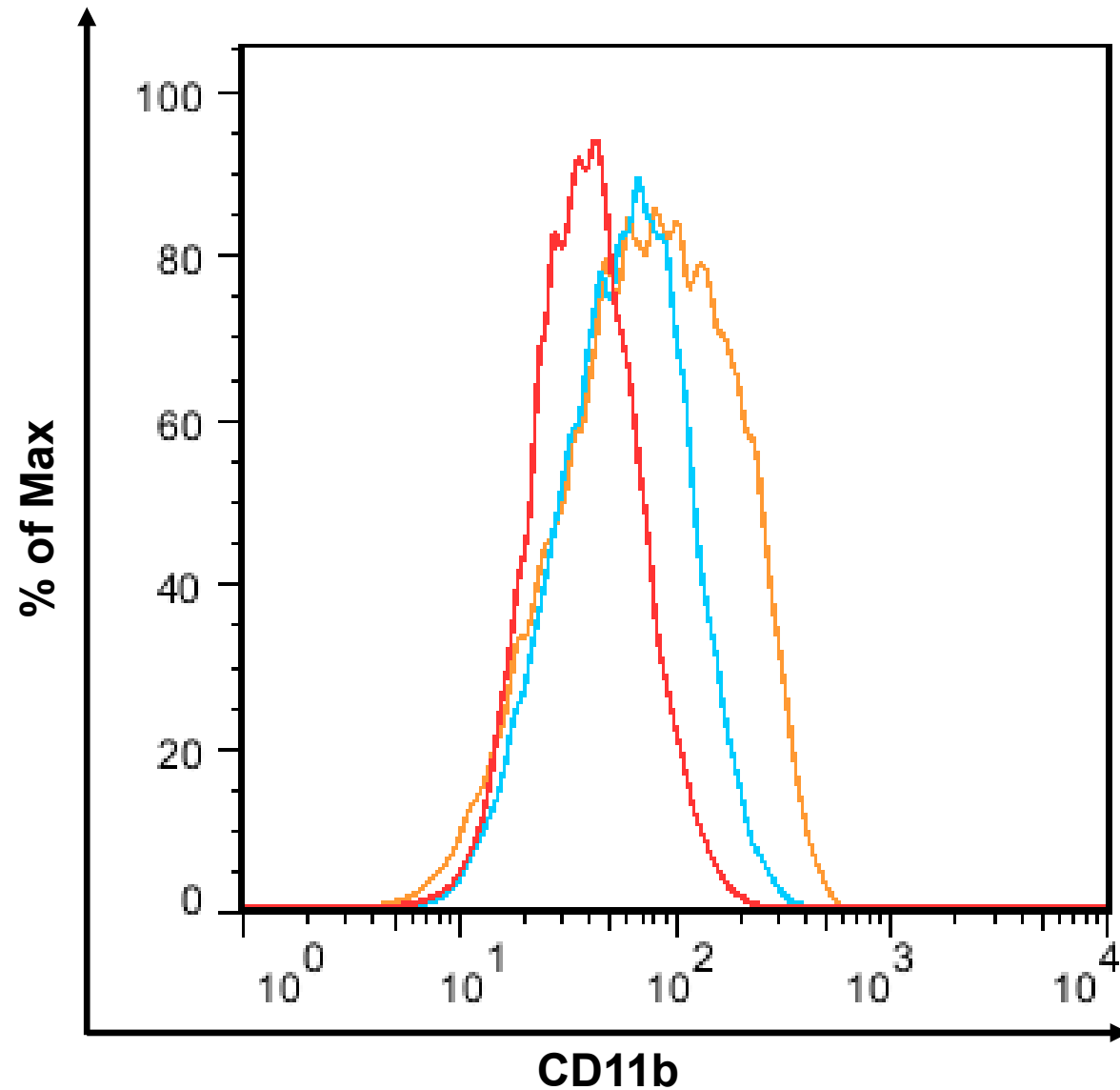


Figure 4H






	Sample Name
	M14_Specimen_001_untreated_001.fcs
	M14_Specimen_001_FC531 2uM_002.fcs
	M14_Specimen_001_FC531 5uM_003.fcs

Figure 4I

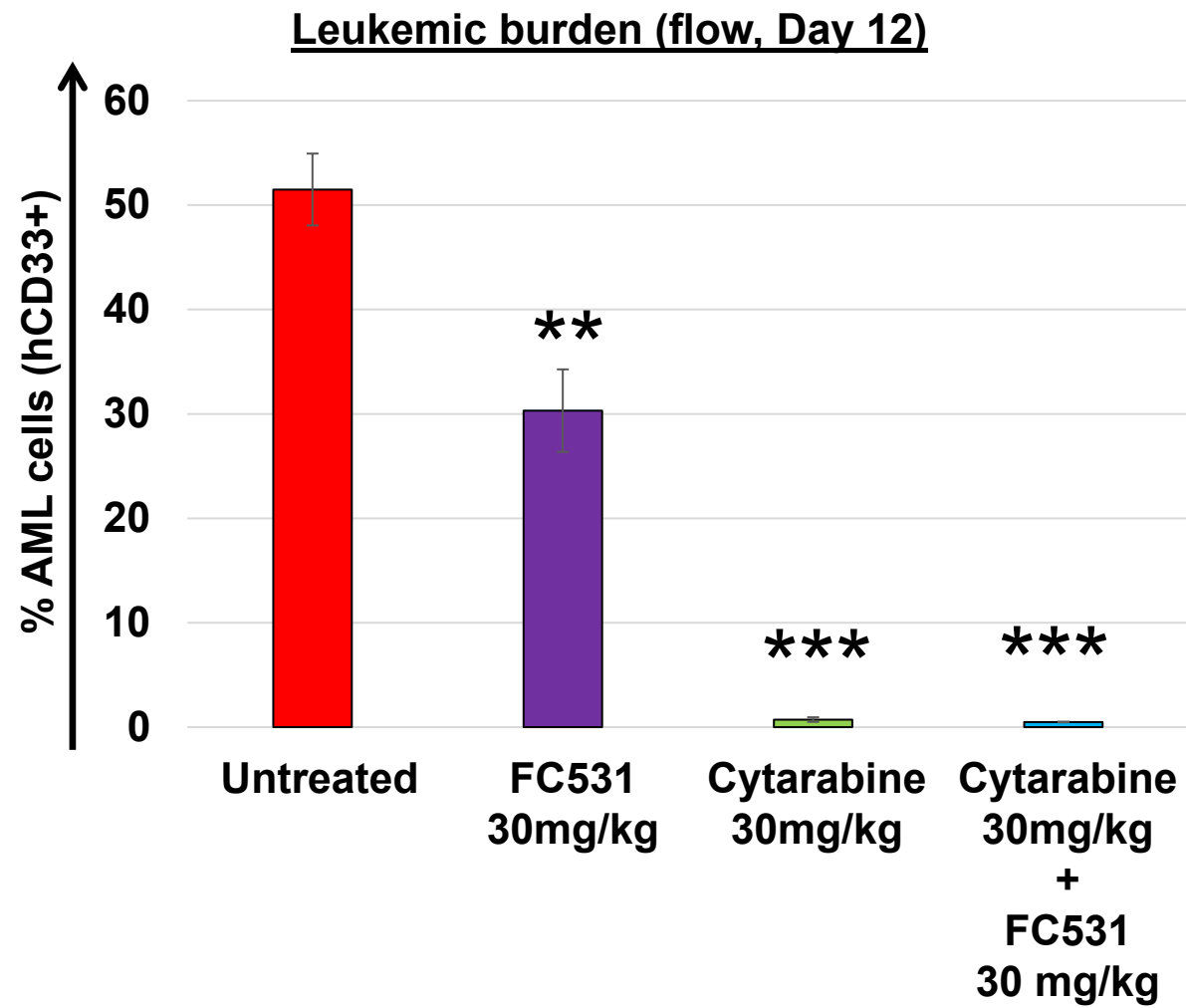


Figure 5A

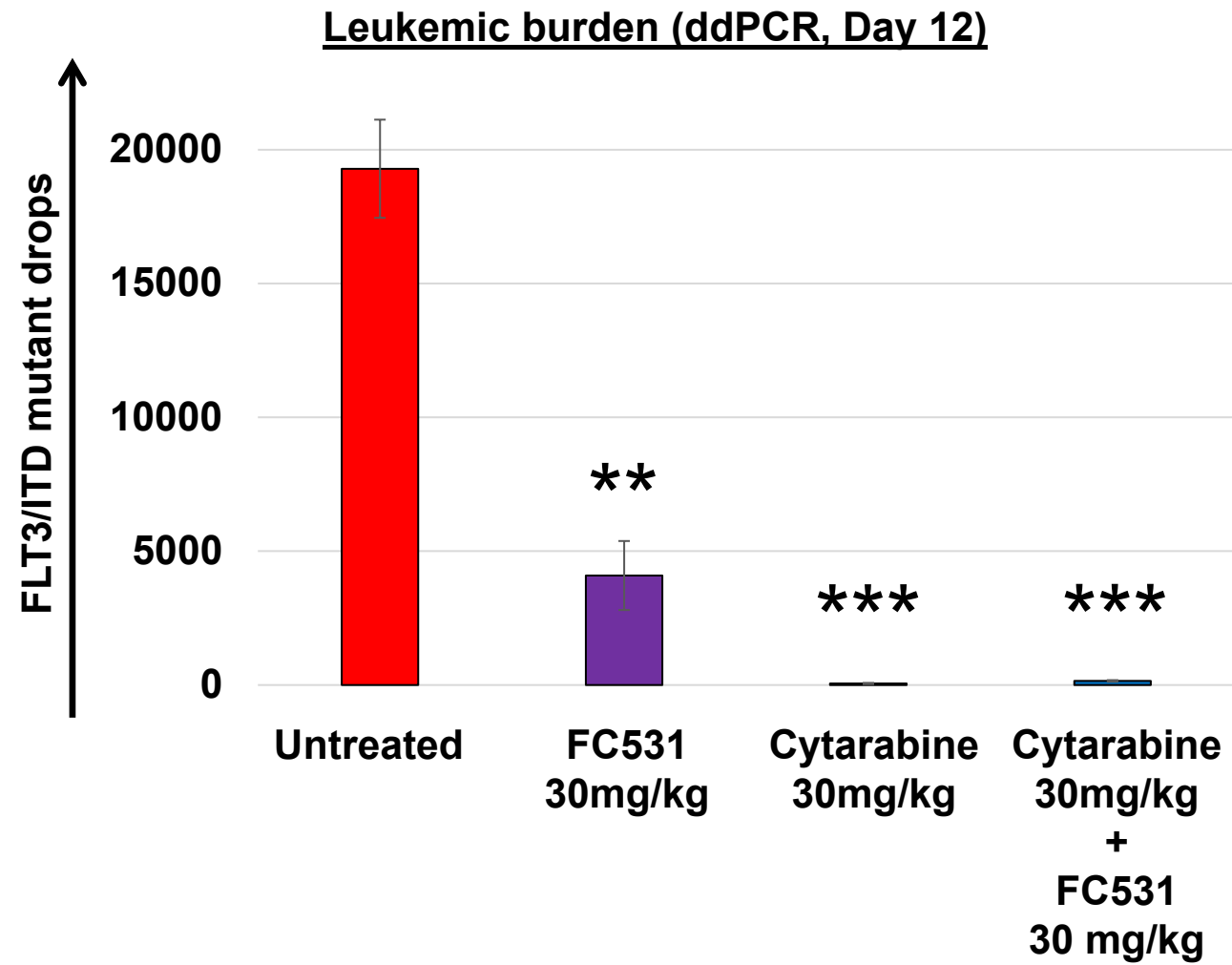
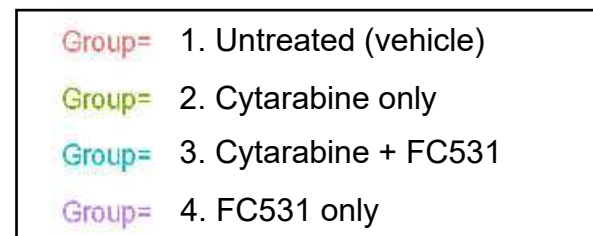
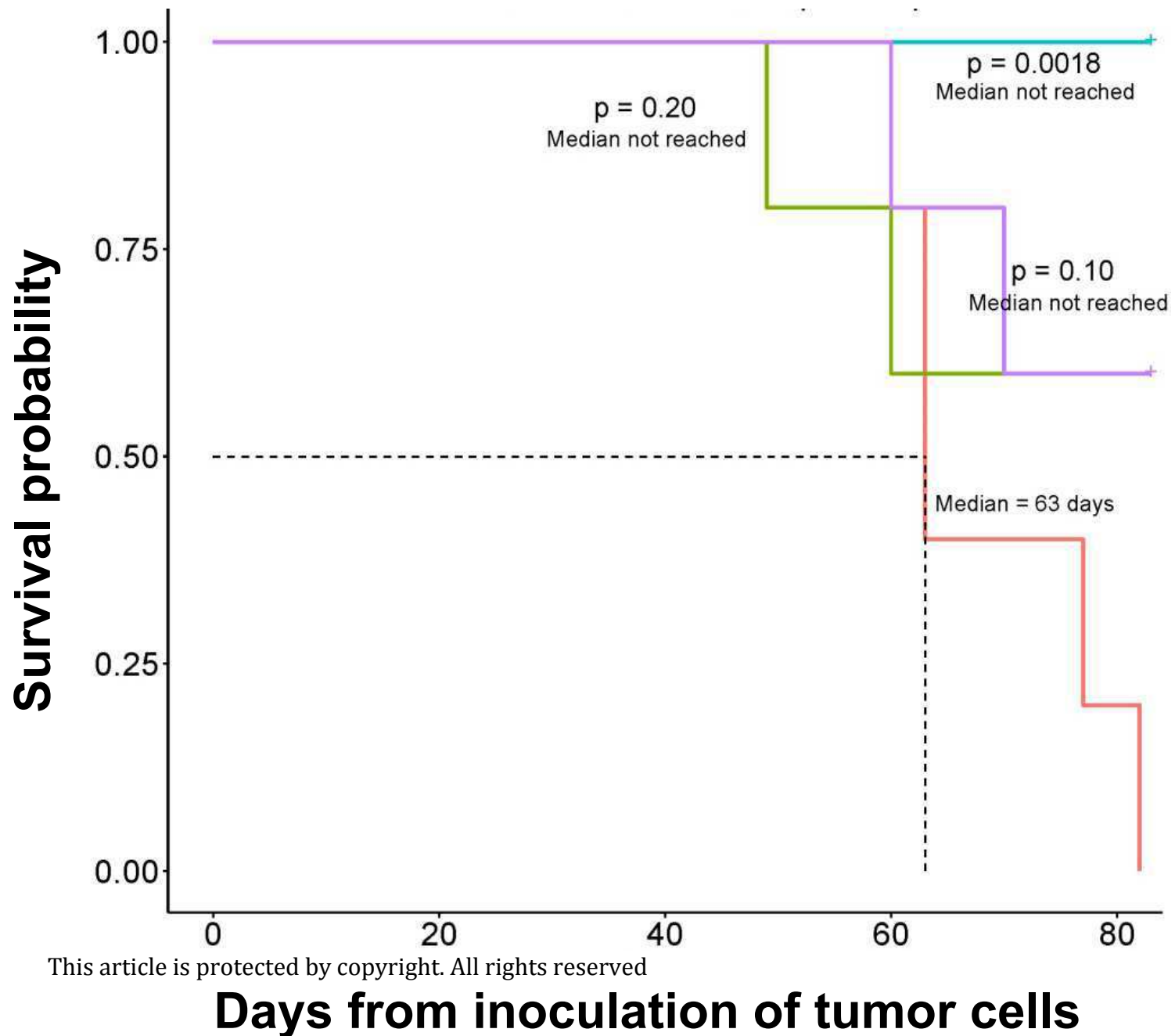


Figure 5B



This article is protected by copyright. All rights reserved

Figure 5C

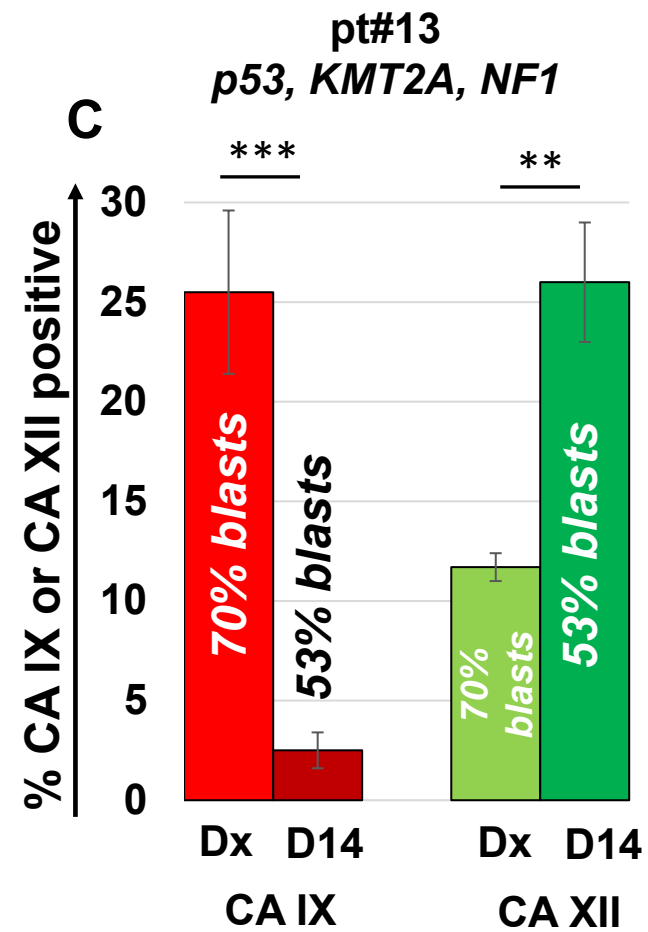
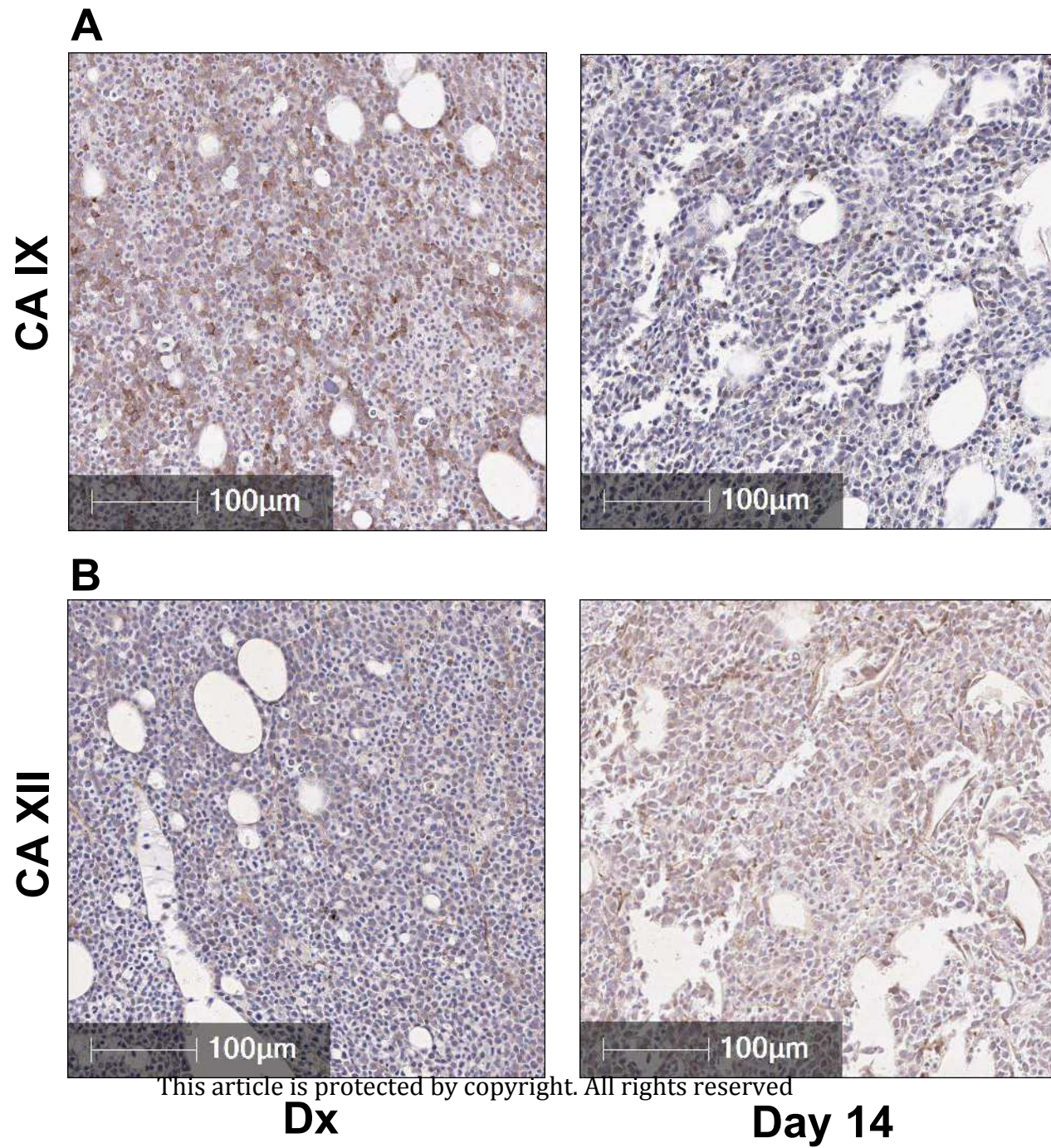
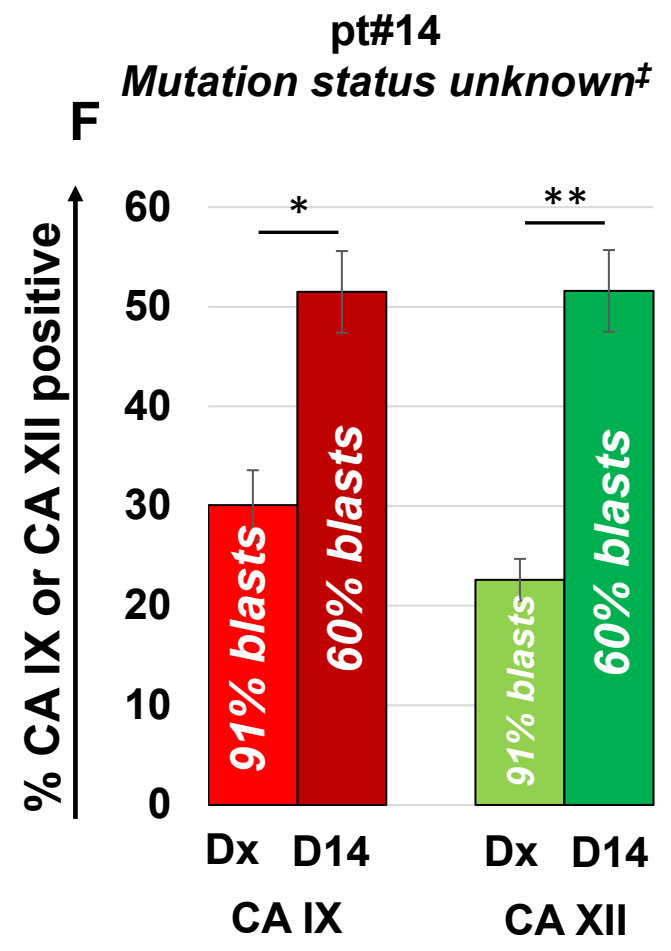
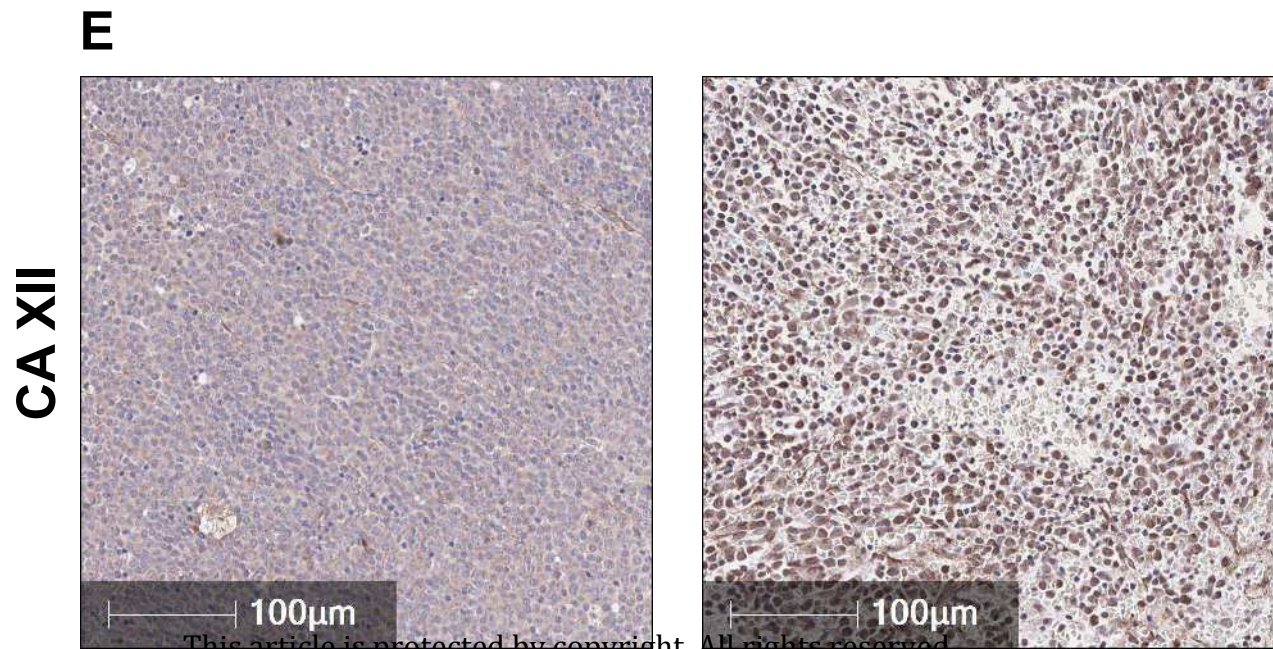
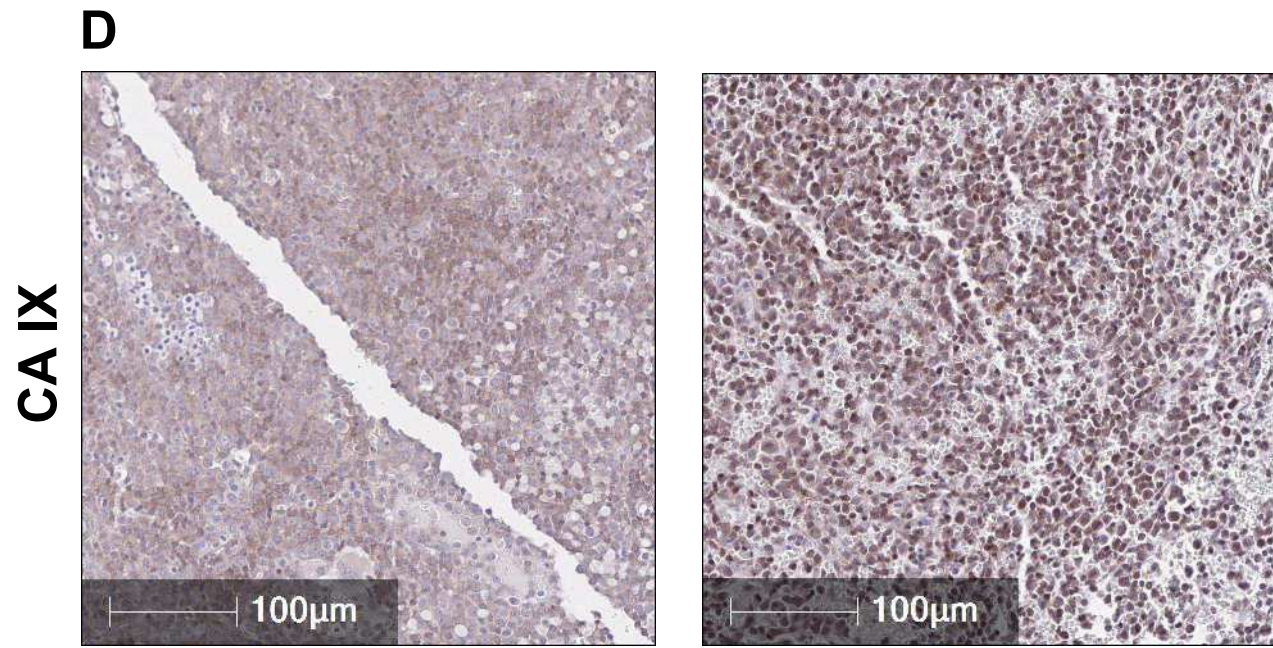


Figure 6



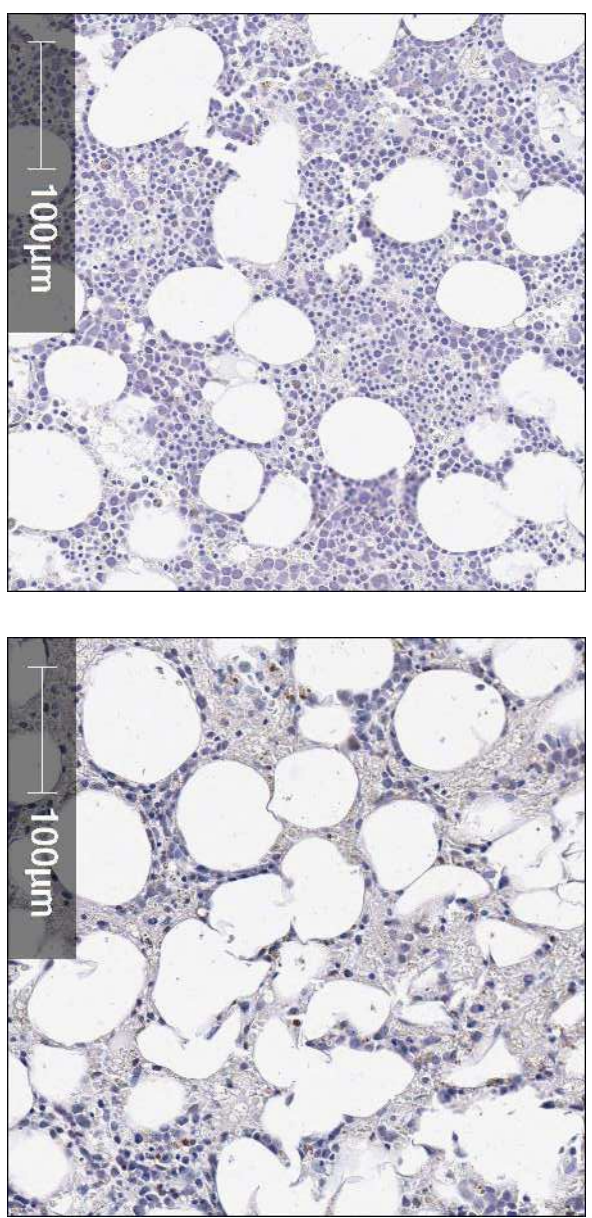
‡ NGS deferred by patient

This article is protected by copyright. All rights reserved

Dx **Day 14**

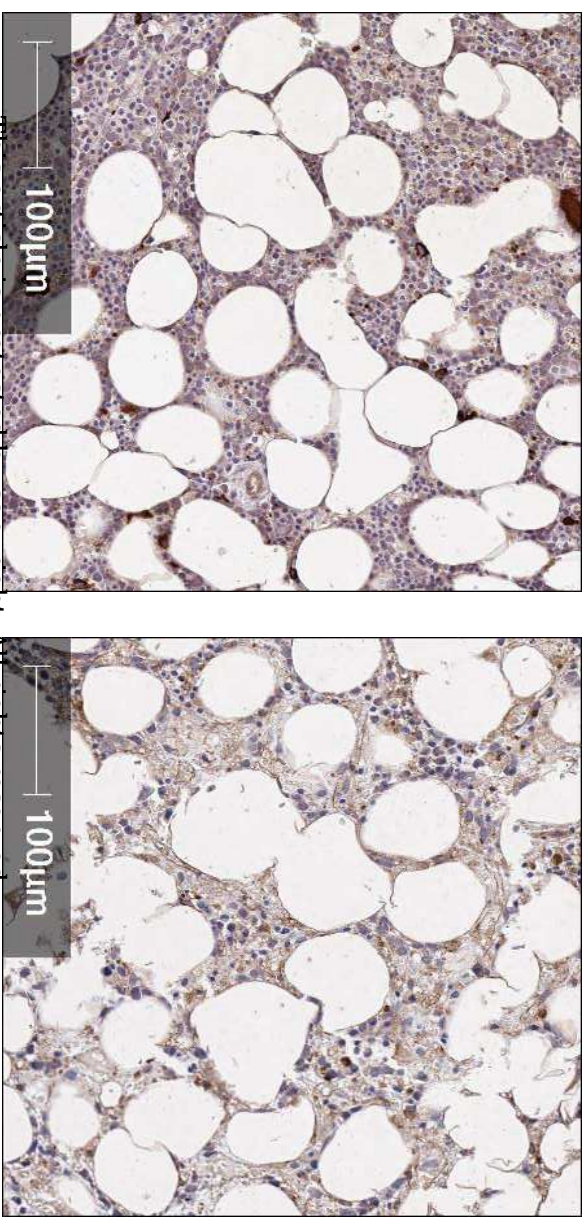
Figure 6

G



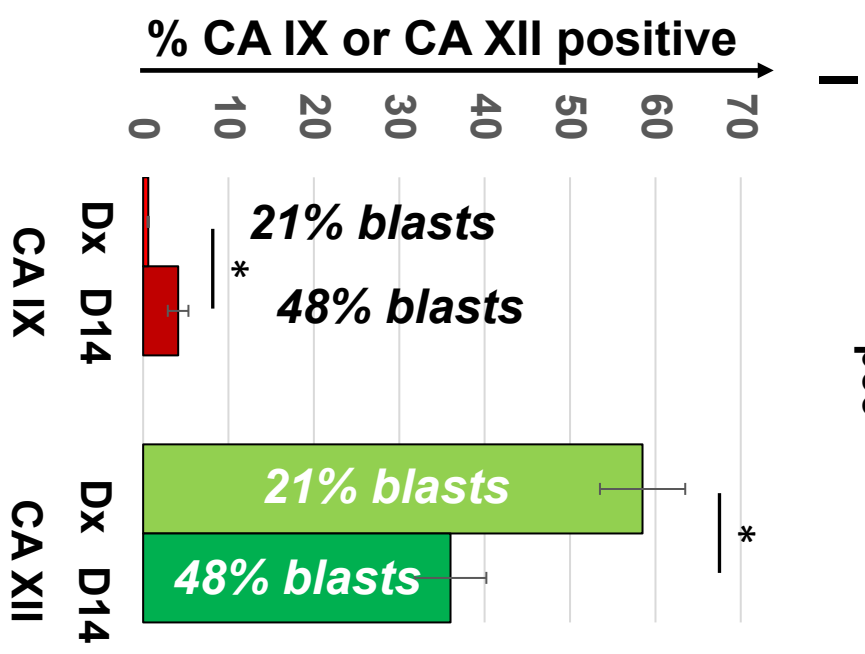
CA IX

H



CA XII

**pt#15
p53**

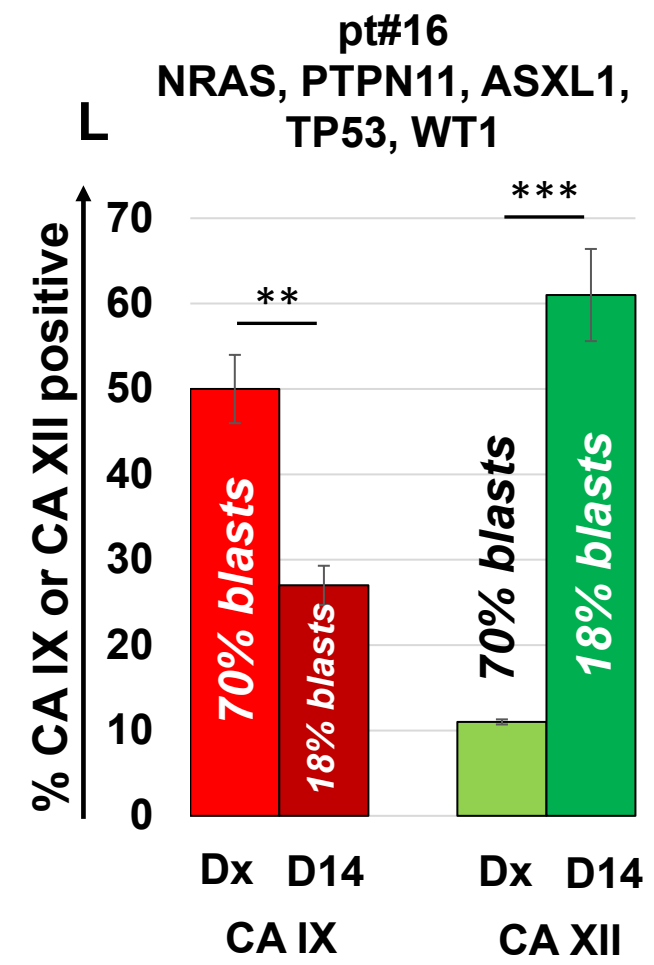
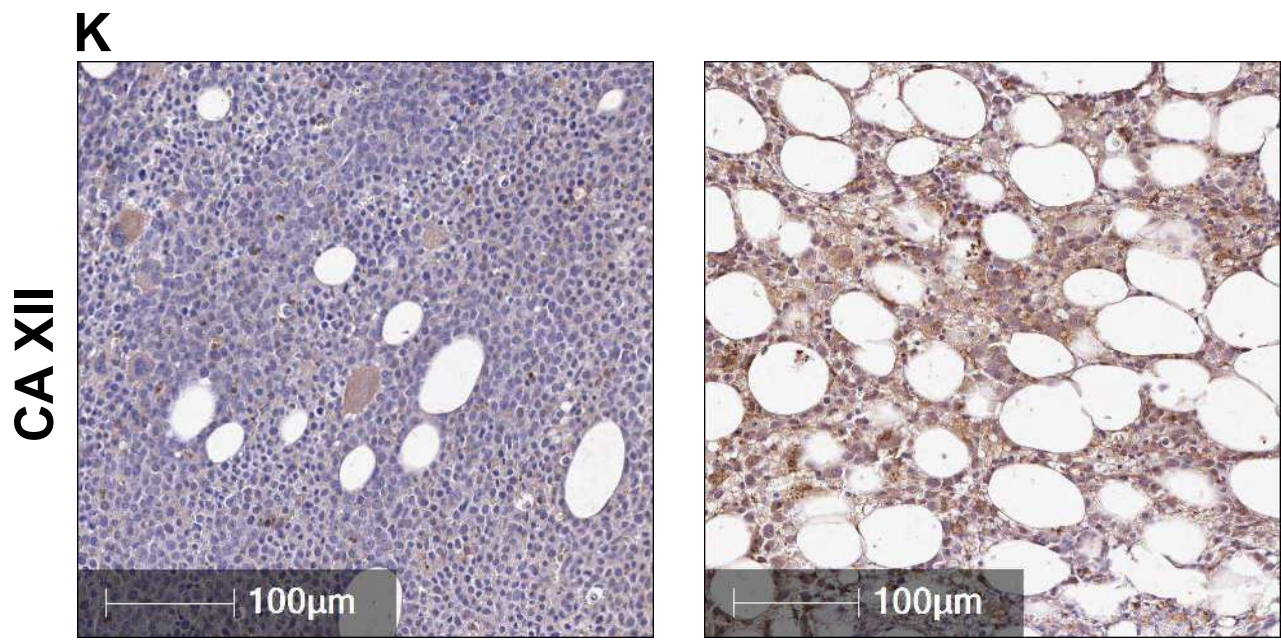
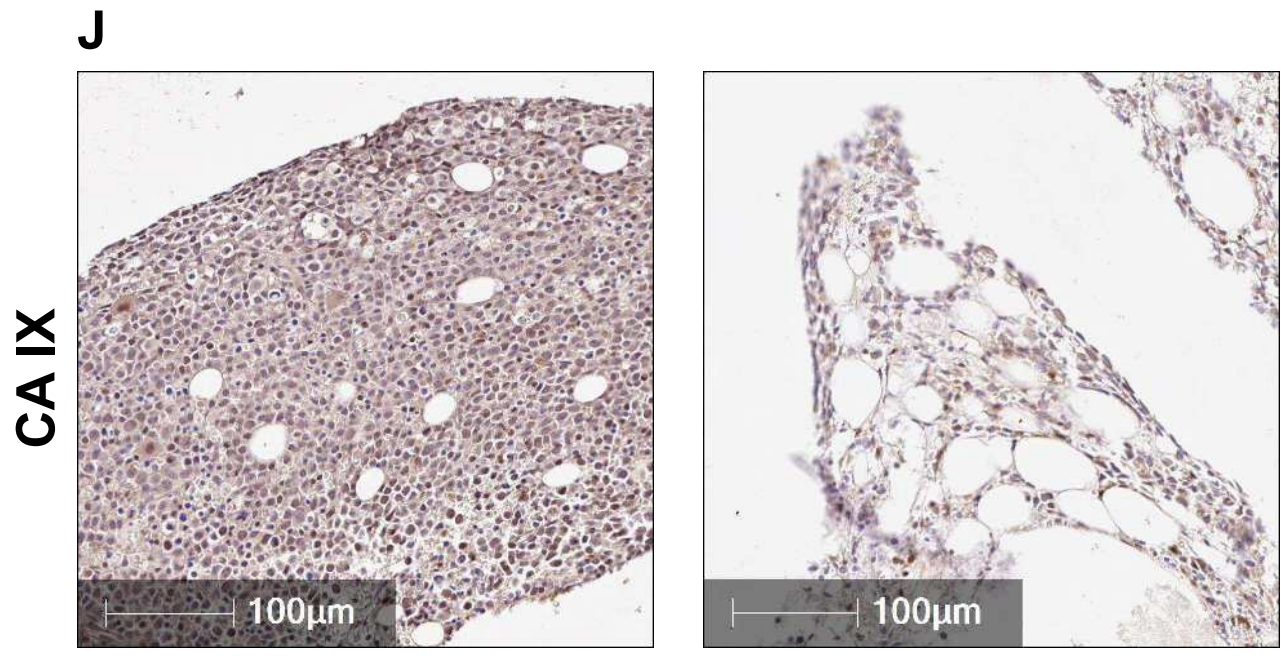


This article is protected by copyright. All rights reserved

Dx

Day 14

Figure 6



This article is protected by copyright. All rights reserved

Dx

Day 14

Figure 6

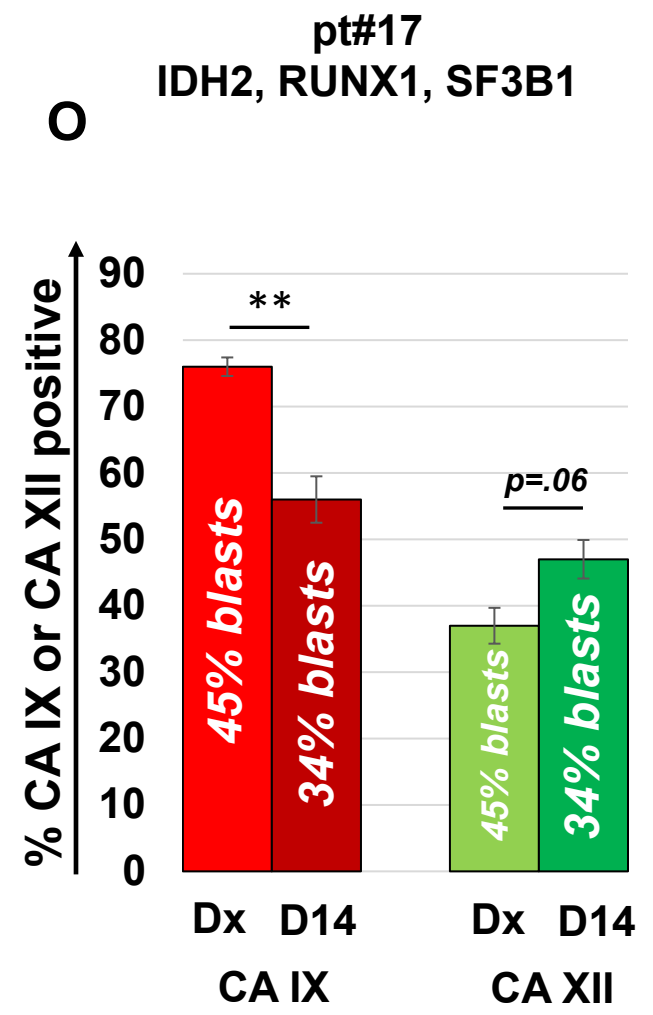
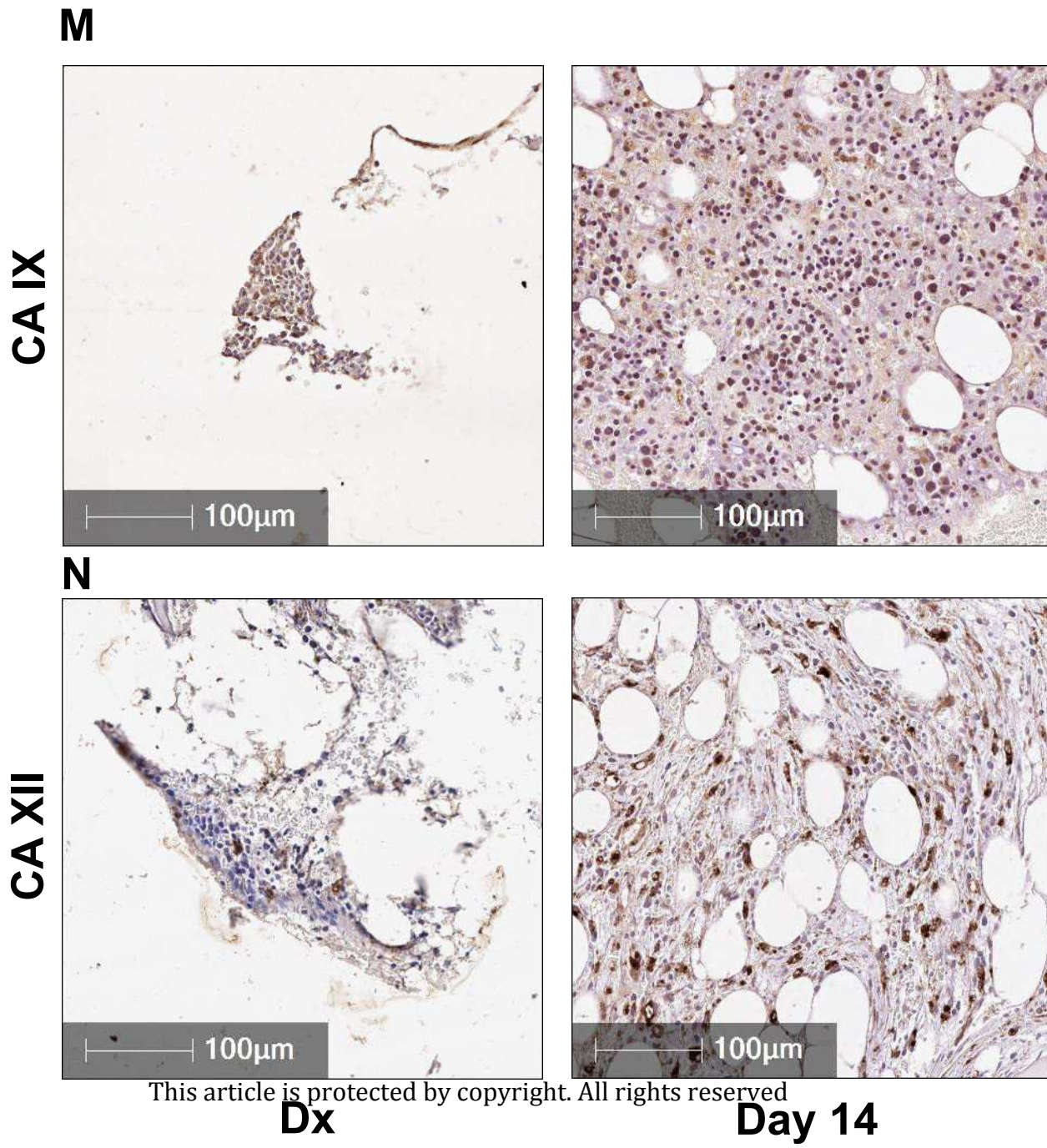


Figure 6

Patient No.	Age (y)	Gender, male (M)/ female (F)	Newly diagnosed (NDx), Relapsed/Refractory (R/R)	Cytogenetics	Molecular alterations identified
1	33	F	NDx	46,XX,inv(12) (p11.2q13)	FLT3/ITD, NPM1
2	75	F	NDx	46,XX	FLT3/ITD, NPM1
3	24	F	NDx	47, XX, +8	FLT3/ITD
4	56	M	NDx	46, XY	FLT3/ITD, ATRX, CCT6B, KMT2C (MLL3), NPM1, PTPN11, RAD21
5	50	F	NDx	46, XX	FLT3/TKD, IDH2, DNMT3A
6	35	F	R/R	46, XX	FLT3/ITD, NPM1
7	60	M	R/R	46, XY	FLT3/ITD
8	36	F	R/R	46, XX	FLT3/ITD, NPM1, ATRX, ASXL1, RUNX1, TET2
9	30	M	NDx	46, XY	FLT3/ITD, WT1
10	39	M	NDx	46,XY,t(5;22)(q35;q11.2)	FLT3/ITD, NRAS, PDCD11, WT1
11	46	M	NDx	47,XY,+11	FLT3/ITD, TET2, KMT2A, SRSF2
12	38	F	NDx	46, XX	FLT3/ITD, FLT3/TKD

Patient No.	Age (y)	Gender, male (M)/ female (F)	Newly diagnosed (NDx), Relapsed/Refractory (R/R)	Cytogenetics	Molecular alterations identified
13	63	M	NDx	46,XY,del(20)(q11.2q13.3)[9]/46,sl,del(5)(q13q33),+7,der(7;17)(q10;q10),+8,add(11)(q23),18,3~6dmin[5]/47,sdl1,+6,3~20dmin[2]/46,sdl2,der(7;17),-8,5~12dmin[2]/46,XY[2]	P53, KMT2A, NF1
14	25	M	NDx	46, XY	Unknown*
15	65	M	NDx	45,XY,add(1)(p22),-2,-5,add(9)(p11), -12,-15, add(16)(q22), add(17)(p11.2), -18,+mar1, +mar4,+mar5,+mar8[7]/ 43~44,idem, -X,-3,-4,-7, -20,+mar2,+mar3, +mar6,+mar7[cp5]/ 46,XY[8]	P53
16	66	M	NDx	45,XX,add(5)(q1?3),add(14)(p12),add(17)(p11.2),-18[2]/ 45,sl,der(16)t(11;16)(q13;p13.3)[11]/ 46,sdl1,+8[5]/ 46,XX[3]	NRAS, PTPN11, ASXL1, TP53, WT1
17	60	F	NDx	92<4n>,XXXX[2]/ 46,XX[18]	IDH2, RUNX1, SF3B1

Intracellular pH		
O₂	21%	1%
Untreated	<i>7.40±0.26</i>	<i>7.31±0.51</i>
FC531 1μM	<i>7.59±0.30</i>	<i>6.80±0.42</i>
FC531 2μM	<i>7.50±0.23</i>	<i>6.32±0.57</i>
FC531 5μM	<i>7.21±0.42</i>	<i>4.60±1.03</i>

Table 2

PDX Group	d1-5	d8-12
1	<i>PBS (untreated)</i>	<i>PBS (untreated)</i>
2	<i>Cytarabine 30 mg/kg/d i.p.</i>	<i>Cytarabine 30 mg/kg/d i.p.</i>
3	<i>Cytarabine 30 mg/kg/d i.p.</i>	<i>FC531 30 mg/kg/d i.p.</i>
4	<i>FC531 30 mg/kg/d i.p.</i>	<i>FC531 30 mg/kg/d i.p.</i>

Table 3

